Molecular characterization of the tetratricopeptide repeat - mediated interactions of murine stress - inducible protein 1 with major heat shock proteins

A thesis submitted in fulfilment of the requirements for the degree of

DOCTOR OF PHILOSOPHY

of

RHODES UNIVERSITY

by

Odutayo Odutola ODUNUGA

December 2002

Declaration

I hereby declare that this submission is my own unaided work and that, to the best of my knowledge and belief, it contains no material previously published or written by another person, nor material which to a substantial extent has been accepted for the award of any other degree of the university or other institute of higher learning, except where due acknowledgment has been made in the text.

O. O. ODUNUGA

This 28TH day of MARCH 2003

Abstract

Murine stress-inducible protein 1 (mSTI1) is a co-chaperone that is homologous with the human heat shock protein 70 (Hsp70)/heat shock protein 90 (Hsp90)-organizing protein (Hop). The two proteins are homologues of the highly conserved stress-inducible protein 1 (STI1) family of co-chaperones. The STI1 proteins interact directly and simultaneously at some stage, with Hsp70 and Hsp90 in the formation of the hetero-multi-chaperone complexes that facilitate the folding of signal transducing kinases and functional maturation of steroid hormone receptors. The interactions of mSTI1 with both Hsp70 and Hsp90 is mediated by a versatile structural protein-protein interaction motif, the tetratricopeptide repeat (TPR). The TPR motif is a degenerate 34-amino acid sequence α-helical structural motif found in a significant number of functionally unrelated proteins. This study was aimed at characterizing the structural and functional determinants in the TPR domains of mSTI1 responsible for binding to and discriminating between Hsp70 and Hsp90. Guided by data from Hop's crystal structures and amino acid sequence alignment analyses, various biochemical techniques were used to both qualitatively and quantitatively characterize the contacts necessary for the N-terminal TPR domain (TPR1) of mSTI1 to bind to the C-terminal EEVD motif of heat shock cognate protein 70 (Hsc70) and to discriminate between Hsc70 and Hsp90. Substitutions in the first TPR motif of Lys^{8} or Asn^{12} did not affect binding of mSTI1 to Hsc70, while double substitution of these residues abrogated binding. A substitution in the second TPR motif of Asn^{43} lowered but did not abrogate binding. Similarly, a deletion in the second TPR motif coupled with a substitution of Lys^{8} or Asn^{12} reduced but did not abrogate binding. Steady state fluorescence and circular dichroism spectroscopies revealed that the double substitution of Lys^{8} and Asn^{12} resulted in perturbations of inter-domain interactions in mSTI1. Together these results suggest that mSTI1-Hsc70 interaction requires a network of electrostatic interactions not only between charged residues in the TPR1 domain of mSTI1 and the EEVD motif of Hsc70, but also outside the TPR1 domain. It is proposed that the electrostatic interactions in the first TPR motif collectively made by Lys^{8} and Asn^{12} define part of the minimum interactions required for successful mSTI1-Hsc70 interaction. In the first central TPR domain (TPR2A), single substitution of Lys^{301} was sufficient to abrogate the mSTI1-Hsp90 interaction. Using a truncated derivative

of mSTI1 incapable of binding to Hsp90, residues predicted by crystallographic data to determine Hsp70 binding specificity were substituted in the TPR1 domain. The modified protein had reduced binding to Hsc70, but showed significant binding capacity for Hsp90. In contrast, topologically equivalent substitutions on a truncated derivative of mSTI1 incapable of binding to Hsc70 did not confer Hsc70 specificity on the TPR2A domain. These data suggest that binding of Hsc70 to the TPR1 domain is more specific than binding of Hsp90 to the TPR2A domain. In addition, residues C-terminal of helix A in the second TPR motif of mSTI1 were shown to be important in determining specific binding to Hsc70. Binding assays using surface plasmon resonance spectroscopy showed that the affinities of binding of mSTI1 to Hsc70 and Hsp90 were 2 μM and 1.5 μM respectively. Preliminary *in vivo* studies revealed differences in the dynamics of binding of endogenous and exogenous recombinant mSTI1 with Hsc70 and Hsp90. The outcome of this study poses serious implications for the mechanisms of mSTI1 interactions with Hsc70 and Hsp90 in the cell.

Dedication

This thesis is dedicated to my loving family, my wife Abolanle, and my son Temitayo; you both stood by me throughout.

And to God the Almighty, who has enabled me in all things to be able to achieve this feat.

Acknowledgements

I would like to acknowledge my supervisor, Professor Gregory Blatch for his enthusiastic support and encouragement throughout this project. His dedication to his students and to excellence in science is unparalleled.

I would also like to acknowledge:

- The Deutscher Akademischer Austauschdienst (DAAD) for the award of a Predoctoral Scholarship to study in South Africa.
- The Volkswagen Foundation (Germany), the Wellcome Trust (United Kingdom), the National Research Foundation (NRF, South Africa) and the Joint Research Committee (JRC, Rhodes University) for funding the project.
- Dr Judith Hornby, University of Arizona, Tucson, U.S.A, for technical assistance and valuable input into the circular dichroism and steady state fluorescence spectroscopy studies.
- Prof. Dr. Richard Zimmermann, Universität des Saarlandes, Homburg, Germany, for allowing me to do surface plasmon resonance (SPR) studies in his laboratory, and Dr Christiane Bies, Universität des Saarlandes, Homburg, Germany, for valuable technical assistance and useful discussions on the SPR experiments.
- Dr David Pugh, University of the Western Cape, Bellville, South Africa, for the use of the Biacore SPR machine in his laboratory and also for useful discussions on the SPR studies.
- Dr David Toft, Mayo Clinic, Minnesota, U.S.A, and Dr David Smith, Mayo Clinic, Scottsdale, U.S.A, for the gifts of purified Hsp90 and anti-Hsp90 antibody.
- Drs Péter Csermely and Csaba Söti, Semmelweis University, Budapest, Hungary for the gift of purified Hsp90.
- All my colleagues in the Chaperone Research Group (Lab 301) for their support and encouragement, especially Fritha Hennessy for her assistance in computer work

Table of Contents

Chapter Four

Quantitation of the affinities of binding of mSTI1 proteins to Hsc70 and Hsp90 using surface plasmon resonance spectroscopy **75**

Chapter 5

Characterization of the binding of mSTI1 to Hsc70 and Hsp90 *in vivo* 82

List of Figures

List of Tables

List of Symbols

Abbreviations of Units

%	Percent or g/100 ml
α	alpha
β	beta
γ	gamma
Å	angstrom
µg	microgram
µl	microlitre
µm	micrometer
µmol	micromole
A_{260}	Absorbance at 260 nanometers
A_{280}	Absorbance at 280 nanometers
bp	base pair
Da	Daltons
g	gram
kDa	kiloDalton
l	litre
M	Molar
mg	milligram
ml	millilitre
mm	millimiter
mol	mole
nm	nanometer
^0C	degree Celcius
pmol	picomole
U	units
V	volts
w/v	weight per volume
v/v	volume per volume
x g	relative centrifugal force to gravity

Prefixes

10^{3}	kilo	k
10^{-3}	milli	m
10^{-6}	micro	μ
10^{-9}	nano	n
10^{-12}	pico	p

Chapter One

Introduction and Literature Review

1.1 Protein folding in the cell

1.1.1 Protein folding *in vitro* and *in vivo*

The observation by Christian Anfisen (1973) of reversible denaturation and renaturation of ribonuclease *in vitro* provided the first clue that the information for folding a protein into its native three-dimensional conformation lies in its amino acid sequence. The native state is the thermodynamically most stable conformation of a polypeptide. To reach the native state, the unfolded polypeptide proceeds via one or more pathways in which rapid formation of compact folding intermediates restricts the conformational space available to a polypeptide (Dill and Chan, 1997; Jaenicke, 1998). It therefore appears that removal of hydrophobic core of the folded protein is a major driving force for formation of folding intermediates (Frydman, 2001). Most *in vitro* studies have used small, single-domain proteins that undergo co-operative and reversible folding reactions, e.g. glutathione-*S*-transferase (GST), barnase, lysozyme e.t.c. In these experiments, a pure protein is unfolded or denatured with chemical reagents such as 8 M urea or 6 M guanidinium hydrochloride. The reaction is then rapidly diluted into aqueous solution, where the protein refolds spontaneously.

This refolding takes place in two phases. First, a very rapid formation of secondary structure such as α-helices and β–sheets, and folding of these structures to form a compact shape, which is presumed to be driven by hydrophobic collapse, so that most of the interior of the protein is occupied by hydrophobic amino acids, which have a low affinity for water. The second phase is slower; the secondary structure elements interact with each other to form the native tertiary structure. These *in vitro* reaction models are manageable systems, as the folding reaction is not complicated by off-pathway side reactions such as aggregation. In nature, proteins fold in a cellular environment that may be substantially different from that of *in vitro* folding experiments that are usually done at very high dilutions and low temperatures (Frydman, 2001). The homogeneous environment of *in vitro* experiments does not mimic the heterogeneous environment in the cell. The interior of a cell is a very crowded and dynamic environment; the effective protein concentration inside a

typical cell has been estimated to be as high as 300 mg/ml (Zimmermann and Trach, 1991). Because of its high concentration of proteins and other macromolecules, the interior of a cell no longer behaves as an ideal fluid. This macromolecular crowding gives rise to excluded volume effects, thus promoting such reactions like aggregation of proteins (Zimmermann and Minton, 1993; Minton, 2000). Another major difference between refolding of a chemically denatured protein and folding as it occurs in the cell is that *in vivo*, newly synthesized polypeptides enter the cytosol vectorially because the N-terminus is synthesized before the C-terminus. Although the N-terminus of a translating polypeptide is available for folding before the rest of the polypeptide, stable folding of a folding unit or domain cannot occur until it is completely synthesized (Jaenicke, 1991). Protein synthesis is considerably slower than formation of collapsed intermediates, which could bury hydrophobic aggregation-prone stretches of the nascent chains away from the solution (Frydman, 2001).

Another distinctive feature of the cellular milieu is its high degree of compartmentalization. Whereas small molecules ($\leq$500 Daltons) diffuse freely in the cytosol, diffusion of larger macromolecules, including proteins, is greatly retarded (Frydman, 2001). This implies that most cellular processes are highly compartmentalized and spatially organized. In conclusion, the efficiency of folding *in vivo* often exceeds that *in vitro* to avoid misfolding and aggregation of proteins.

The cell is equipped with several structurally unrelated classes of proteins to ensure correct protein folding. First, there are enzymes that catalyse specific folding steps, the protein disulphide isomerases (PDIs) and *cis-trans* prolyl isomerases. These enzymes accelerate intrinsically slow steps in the folding of some proteins, namely the rearrangement of disulphide bonds in secretory proteins and the *cis-trans* isomerization of peptide bonds preceding proline residues, respectively (Schmid, 1993; Freedman, 1994). Second, there are proteins that bind to and stabilize otherwise unstable conformers of other proteins, and by controlled binding and release, facilitate its correct fate *in vivo*, be it folding, oligomeric assembly, transport to a particular subcellular compartment, or disposal by degradation (Hendrick and Hartl, 1993). In addition, this set of proteins, prevents potential aggregation or misfolding of newly

synthesized or translating proteins. This second class of proteins is generally referred to as "molecular chaperones" and discussed in section 1.2.

1.1.2 Protein folding and diseases

In order to function, a protein must fold into a specific conformation following synthesis on the ribosome. The folding process is therefore a second stage of the translation of genetic information into biological activity. The failure of proteins to fold correctly, or the subsequent misfolding of correctly folded proteins could be lethal to the cell. The misfolding of protein can be caused by many factors such as mutation in the DNA so that the amino acid sequence differs from normal, lack of an enzyme or chaperone needed to fold a protein, correctly folded protein becoming misfolded by accumulated damage due to oxidation or other chemical reactions, and interaction with other misfolded proteins. The misfolding of a protein can be lethal to the cell in many ways (Ellis, 2002). For instance, a protein could be non-functional, in short supply, or unable to be translocated to the right subcellular organelle.

Finally, protein aggregates have damaging effect on the cell (Thomas, 1995; Shaw, 1995). A number of diseases, both in human and other organisms, have recently been shown to be due to incorrect protein folding. These disorders include the amyloidal diseases, such as Alzheimer's disease (Walsh *et al.*, 2002), bovine spongiform encephalopathy (BSE, mad cow disease), primary systemic amyloidoisis, and type II diabetes (Sunde, 1999). These diseases are disorders of protein folding in which proteins and peptides take up an incorrect, fibrillar structure (Terry *et al.*, 1993; Hamilton *et al.*, 1993; Serpell *et al.*, 1995; Kelly, 1996; Blake and Serpell, 1996; Wetzel, 1996; Kelly, 1997; Bucciantini *et al.*, 2002). Other protein folding related diseases include onset neurodegenerative diseases e.g. Huntington's disease, caused by expansion of a translated CAG repeat that encodes glutamine in the respective gene products (Zoghbi and Botas, 2002). Cystic fibrosis is an autosomal recessive disease caused by mutations in the gene coding for the cystic fibrosis transmembrane conductance regulator (CFTR). It is therefore extremely important that the cell ensures the correct folding of polypeptides, prevents aggregation of proteins and refolds or degrades as soon as possible misfolded proteins.

1.2 Molecular chaperones and Heat shock proteins

1.2.1 Historical background

In 1962, Ritossa reported the effects of temperature on the puffing patterns of the salivary glands chromosome of *Drosophila busckii*. He observed that temperature shocks induced well-defined variations in the puffing patterns of the same set of bands, and that chemicals such as 2, 4-dinitrophenol and sodium salicylate could induce the same puffing patterns. In 1978, Laskey *et al* observed that the nucleosome subunits of chromatin were assembled from histones and DNA by the abundant acidic nuclear protein nucleoplasmin and described the protein as a molecular chaperone. In 1980, Hightower reported the induction of some acidic polypeptides, with molecular weights ranging from 23 to 110 kDa, in cultured chick embryos exposed to puromycin and the arginine analogue, canavanine. The proteins were divided into two groups based on their level of inducibility. The major ones were the 88, 72, 71 and 23 kDa proteins while the minors comprised of the 110, 50, 38 and 30 kDa proteins. In 1987, Ellis first proposed the words "molecular chaperones" to describe the class of cellular proteins whose function is to ensure that the folding of certain other polypeptide chains and their assembly into oligomeric structures occur correctly.

1.2.2 Definition and properties of molecular chaperones

By definition, molecular chaperones are a large group of structurally unrelated protein families whose role is to minimise non-specific protein aggregation by stabilizing unfolded proteins, ensure proper folding of nascent proteins, maturation, assembly and disassembly of proteins and/or their translocation across membranes or for degradation. Therefore their main role is to prevent inappropriate association or aggregation of exposed hydrophobic surfaces and direct their substrates into productive folding, transport or degradation pathways. They exist as large gene families with functional homologues in different subcellular locations including the nucleus, cytosol, endoplasmic reticulum, and mitochondria (Morimoto *et al.*, 1994). The general properties of molecular chaperones are itemised in Table 1.1.

Table 1.1: Families of Molecular Chaperones

Chaperone family	Functions
Small heat shock proteins (Hsp25)	Protect cell against stress and prevent aggregation during heat shock.
Heat shock protein 60 (Hsp60) e.g. Cpn60, GroEL	Facilitate folding of polypeptides to the native state in an ATP-dependent manner.
Heat shock protein 70 (Hsp70) e.g. DnaK, Bip	They are ATPases involved in stabilization of hydrophobic regions in extended polypeptide segments, membrane translocation and regulation of the heat response.
Heat shock protein 90 (Hsp90)	They are ATPases involved in binding, stabilization, maturation and regulation of steroid hormone receptors and signal transducing protein kinases.
Heat shock protein 100 (Hsp100) (Clp)	They are ATPases involved in thermotolerance, proteolysis and disaggregation and resolubilization of protein aggregates.
Calnexin and calreticulin	Involved in glycoprotein folding and maturation in the endoplasmic reticulum in cooperation with glucosyltransferase, and in quality control.
Protein disulphide isomerases (PDIs) and cis/trans prolyl isomerases	Catalyse specific steps in the folding process.

1.2.3 Major Heat shock proteins

Heat shock proteins (Hsps) are a large family of molecular chaperones whose synthesis is sharply and dramatically induced at high temperatures. The various Hsps are referred to on the basis of their mode of induction, and apparent molecular mass on sodium dodecyl sulphate (SDS) polyacrylamide gels (Kaufmann, 1990). Other stress stimuli that could lead to over-expression of Hsps include: nutrient deprivation, hypoxia, exposure of tissues to uncouplers of oxidative phosphorylation, inhibitors of electron transport, amino acid analogues, enzyme inhibitors and heavy metal ions (Georgopoulos, 1992). The induction of Hsps upon exposure to environmental, chemical or oxidative stress is a common feature of all organisms from archabacteria to eubacteria, plants, yeasts, invertebrates and vertebrates (Bonnefoy *et al.*, 1994). Even though the concentrations of Hsps increase after heat stress or general cell stress, they are essential for cell growth under normal conditions (Morimoto *et al.*, 1994). Heat shock proteins prevent accumulation of stress-damaged proteins in two

ways: some restore the native structures of misfolded proteins; others facilitate the degradation of damaged proteins by presenting them for proteolytic degradation (Boguski *et al.*, 1990).

Although sequence homologies between Hsp counterparts of different organisms are high, there is no obvious sequence homology between Hsps of different families (Jindal, 1996). The ability to recognise non-native conformations of proteins is a common feature among the Hsps. Majority of the Hsps recognise hydrophobic regions that are exposed on the surfaces of the unfolded proteins, either nascent or denatured, and facilitate refolding by secluding such proteins, thereby preventing aggregation (Beckmann *et al.*, 1992).

1.2.3.1 Heat shock protein 70 (Hsp70)

The 70 kDa heat shock proteins constitute a large family of highly conserved chaperones that assist folding processes including *de novo* folding of proteins, prevention of aggregation and refolding of stress denatured proteins, disaggregation of protein aggregates, translocation and control of activity and stability of regulatory proteins and degradation of unfolded proteins (Bukau and Horwich, 1998; Mayer *et al.*, 2001; Hartl and Hayer-Hartl, 2002). There are two major cytosolic forms of Hsp70, the constitutive heat shock cognate protein 70 (Hsc70) and the stress-inducible heat shock protein 70 (Hsp70) (Hartl, 1996). Hsp70 is present in multiple compartments of most cells (Gething and Sambrook, 1992; Craig *et al.*, 1993). In humans, the Hsp70 multi-gene family includes the cytosolic and nuclear localized Hsc70 and Hsp70, endoplasmic reticulum localized Grp78 (Bip) and mitochondrial mtHsp75 (Bhattacharya *et al.*, 1995; Moro *et al.*, 2002). The protein has been widely studied and extensively characterized in *Escherichia coli* (*E. coli*) (DnaK). The Hsp70 chaperones are composed of two domains. The more highly conserved N-terminal ATPase domain of 45 kDa (Rudiger *et al.*, 1997), which binds to and hydrolyses ATP and the more variable C-terminal domain that is further divided into a polypeptide-binding subdomain ~ 15 kDa (Wang *et al.*, 1993) and a C-terminal subdomain of 10 kDa with binding sites for certain co-chaperones, e.g. stress-inducible protein 1 (STI1) (Chen and Smith, 1998).

The crystal structures of bovine and human Hsc70 ATPase domains (Figure 1.1) have been determined (Flaherty *et al.*, 1990; Siriam *et al.*, 1997). Also, the ATPase domain of DnaK in complex with its dimeric cofactor GrpE has been determined (Harrison *et al.*, 1997). Zhu *et al* (1996) crystallized and determined the structure of the substrate-binding domain of DnaK in complex with a substrate peptide, NRLLLTG (Figure 1.1). The structural similarity of hATPase (human) and bATPase (bovine) and the sequence similarity within the Hsp70 chaperone family (>50% amino acid identity) suggest a universal mechanism of ATP hydrolysis among all Hsp70 molecular chaperones (Siriam *et al.*, 1997). The Hsp70 chaperones exhibit a high binding affinity for ATP and a weak ATPase activity. However, ADP binds to Hsc70 with 5-fold higher affinity than does ATP. Through a cycle of ATP binding, hydrolysis, and nucleotide exchange, denatured proteins are alternately bound to Hsc/Hsp70 and released to effect protein folding (Hartl, 1996).

In the ATP-bound state, Hsp70 binds and releases substrates rapidly, whereas the ADP-bound form binds and releases slowly. In DnaK, cycling between its different nucleotide-bound states is regulated by two cofactors, DnaJ and GrpE (Harrison *et al.*, 1997; Bukau and Horwich, 1998). The 41 kDa DnaJ protein is itself a chaperone, which can bind to unfolded polypeptides and prevent their aggregation (Langer *et al.*, 1992; Szabo *et al.*, 1996). DnaJ binds to DnaK and stimulates its ATPase hydrolysis, generating the ADP-bound state of DnaK, which interacts stably with the polypeptide substrate (Liberek *et al.*, 1991; Laufen *et al.*, 1999; Suh *et al*, 1999). The 23 kDa GrpE protein acts as a nucleotide exchange factor; it binds to the ATPase domain of DnaK and, by distorting the nucleotide-binding pocket, induces the release of bound ADP (Harrison *et al.*, 1997). Re-binding of ATP triggers dissociation of the DnaK-substrate complex and the protein is ready for another round of ATPase cycle.

One exception to this generally accepted view is HscC, the *E. coli* member of a novel subfamily of specialized Hsp70 chaperones (Kluck *et al.*, 2002). HscC has a higher ATPase activity than DnaK, which is not affected by the nucleotide exchange factor, GrpE. In addition, its ATPase activity is stimulated 8-fold by Dj1C, a DnaJ protein with putative transmembrane domain but not by other DnaJ proteins (Kluck *et al.*, 2002). HscC has been shown not to have a general chaperone activity (Kluck *et al.*, 2002).

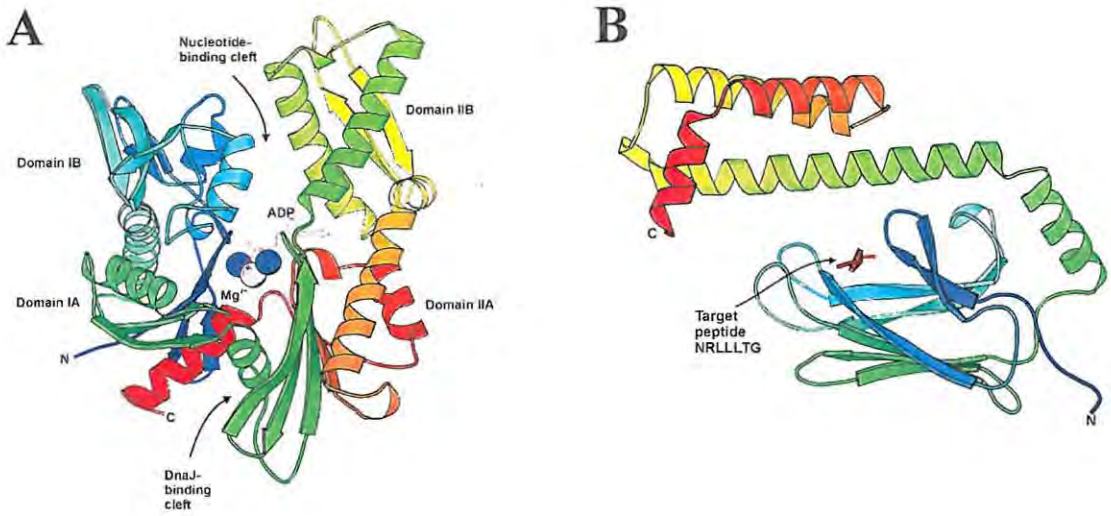

Figure 1.1: Ribbon representations of the N-terminal ATPase and the C-terminal substrate-binding domains of heat shock protein 70
A: Bovine Hsc70 ATPase domain in complex with adenosine 5' diphosphate (PDB code: 3HSC; Flaherty *et al.*, 1990) and **B:** DnaK substrate binding domain with a substrate peptide NRLLLTG (PDB code: 1DKX; Zhu *et al.*, 1996). Figures were drawn with MOLSCRIPT (Kraulis, 1991)

1.2.3.2 Heat shock protein 90 (Hsp90)

The 90 kDa heat shock protein is one of the most abundant cytosolic proteins in eukaryotes, constituting up to 2% of the cellular protein even when the cell is not under stress (Buchner, 1999). Its expression level increases up to ten folds in response to stress (Yonehara *et al.*, 1996; Buchner, 1999). Hsp90 is necessary for viability in yeast (Picard *et al.*, 1990; Parsell and Lindquist, 1993), and for proper folding, processing, and function of proteins involved in several transduction pathways. Hsp90 is distinguished from other chaperones in that most of its known substrates are signal transduction proteins such as steroid receptors (SHRs) e.g. glucocorticoid receptor (GR) and progesterone receptor (PR), the Raf serine kinases, cyclin-dependent kinase 4 (cdk4) and other cell cycle kinases (Chen *et al.*, 1996; Dittmar *et al.*, 1996; 1997a; 1997b; Buchner, 1999; Young *et al.*, 2001; Basso *et al.*, 2002). Other Hsp90 substrates include kinases, p53, luciferase, tubulin, nitric oxide synthase, β-galactosidase, and tumor necrosis factor (Buchner, 1999). Rutherford and Lindquist (1998) reported that that in *Drosophila*, when Hsp90 is mutated or pharmacologically impaired, phenotypic variation affecting nearly any adult structure was produced, with specific variants depending on the genetic background and occurring both in laboratory strains and in wild populations. This implies that Hsp90 acts as a capacitor

to buffer genetic morphological variations (Queitsch *et al.*, 2002). The highly conserved Hsp90 chaperone family includes the Hsp90 of the eukaryotic cytosol (both Hsp90α and Hsp90β, corresponding to major and minor isoforms), Hsp86 and Hsp84 in mice, Hsp83 in *Drosophila*, Hsc82 and Hsp82 in yeast, HtpG in the bacterial cytosol,

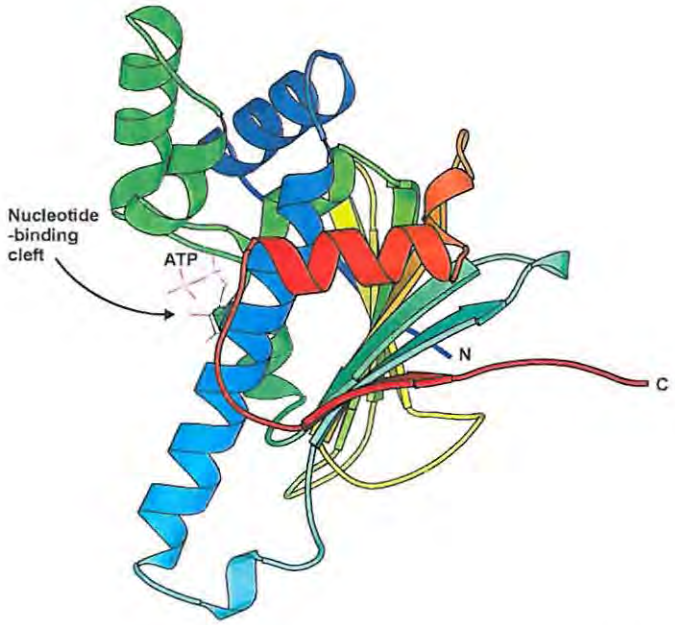

Figure 1.2: Ribbon representation of the N-terminal ATPase domain of Human Hsp90.
The figure was drawn with MOLSCRIPT (Kraulis, 1991) using the co-ordinates of the human Hsp90 ATPase domain (PDB code: 1AMW).

Grp94/gp96 in the ER and Hsp75/TRAP1 in the mitochondrial matrix (Czar *et al.*, 1997; Buchner, 1999; Argon and Simen, 1999; Felts *et al.*, 2000; Thomas and Baneyx, 2000; Young *et al.*, 2001; Basso *et al.*, 2002). Hsp90 is a constitutive elongated homodimer with its main intersubunit contacts within the C-terminal 190 residues (Nemoto *et al.*, 1995). Electron microscopy and antibody studies suggest that the C-terminal parts of the protein meet in the middle and that the N-terminal domains point in opposite directions (Maruya *et al.*, 1999). The three-dimensional structures of N-terminal fragments of both yeast and human Hsp90 (Figure 1.2) have been solved by X-ray crystallography (Prodromou *et al.*, 1997a; 1997b; Stebbins *et al.*, 1997). The N-terminal domain consists of an eight-stranded antiparallel β-sheet and nine α-helices, forming an α/β sandwich (Figure 1.2). The highly conserved 25 kDa N-terminal domain of Hsp90 is the binding site for ATP and for geldanamycin.

Geldanamycin inhibits the ATPase activity of Hsp90 by competitively binding to the nucleotide-binding cleft (Whitesell *et al.*, 1994; Panaretou *et al.*, 1998). A charged sequence of about 36 amino acids separates the N-terminal domain from the conserved but flexible 35 kDa middle domain and the 12 kDa C-terminal domain.

Both N- and C-terminal domains have been implicated in binding of substrate polypeptides (Young *et al.*, 1997; Scheibel *et al.*, 1998; 1999). The ATPase cycle of Hsp90 has not been fully elucidated. The ATP-bound state of Hsp90 binds stably to the substrate polypeptides. ATP binding is believed to induce inter-subunit contacts between the N-terminal nucleotide-binding domains in the homodimer to form a so-called "molecular clamp" to which the substrate binds (Dutta and Inouye, 2000; Prodromou *et al.*, 2000). The release of substrate is achieved by ATP hydrolysis, which causes a series of conformational changes in the protein or opens the N-terminal clamp (Young and Hartl, 2000). The turnover rate of the enzyme is mainly controlled by intermolecular interactions between the N terminal domains (Richter *et al.*, 2002).

Recently, it has been proposed based on experimental evidence that a second ATP-binding site exists in the C-terminal domain of Hsp90 (Csaba *et al.*, 2002). The protein, p23, seems to play a key role in regulating the ATPase cycle of Hsp90 by binding to the ATP-bound state of Hsp90, hence enhancing substrate release (Young and Hartl, 2000; Sullivan *et al.*, 2002). Other proteins that regulate the chaperoning activity of Hsp90 include cell division control protein 37 (Cdc37), *Caenorhabditis elegans UNC*45, Hsp70/Hsp90 organising protein (Hop), the FK506/rapamycin binding proteins (FKBP51 and FKBP52), cyclophilin-40 (CyP40), protein phosphatase 5 (PP5), translocator outer membrane protein 70 (Tom70), cyclophilin seven suppressor (Cns1), aryl hydrocarbon receptor-interacting protein (AIP), C-terminus of Hsc70-interacting protein (CHIP) e.t.c. Most of these so-called co-chaperones contain a protein motif called the tetratricopeptide repeat motif, which is discussed in detail in section 1.7.

1.3 Cooperation among different chaperone systems

Many newly translated or translocated proteins interact with more than one class of chaperone (reviewed in Frydman, 2001). There is ample compelling evidence which show that distinct chaperone systems cooperate to form defined chaperone pathways. The first indication that different chaperone systems might cooperate in a folding reaction was provided by studies on the import of proteins into the mitochondria (Hohfeld and Hartl, 1994). Firefly luciferase imported into mitochondria interacts sequentially with Hsp70 and then Hsp60 (Heyrovska *et al.*, 1998). This mechanism involves transient interaction of the unfolded translocating polypeptide with mitochondrial Hsp70 and the chaperonins. How is the polypeptide transferred between the chaperone players? There are two schools of thought.

First, the cooperation of different chaperones might involve the release of a previously chaperone-bound polypeptide into the cellular milieu in a non-native conformation that is recognised by another chaperone system. Second, the cooperating chaperones might interact physically and form a multi-functional chaperone complex, which could mediate the folding of the polypeptide substrate without its exposure to the surrounding cytosol (Frydman and Hohfeld, 1997). Experimental evidence seems to support the latter model (Frydman *et al.*, 1994; Frydman and Hartl, 1996). For example, analysis of the transit of newly made polypeptides through *E. coli* chaperones indicated that overexpression of GroEL increases the flux of substrates through DnaK if GroEL is downstream of DnaK in the folding pathway (Teter *et al*, 1999). Also, in eukaryotes, TCP-1 ring complex protein (TriC), and Hsp70 associate *in vivo* and this suggests that the proteins co-operate functionally (Feldman *et al.*, 1999). In view of these examples, it appears that in the cell, polypeptides are transferred from holding chaperones e.g. Hsp70, which prevent aggregation, to the chaperones that recognise more compact structures such as the chaperonins or the Hsp90 system (reviewed in Frydman, 2001).

1.3.1 Hsp90-dependent activation of steroid hormone receptor

Extensive studies have been done on the Hsp70/Hsp90-dependent multichaperone complex involved in the folding of steroid hormone receptors (Pratt, 1990; Smith and Toft, 1993; Pratt, 1993; Pratt and Toft, 1997; Pratt, 1998; reviewed in Buchner, 1999;

Caplan, 1999; Cheung and Smith, 2000; Pearl and Prodromou, 2000; Young *et al.*, 2001; Frydman, 2001). Steroid hormone receptors must associate with Hsp90 to adopt the conformation competent for hormone binding (reviewed in Caplan, 1999; Cheung and Smith, 2000; Young *et al.*, 2001). Genetic evidence and *in vitro* reconstitution experiments indicate that Hsp90 function requires its sequential interaction with different subsets of cofactors some of which are chaperone themselves, e.g. Hsp70 and Hsp40 (Johnson and Toft, 1994; Kimura *et al.*, 1995; Dey *et al.*, 1996; Dittmar and Pratt, 1997; Johnson *et al.*, 1998; Morishima *et al.*, 2000; Johnson and Craig, 2000). In their review, Cheung and Smith (2000) reported that the assembly pathway for steroid receptor-chaperone complexes could involve at least 10 chaperone components. Five of these proteins are obligatory *in vitro* for maturation of hormone binding ability by GR. Three of the obligatory chaperones are the constitutively expressed isoforms of Hsp70, Hsp40 and Hsp90.

In addition, two co-chaperones are required for minimal *in vitro* hormone-binding assays; the Hsp90-binding protein p23 and the Hsp70/Hsp90 organising protein (Hop; also known as p60 or extendin in mammals and STI1 in yeast), which acts as an adaptor in bringing Hsp70 and Hsp90 together in the multichaperone complex (Prapapanich *et al.*, 1996; Chen *et al.*, 1996; Chen and Smith, 1998). In addition, Hsp70-interacting protein (Hip) (Hohfeld *et al.*, 1995; Hohfeld and Frydman, 1997) and BCL-2 binding athanogene-1 protein (BAG-1) (Takayama *et al.*, 1995) have been identified as part of the complex *in vivo*, but their roles are not essential *in vitro* (Prapapanich *et al.*, 1998; Kanelakis *et al*, 1999; Cheung and Smith, 2000). In addition, there are four additional proteins that have been recovered in native receptor complexes but which are not essential in minimal *in vitro* hormone-binding assays; these are FKBP51, FKBP52, CyP40 and PP5 (Cheung and Smith, 2000).

Mechanistically, ATP is required for assembly of receptor complexes, especially in the formation of the Hsp70-dependent early complex and Hsp90-dependent intermediate complex (Figure 1.3) (reviewed in Cheung and Smith, 2000; Frydman, 2001). In complete reticulocyte lysate, free receptor initially associates with Hsp40 and Hsp70 in an ATP-dependent manner. Recent experimental evidence showed that the actual first step is the binding of the receptor to Hsp40 (Hernandez *et al.*, 2002). This step occurs rapidly and does not require ATP (Hernandez *et al.*, 2002). Hsp40

then transfers the PR or GR substrate to Hsp70 and stimulates Hsp70-ATP hydrolysis to generate the ADP-bound form of Hsp70 necessary for both Hop and Hip to bind. *In vivo*, a steroid hormone receptor may enter the maturation pathway through a cotranslational or posttranslational interaction with Hsp70, which may induce conformational changes of the receptor molecule necessary for its subsequent interaction by Hsp90. Substrate transfer from Hsp70 to Hsp90 is facilitated by the action of Hop. Since Hop binds independently to Hsp90, it may form a pre-existing complex with the ADP-form of Hsp90 (Figure 1.3). It then functions as an adaptor in binding Hsp70 to promote the formation of an Hsp70-Hop-Hsp90 complex, thus mediating the transfer of the receptor to Hsp90 (reviewed in Cheung and Smith, 2000; Frydman, 2001). Hop's interaction with both Hsp70 and Hsp90 is mediated by a structural protein-protein interaction motif, the tetratricopeptide repeat (Das *et al.*, 1998; Young *et al.*, 1998; Liu *et al.*, 1999; van der Spuy *et al.*, 2000; Scheufler *et al.*, 2000; Brinker *et al.*, 2001).

At the final stage of receptor maturation, Hsp90 becomes directly associated with the receptor ligand-binding domain in the presence of an additional set of proteins comprising p23 and different peptidylpropyl isomerases (Figure 1.3) (reviewed in Cheung and Smith, 2000). Even though the functions of the Hsp90-associated peptidylpropyl isomerases have not been fully elucidated, they may induce additional conformational changes of the receptor molecule at this stage (Prapapanich *et al.*, 1996; Ratajczak and Carrello, 1996). In like manner, the interactions of the immunophilins, Hip, and CyP40 with either Hsp70 or Hsp90 are mediated by their TPR motifs. Tyrosine kinases, such as src, also recruit an additional cofactor, Cdc37 (Kimura, 1997). Recently, it has been shown using yeast extracts that Cdc37 and STI1 interact both physically and genetically (Abbas-Terki *et al.*, 2002), though the function of this interaction *in vivo* is not clear. In the functionally matured receptor complex, Hsp90-associated Hop has been replaced by one of the immunophilins (reviewed in Cheung and Smith, 2000). The p23 associates with Hsp90 only in its ATP-bound state (Grenert *et al.*, 1999; Sullivan *et al.*, 2002) and stimulates the release of the receptor from Hsp90 upon ATP hydrolysis (Young and Hartl, 2000; Sullivan *et al.*, 2002).

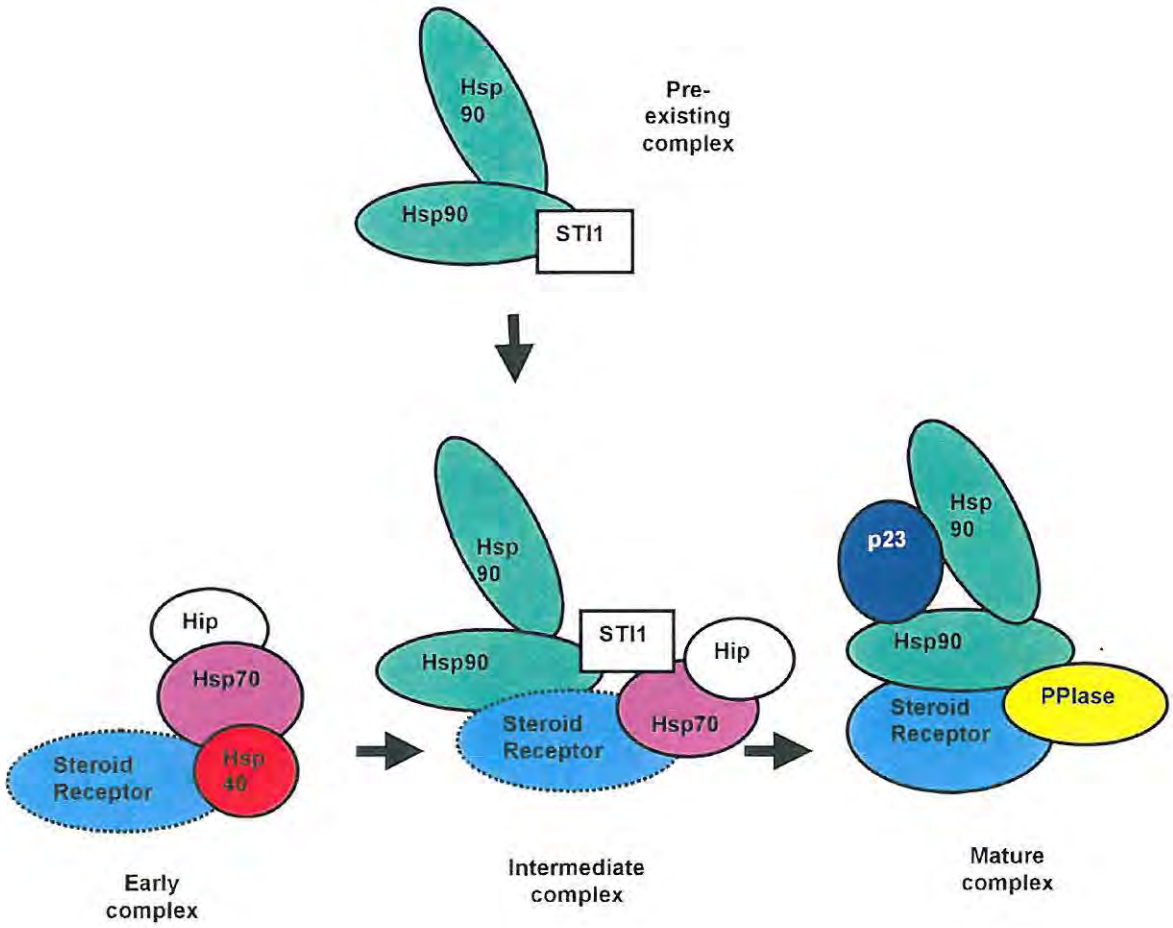

Figure 1.3: Schematic representation of the chaperone-mediated assembly and functional maturation of the steroid hormone receptor.
The early complex is an Hsp40-mediated association of Hsp70 with the steroid receptor. The intermediate complex contains Hsp70, Hip, Hsp90 and Hop. Hop brings Hsp70 and Hsp90 together. The mature complex contains Hsp90, p23 and immunophilins. The mature complex is capable of binding to steroid hormone. Hormone-binding incompetent steroid receptor is represented as broken circle. The mature, hormone-binding competent steroid receptor is shown as solid circle.

1.4 Stress-inducible protein 1 family of co-chaperones

In 1989, Nicolet and Craig first reported the presence of a stress-inducible gene in the yeast, *Saccharomyces cerevisiae* and designated it as STI1, for stress inducible. They observed that cells carrying a disruption mutation of the STI1 (ySTI1 for yeast STI1) gene grew normally at 30°C but showed impaired growth at higher and lower temperatures. Overexpression of the gene resulted in substantial trans-activation of SSA4 promoter-reporter gene fusions, indicating that STI1 might play a role in mediating the heat shock response of some Hsp70 genes. The STI1 open reading frame of approximately 2 kilobases (kb) was predicted to encode a 66-kilodalton

(kDa) protein. The presence of isoforms of the STI1 protein, with different isoelectric points indicated the possibility of post-translational modification(s) of the protein. STI1 was found to be responsive to a number of different stresses. For instance, an increase in temperature from 23^0C to 39^0C or addition of the amino acid analogue canavanine both resulted in a 10-fold increase in the levels of STI1 mRNA in yeast (Nicolet and Craig, 1989). Also, a 6-fold increase in STI1 mRNA level was detected as the cells progressed into the stationary phase of the cell cycle. *In vivo* analysis showed that deletion of STI1 in yeast resulted in the impairment of the glucocorticoid receptor hormonal response and the activity of Hsp90 substrate, v-Src (Chang *et al.*, 1997). Overexpression of ySTI1 has been reported to confer resistance to quinoline ring-containing antimalarial drugs in yeasts (Delling *et al.*, 1998).

The human stress-inducible protein 1 (hSTI1, also known as p60 or Hop) was identified from SV40-transformed MRC-5 fibroblasts and shares 42 % homology with the yeast STI1 (Honore *et al.*, 1992). The human homologue of STI1 co-migrated with the isoelectric focusing sample spot protein number 3521, and hence designated IEF SSP 3521. The 2.1 kb cDNA fragment was found to encode a protein of 543 amino acids and a molecular mass of 62.2 kDa. In normal MRC-5 fibroblasts, two charge variants of IEF SSP 3521 were detected. In SV40-transformed MRC-5 fibroblasts however, up to five charge variants were detected of which the acidic forms were phosphorylated. This phosphorylation indicated a potential mechanism of regulation of IEF SSP 3521 within the cell. Increase in temperature from 37^0C to 42^0C led to approximately 2-fold increase in the levels of IEF SSP 3521 protein in SV40-transformed MRC-5 fibroblasts and human embryonic fibroblasts (Celis *et al.*, 1990) compared to the untransformed cells. However, the levels of IEF SSP 3521 mRNA were increased several folds in SV40-transformed MRC-5 fibroblast cells. Immuno-fluorescence analysis localized hSTI1 in the nucleus of transformed MRC-5 cells, whereas the same protein was found in the Golgi apparatus and small vesicles in normal cells (Honore *et al.*, 1992).

Blatch *et al* (1997) isolated STI1 homologue from mouse M27 Lewis lung carcinoma cDNA expression library, and termed it mSTI1, for mouse STI1. This protein showed 97 % amino acid identity to hSTI1, 42 % identity to ySTI1, 44 % identity to *Glycine max* STI1 (gmSTI1), and 32 % identity to *Leishmania donovanii* STI1 (lmSTI1)

(Blatch *et al.*, 1997). The predicted open reading frame encoded a protein of 543 amino acids with a molecular size of approximately 63 kDa. Elevated temperature significantly increased the levels of mSTI1 transcript, but had no effect on the steady-state levels of mSTI1 protein in NIH3T3 mouse fibroblast whole cell extracts (Lässle *et al.*, 1997). In addition, increased temperature altered the isoform composition of mSTI1 favouring a more acidic isoform (phosphorylated) and the appearance of a basic isoform of the protein (Lässle *et al.*, 1997). Hence the heat stress mediated a post-translational modification of the protein. Using immuno-fluorescence, Lässle *et al* (1997) localized mSTI1 predominantly in the cytoplasm with a sub-population in the nucleus. Recently, Zanata *et al* (2002) reported that mSTI1 was a prion-binding protein that associated with the cell membrane. In addition, they showed that prion proteins (PrP^{c}) interaction with either the full-length mSTI1 or its prion-binding domain (residues 230 – 245) induced neuroprotective signals that rescued cells from apoptosis in mice.

Other homologues have been identified in human, mouse, rat, yeast, plants and several parasites (See Figure 1.4 for a sequence alignment of STI1 homologues and Appendix C for a list of homologues of STI1). An essential homologue of STI1 was identified in yeast and shown to bind to both Hsp90 and the CyP40 homologue, cyclophilin seven suppressor 1 (Cpr7) (Dolinski *et al.*, 1998). Using lysates from chick, human, rat, rabbit and *Xenopus* tissues, Smith *et al* (1993) showed that STI1 co-purified with both Hsp90 and Hsp70. A major structural feature found in STI1 proteins is the tetratricopeptide repeat (TPR) motif.

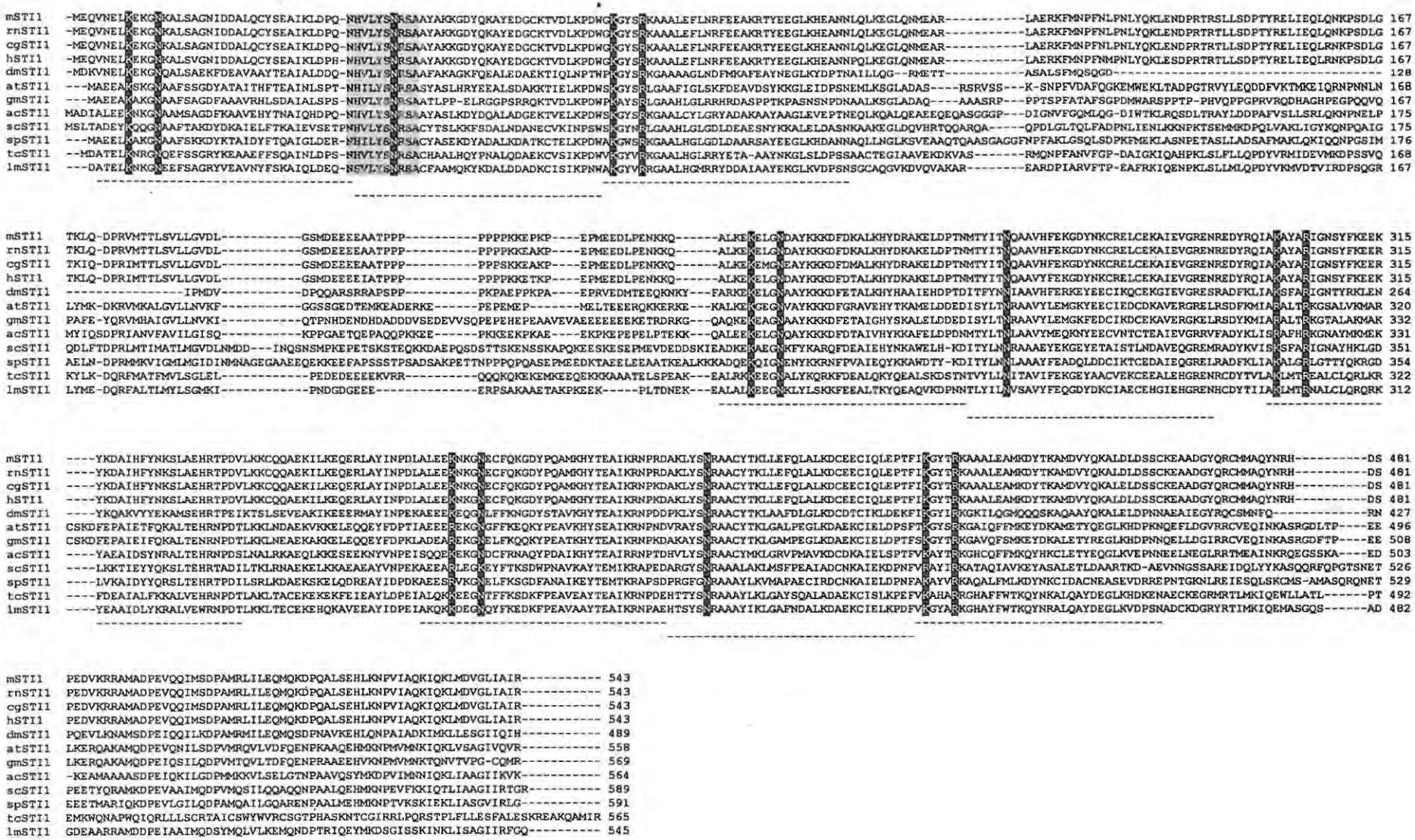

Figure 1.4: Sequence alignment of STI1 homologues.
m, *Mus musculus* (AAC53267.1); rn, *Rattus norvegicus* (CAA75351.1); cg, *Cricetulus griseus* (AAB94760.1); h, *Homo sapiens* (AAA58682.1); dm, *Drosophila melanogaster* (AAC12945.1); at, *Arabidopsis thaliana* (CAB45987.1); gm, *Glycine max* (S56658); ac, *Achantamoeba castellanii* (AAB49720); sc, *Saccharomyces cerevisiae* (CAA60743.1); sp, *Schizosaccharomyces pombe* (CAB39910.1); tc, *Trypanosoma cruzi* (AAC97378.1); lm, *Leishmania major* (AAB37318). A highly conserved block of amino acids is shown in grey background. Residues in black background are involved in the interaction of STI1 proteins with Hsp70 and Hsp90. A strictly conserved tryptophan residue is indicated by asterisk (*). Dashed lines represent the extent of each TPR motif comprising two α-helices, based on the crystal structures of hSTI1 (Hop) (Scheufler, *et al.*, 2000). The alignment was generated using CLUSTAL W (Thompson *et al.*, 1994)

1.5 The Tetratricopeptide repeat motif

1.5.1 Tetratricopeptide repeat-containing proteins

Sikorski *et al* (1990) first reported the tetratricopeptide repeat (TPR) motif, when a database search for amino acid sequences similar to the *Saccharomyces cerevisiae* Cdc2 gene revealed statistically significant similarities to the products of five genes: *nuc*2^{+} from *Schizosaccharomyces pombe*, *bim*A from *Aspergillus nidulans*, and Cdc16, *SK*13 and *Ssn*6 from *Saccharomyces cerevisiae*. Further analysis revealed that the TPR motif is a degenerate 34 amino acid sequence occurring in multiple copies in proteins and form scaffolds to mediate a variety of different protein-protein interactions (Sikorski *et al.*, 1990; Das *et al.*, 1998; Blatch and Lässle, 1999). Most TPR-containing proteins are associated with multi-protein complexes (Blatch and Lässle, 1999).

Majority of the TPR-containing proteins participate in cell cycle control, transcription, protein translocation, phosphate turnover, signal transduction, and protein folding. TPR-containing proteins are found in bacteria, cyanobacteria, yeast and other fungi, insects, plants, and animals, and in various subcellular locations, such as the cytosol, nucleus, mitochondria, chloroplasts, and peroxisomes (Lamb *et al.*, 1995; Blatch and Lässle, 1999). The number of TPR motifs varies in different proteins, and there is no preferential positioning along the primary sequence of the protein (Blatch and Lässle, 1999). Studies have shown that while the TPR motif may be sufficient for protein-protein interactions in some proteins (Liu *et al.*, 1999), others may require the participation of other structural regions such as the J domain (Gale *et al.*, 1996) and the SH2-binding domain (Malek *et al.*, 1996), or binding groups (Ratajczak and Carrello, 1996; Irmer and Hohfeld, 1997).

van der Spuy *et al* (2000) have classified TPR proteins involved in chaperone-co-chaperone interactions into two different groups: class I which does not require extensive TPR flanking regions in interacting with heat shock proteins e.g. murine STI1 (mSTI1; Blatch *et al.*, 1997), colon cancer antigen 7 (NY-CO-7; Scanlan *et al.*, 1998), tetratricopeptide repeat domain 1 (TPR1; Murthy *et al.*, 1996), human small glutamine-rich protein (hSGT; Kordes *et al.*, 1998); and class II which requires extensive TPR flanking regions (more than 20 amino acid residues) e.g.

immunophilins, Hsc70-interacting protein (Hip; Hohfeld *et al.*, 1995) and Protein phosphatase 5 (PP5; Chen *et al.*, 1994). Apart from molecular chaperone complexes, other complexes that involve TPR proteins include: the anaphase-promoting complex (Irniger *et al.*, 1995), transcription repression complex (Tzamarias and Struhl, 1995), nucleotide excision repair (NER) complex (Nakatsu *et al.*, 2000), and protein import complex (Dodt *et al.*, 1995). Among the Hsp70- interacting TPR proteins are, ySTI1 (Nicolet and Craig, 1989), hSTI1 (Honore *et al.*, 1992), mSTI1 (Blatch *et al.*, 1997), SGT (Kordes *et al.*, 1998), TPR1, TPR2, (Murthy *et al.*, 1996), NY-CO-7 (Scanlan *et al.*, 1998), CHIP (Ballinger *et al.*, 1999), and Hip (Hohfeld *et al.*, 1995). TPR proteins that interact with Hsp90 include the immunophilins, PP5 (Chen *et al.*, 1994), mSTI1 (Blatch *et al.*, 1997), and hSTI1 (Honore *et al.*, 1992).

1.5.2 Primary structure of the TPR motif

The TPR is a degenerate 34-amino acid repeat motif often found in tandem arrays, although one or more repeats separated from such arrays do occur (Lamb *et al,*. 1995). In general, comparison of TPR motifs from various proteins reveals a defined conservation of some amino acids in terms of size, hydrophobicity and spacing especially at positions 4 (W/L/F), 7 (L/I/M), 8 (G/A/S), 11/12 (Y/L/F), 20 (A/S/E), 24 (F/Y/L), 27(A/S/L), and 32 (P/K/E) (Figure 1.5) (Sikorski *et al.*, 1990; Goebl and Yanagida, 1991; Das *et al.*, 1998; Blatch and Lässle, 1999). Sequence conservation is limited to the so-called TPR consensus residues in functionally diverse TPR motifs and in particular at positions 8, 20, 24 and 27. However, comparison of functionally equivalent TPR motifs reveals conservation outside the signature residues and this suggests functional specialisation of the motif (Blatch and Lässle, 1999). For instance, alignment of the TPR motifs responsible for mediating interactions with Hsp70 (e.g. those found in Hop, TPR1, hSGT and NY-CO-7), revealed a number of small, hydrophobic, and charged residues that are conserved outside the eight consensus residues (Figure 1.5). Furthermore, it was proposed that some of these residues, especially the charged ones, were potentially important in mediating interactions of the TPR-containing proteins with Hsp90 Blatch and Lässle, 1999).

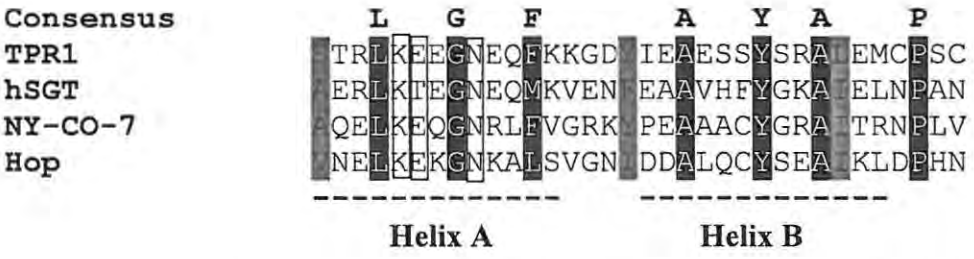

Figure 1.5: Sequence alignment of the first tetratricopeptide repeat motifs of Hsp70-binding proteins.
TPR1; (Tetratricopeptide repeat 1; NP_003305), hSGT; (human small glutamine-rich protein; NP_003012), NY-CO-7; (colon cancer antigen 7; AAC18038), Hop; (Hsp70/Hsp90 organising protein; AAA58682.1). The TPR consensus residues are shown in black background. The boxed and grey residues represent conserved charged and hydrophobic residues respectively, outside the consensus. The broken lines represent the extent of helices A and B of the TPR motif.

1.5.3 Secondary and tertiary structures of the TPR motif

Circular dichroism, limited proteolysis of the repeats, and model fitting indicated that TPR motifs are approximately 50 % α-helical structures connected by protease-sensitive hinges (Hirano *et al.*, 1990). Crystallographic studies have confirmed earlier propositions that each TPR motif forms two α-helical domains A and B, in which domain A spans the consensus residues 4, 7, 8, 10 and 11 while domain B spans the consensus residues 20, 24 and 27 (Das *et al.*, 1998; Lapouge *et al*, 2000; Scheufler *et al.*, 2000). Analysis of the PP5 TPR motif has provided an explanation for the consensus sequence pattern of small and large hydrophobic residues (Das *et al.*, 1998). The small hydrophobic residues 8, 20 and 27 are located at the position of closest contact between the A and B α- helices of a TPR. The large hydrophobic residues occupy positions 4, 11 and 24 and form the interfaces between adjacent α-helices. Position 32 is commonly a hinge-inducing proline residue. Thus the consensus residues may be critical for structural integrity of the TPR domain by ensuring correct intra and inter-helix packing (Figure 1.6, A and B).

Recently however, an unusual TPR motif conformation has been reported in peroxin PEX5 from *Trypanosoma brucei* in which the two helices form a single continuous helix rather than the generally accepted antiparallel helix hairpin (Kumar *et al.*, 2001). In PP5 N-terminal domain (Das *et al.*, 1998), the three TPR motifs are structurally identical and each is composed of a pair of antiparallel α-helices, A and B. The

packing of the helices within a tandem array of TPR motifs occurs such that the sequentially adjacent α-helices are antiparallel and each α-helix shares two immediate neighbours. The amphipathic α-helices are related by an angle of 24^0 and bundled together to form a globular domain with an amphipathic groove or channel on one face (Das *et al.*, 1998). The inner surface of the groove is formed mainly by the side chains of the amino acids in the helix A of each TPR motif, while the outer part is formed by amino acids from both helices A and B (Figure 1.6C). Das *et al* (1998) have proposed that tandem TPR motifs fold into a right-handed super-helical structure with a helical repeat of approximately seven TPR motifs, a pitch of 60 Å and a width of 42 Å. Five to six TPR motifs could accommodate an α-helix of a target protein.

TPRs come in many different ways that form distinct sequence subfamilies. These subfamilies include repeats in kinesin light chains (Ginhart and Goldstein, 1996), SNAP secretory proteins (Ordway *et al.*, 1994), clathrin heavy chains, and bacterial aspartyl-phosphate phosphatases (Andrade *et al.*, 2000). In depth studies of helical repeats showed that repeat families, such as HAT repeats (Preker and Keller, 1998), protein farnesyl transferase α-subunit repeats (Boguski *et al.*, 1992) and Sel-1 repeats are distantly homologous to the TPR motif (Andrade *et al.*, 2000). Other protein interaction motifs that resemble the TPR have been reported such as the paired amphipathic helix (PAH) motif (Wang and Stillman, 1993), the helix-loop-helix (HLH) (Murre *et al.*, 1998) and the PPR motif (Small and Peeters, 2000).

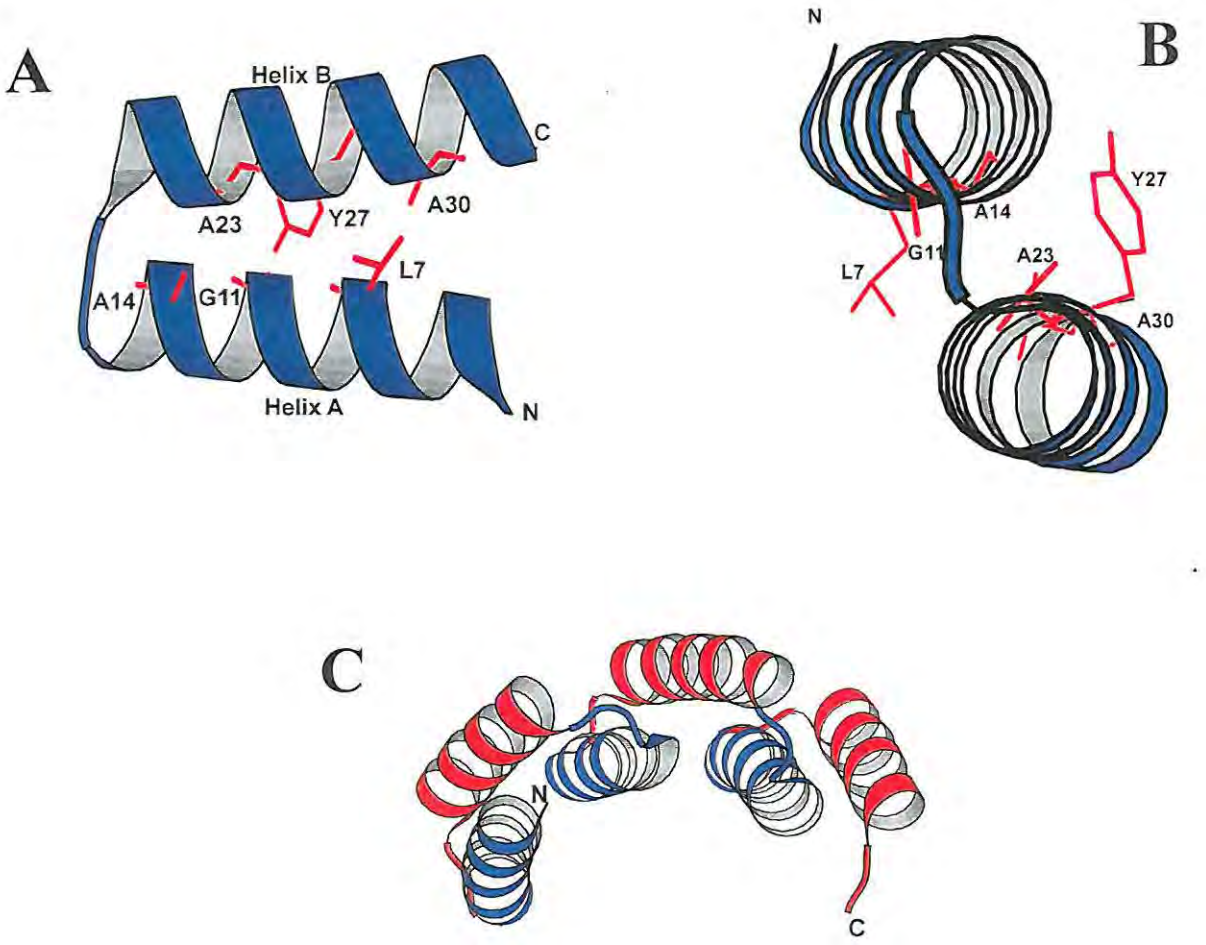

Figure 1.6: Ribbon representations of the TPR domains of Hop.
A and B: Side view and end-on view respectively, of the first TPR motif of the N-terminal TPR1 domain of Hop to show the positions and roles of the TPR consensus residues in the intra- and inter helix packing. **C:** View parallel to the helical axis of the first central TPR2A domain of Hop showing the inner surface of the TPR groove formed by helices A (blue) of the motifs. The residues are labeled using the single letter code, and the numbering refers to the position of the residues in Hop primary sequence. The figures were drawn using MOLSCRIPT (Kraulis, 1991).

1.6 Mechanism of TPR-mediated protein-protein interactions

Experimental evidence suggest that charged residues, especially basic residues, that project into the groove of the TPR domains of proteins that interact with Hsp70 and/or Hsp90, (e.g. PP5, Hop/mSTI1, CyP40), may be critical for binding to these molecular chaperones (Russell *et al.*, 1999; Scheufler *et al.*, 2000; Brinker *et al.*, 2002; Ward *et al*, 2002). These charged residues form part of a binding groove and appear to be highly conserved among the different Hsp70/Hsp90 interacting proteins (Russell *et*

al., 1999; Bell and Poland, 2000; Brinker *et al.*, 2002; Ward *et al.*, 2002). In other complexes of TPR-containing proteins, there are slight modifications to this 'binding groove' model, such as in the Rac.GTP/$p67^{phox}$ complex (Lapouge *et al.*, 2000). The $p67^{phox}$ TPR fragment contains nine α-helices, eight of which form four motifs. Each repeat folds into two antiparallel α-helices, which pack together in a similar manner to that of the TPR domain structures of Hop and PP5 (Das *et al.*, 1998; Scheufler *et al.*, 2000). There is a C-terminal helix (helix C) that packs against helix A of the fourth TPR motif. The nine-helical bundle exhibits the canonical right-handed super-helical twist generating a groove on the A helix face of the TPR domain. Interestingly, the 18 ordered residues C-terminal to helix C in an extended conformation occupy this groove. In addition, the inside of the groove is hydrophobic and formation of the intramolecular complex with the $p67^{phox}$ TPR C terminus buries 2742 Å of solvent-accessible surface, 75 % of which is contributed by non-polar side chains. Notably, the binding surface presented by $p67^{phox}$ TPR to Rac is confined to one face of the TPR domain and is created by the β-hairpin insertion (an insertion of 20 amino acids between the third and fourth repeats that form two short antiparallel β strands and a 3_{10} helical turn) and the loops that connect TPR1 with TPR2, and TPR2 with TPR3. No part of Rac appears to dock in the TPR groove of $p67^{phox}$ TPR.

Similar observations have been reported in the TPR-mediated interaction of the repressor proteins, Ssn6 and Tup1 (Gounalaki *et al.*, 2000). Using random mutagenesis and molecular modeling, Gounalaki *et al* (2000) showed that the interaction of Ssn6, via its TPR domain, with Tup1 protein is mainly hydrophobic and that no specific residue is responsible for direct binding to Tup1 via electrostatic interactions. They further concluded that the interaction of Ssn6 with Tup1 does not seem to be performed via the "authentic" groove created by the three tandemly arranged TPRs of Ssn6.

The crystal structures of the N-terminal TPR domain (TPR1) of Hop in complex with the C-terminal heptapeptide of Hsp70 and the central TPR domain (TPR2A) in complex with the C-terminal pentapeptide of Hsp90 have been determined (Scheufler *et al.*, 2000) (See section 1.6.1 for details on Hop's TPR structures). The structures predict that binding involves a network of electrostatic interactions between basic

amino acid residues in the N-terminal and central terminal TPR domains of Hop and the C-terminal EEVD motifs of Hsp70 and Hsp90, respectively.

Although there are exceptions, the hypothesis that binding of EEVD-containing proteins to their TPR-containing partners involves mainly electrostatic interactions and that specificity is largely determined by hydrophobic contacts seems to be generally accepted. All evidence so far presented do suggest that, (i) TPR domains are more versatile in their mechanisms of interactions with partner proteins, (ii) the structural integrity of the TPR domain is critical in all the models so far described, (iii) the groove is not always empty and (iv) the interaction interface may differ as well as the residues involved, from protein to protein. TPR assemblies show multiple modes of ligand binding and do not appear to possess a single "super-site".

1.7 Murine stress-inducible protein 1

Murine stress-inducible protein 1 (mSTI1; Blatch *et al.*, 1997) is a member of the heat-inducible STI1 family of co-chaperones (See section 1.4 for details). Secondary structure predictions indicated that mSTI1 might be composed mainly of α-helices and random coils. This prediction has been confirmed by the crystal structures of Hop with which mSTI1 shares 97 % amino acid identity (Scheufler *et al.*, 2000). Biochemical characterization of mSTI1 suggested that the 6 x histidine tagged recombinant mSTI1, $(His)_6$-mSTI1, existed as both a monomer and a dimer (van der Spuy *et al.*, 2001).

Studies on the interaction of $(His)_6$-mSTI1 with Hsc70 using gel filtration detected species of molecular mass consistent with a dimeric STI1 species or a 1:1 complex of STI1 and Hsc70 (van der Spuy *et al.*, 2001). Similar results were obtained for the yeast STI1 homologue that binds to dimeric Hsp82 as a dimer and induces a conformational change in Hsp82 (Prodromou *et al.*, 1999). Lässle *et al* (1997) showed that heat shock causes changes in the isoform composition of mSTI1. *In vitro* studies showed that casein kinase II (CKII) and Cdc2 kinase phosphorylated mSTI1 at positions S189 and T198 respectively (Figure 1.7) (Longshaw *et al.*, 2000). There are implications that mSTI1 has one or two putative nuclear localization signals (NLS) of the bipartite type (Figure 1.7) (Lässle *et al.*, 1997; Longshaw *et al.*, 2000). Statistical analysis and homology modeling showed that mSTI1 and Hop are almost identical;

henceforth these two homologous proteins are discussed together under the name Hop/mSTI1.

1.7.1 Structures of the TPR domains of Hop/mSTI1

Hop/mSTI1 has nine TPR motifs arranged into three domains, each comprising three motifs. The N-terminal TPR domain (TPR1) spans amino acid residues 4 to 119; the central domain (TPR2A) spans residues 225 to 347, and the C-terminal domain (TPR2B) spans residues 360 to 475. Scheufler *et al* (2000) crystallized and solved the structures of TPR1 and TPR2A domains of Hop in complexes with the C-terminal heptapeptide of Hsp70 and the C-terminal pentapeptide of Hsp90 respectively. Both TPR domains form a meander of seven α-helices that are arranged in a head to tail manner similar to that of the peptide-free TPR domain of PP5 (Das *et al.*, 1998). TPR2A domain contains an insertion of about seven residues between repeats two and three resulting in the elongation of helices B2 and A3 by one turn each. In both structures, helix C, which is positioned C-terminal to the three TPR consensus motifs, appears to be an integral part of the TPR domain. The TPR meanders form cradle-shaped grooves that accommodate the peptides in an extended conformation. The bound peptides only make contact with side-chains of the helices A of the TPR domains that line the inner surfaces of the cradles. The extended conformations of the peptides allows for the display of a maximized surface for binding to the TPR domains and thus facilitates the specific recognition of short amino acid stretches with sufficient affinity.

1.7.2 Hop/mSTI1 binds to Hsp70 and Hsp90 via its N-terminal and central TPR domains respectively

Mutational analysis and crystal structures showed that Hop/mSTI1 binds C-terminal EEVD motif of Hsp70 and Hsp90 by its N-terminal and central TPR domains respectively (Chen *et al.*, 1996; Lässle *et al.*, 1997; Chen and Smith, 1998; van der Spuy *et al.*, 2000; Scheufler *et al.*, 2000). It has been shown in the yeast STI1 that the N-terminal TPR domain also binds Hsp104 (Abbas-Terki *et al.*, 2001). Mutations of two highly conserved C-terminal motifs in Hop/mSTI1, DPEV and DPAM, caused significant disruption in its ability to bind to Hsp70 whereas these mutations did not affect binding to Hsp90 (Chen and Smith, 1998). The effect was thought to be due to

perturbations of inter-domain interactions in Hop/mSTI1 necessary for a complete and tight interaction with Hsp70. Hop/mSTI1 competes with CyP40 and FKBP52 to bind to Hsp90 and in addition prevents the ATP-dependent conversion of ADP-Hsp90 to p23-binding form (Owens-Grillo *et al.*, 1996; Chang *et al.*, 1997; Johnson *et al.*, 1998). Hop/mSTI1 was initially thought to act as an ADP/ATP exchange factor for Hsc70 (Gross and Hessefort, 1996) but latter experimental evidence showed that the protein bound to the ADP-bound Hsp70 and did not act as a nucleotide exchange factor (Johnson *et al.*, 1998).

1.7.3 General binding of Hop/mSTI1 TPR domains to Hsp70 and Hsp90 is mediated by electrostatic interactions

The crystal structures of Hop's TPR domains showed that all electrostatic contacts between the TPR domains and the target peptides occur in the regions of the EEVD motif (Scheufler *et al.*, 2000). The structures identify three kinds of hydrogen-bonding interactions, which mediate peptide binding to both TPR domains. First, hydrogen bonds between the side chains of charged residues in the TPR domain and the peptide backbone. Second, hydrogen bonds between the side chains of charged residues in the TPR domain and the peptide side chains. Third, hydrogen bonds between the side chains of charged residues in the TPR domain and the main-chain carboxylate of the C-terminal aspartic acid in the peptide ligands. The electrostatic interactions between the TPR domains and the C-terminal aspartate (Asp 0) form a two-carboxylate clamp that is considered necessary for binding of Hop to Hsp70 and Hsp90. Residues in the TPR1 domain predicted to be involved in forming this clamp include Lys^{8}, Asn^{12}, Asn^{43}, Lys^{73}, and Arg^{77} while the topologically equivalent residues in the TPR2A domain are Lys^{229}, Asn^{233}, Asn^{264}, Lys^{301}, and Arg^{305} (Figures are shown in Chapter Two). The amino acid residues that form the two-carboxylate clamp are highly conserved in TPR-containing proteins that bind to the C-terminal EEVD motif of Hsp70 and Hsp90 (Liu *et al.*, 1999; Scheufler *et al.*, 2000) (Figures are shown in Chapter Two).

1.7.4 Hydrophobic interactions determine the specificity of binding of Hop/mSTI1 TPR domains to Hsp70 and Hsp90

Crystal structures predict that discrimination between the C-termini of the two molecular chaperones depends largely on hydrophobic and van der Waals interactions between residues in Hop's TPR domains and residues upstream of the EEVD motif. For example, Ala^{46}, Ala^{49} and Lys^{50}, all in helix A of the second TPR motif (helix 2A) in TPR1 of Hop make hydrophobic contacts with Ile -4 immediately upstream of the EEVD in Hsp70 while Tyr^{236} and Glu^{271} in helix A of the first TPR motif (helix 1A) and helix A of the second TPR motif (helix 2A) of TPR2A, respectively, make critical hydrophobic contacts with Met -4 upstream of the EEVD motif in Hsp90 (Figures are shown in Chapter Two). Pro -6 which is further upstream of the EEVD motif in Hsp70 exits in a hydrophobic cavity formed by Glu^{83} and Phe^{84} of helix A of the third TPR motif (helix 3A) in TPR1. Val -1 in the EEVD motif of Hsp70 makes hydrophobic contacts with Asn^{12} and Leu^{15} in helix 1A and with Asn^{43} in helix 2A of TPR1. In the TPR2A complex, Val -1 in the EEVD motif of Hsp90 is in hydrophobic contacts with Asn^{233}, Asn^{264} and Ala^{267}.

1.7.5 Hop/mSTI1 TPR domains prefer hydrophobic residues in positions - 4 and - 6 of their respective peptide ligands

Recently, the sequence motifs for the binding of TPR1 and TPR2A domains of Hop to their respective peptides were defined by alanine scanning of the C-terminal octapeptides of Hsp70 and Hsp90 and by screening of combinatorial peptide libraries (Brinker *et al.*, 2002). In both cases, Asp 0 and Val -1 of the EEVD motifs were identified as general anchor residues, thus confirming the predictions from the crystal structures. The highly conserved glutamate residues were found to be critical in binding Hsp90 by TPR2A whereas they did not contribute appreciably to the interaction of Hsp70 with TPR1. Rather, TPR1 preferred hydrophobic amino acids in these positions. In addition, the TPR domains displayed a high tendency to interact preferentially with hydrophobic aliphatic and aromatic side chains in positions -4 and -6 of their respective ligands, Ile -4 in Hsp70 and Met -4 in Hsp90 (Brinker *et al.*, 2002).

A

```
1   MEQVNELKEKGNKALSAGNIDDALQCYSEAIKLDPQNHVLYSNRSAAYAK
          TPR1-1A          TPR1-1B          TPR1-2A

51  KGDYQKAYEDGCKTVDLKPDWGKGYSRKAAALEFLNRFEEAKRTYEEGLK
          TPR1-2B          TPR1-3A          TPR1-3B

101 HEANNLQLKEGLQNMEARLAERKFMNPFNLPNLYQKLENDPRTRSLLSDP

151 TYRELIEQLQNKPSDLGTKLQDPRVMTTLSVLLGVDLGSMDEEEEAATPP

201 PPPPPKKEPKPEPMEEDLPENKKQALKEKELGNDAYKKKDFDKALKHYDR
                    TPR2A-1A          TPR2A-1B

251 AKELDPTNMTYITNQAAVHFEKGDYNKCRELCEKAIEVGRENREDYRQIA
          TPR2A-2A          TPR2A-2B

301 KAYARIGNSYFKEEKYKDAIHFYNKSLAEHRTPDVLKKCQQAEKILKEQE
          TPR2A-3A          TPR2A-3B

351 RLAYINPDLALEEKNKGNECFQKGDYPQAMKHYTEAIKRNPRDAKLYSNR
          TPR2B-1A          TPR2B-1B          TPR2B-2A

401 AACYTKLLEFQLALKDCEECIQLEPTFIKGYTRKAAALEAMKDYTKAMDV
          TPR2B-2B          TPR2B-3A          TPR2B-

451 YQKALDLDSSCKEAADGYQRCMMAQYNRHDSPEDVKRRAMADPEVQQIMS
    3B

501 DPAMRLILEQMQKDPQALSEHLKNPVIAQKIQKLMDVGLIAIR*
```

B

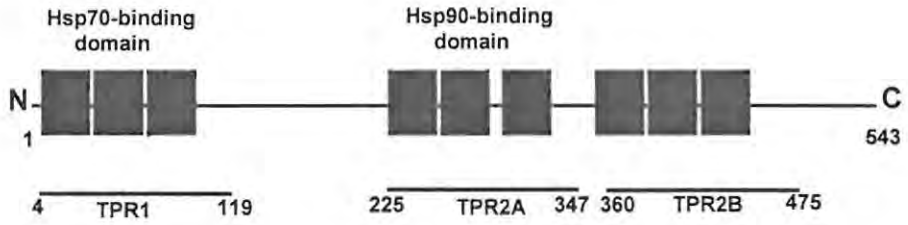

Figure 1.7: Primary structure of mSTI1 showing some structural features
A: Amino acid sequence of mSTI1. Dashed line represents the extent of each TPR α-helix based on the structures of Hop (Scheufler *et al.*, 2000). TPR1, TPR2A and TPR2B represent N-terminal, central and C-terminal TPR domains respectively. Each TPR helix is named by a number and a letter showing its position within the motif. A highly conserved stretch of residues in STI1 homologues (residues 37 – 47) is shown in black background. A polyproline stretch (residues 199 – 205) is shown in black background and italics. Potential nuclear localization signals are shown in grey background. Solid boxes represent potential casein kinase II (ckII) phosphorylation sites while dashed boxes represent potential cell division control (cdc) protein 2 phosphorylation sites. **B:** Organization of TPR motifs in mSTI1. Each closed box represents a TPR motif comprising two α-helices. Each TPR domain is composed of three TPR motifs and an additional helix C at the C-terminal of the domain (Scheufler *et al.*, 2000). Solid line and numbering represent the extent of each TPR domain.

1.8 Research Hypothesis

The relevance of the individual amino acids in the C-terminal peptides of Hsc70 (PTIEEVD) and Hsp90 (MEEVD) to the Hsp70-Hop-Hsp90 complex, and in particular the Hsp90-Hop complex, has been characterised (Brinker *et al.*, 2002). However, the relative significance of the individual amino acids in the TPR1 domain groove to general binding and specificity of the Hsc70-Hop complex are yet to be experimentally characterised. This study was designed to address these issues based on the following broad hypothesis that: 'The mechanism by which the co-chaperone mSTI1 binds to Hsc70 and Hsp90 involves a network of electrostatic interactions between mainly charged amino acid residues and that TPR domains discriminate between Hsc70 and Hsp90 by hydrophobic interactions.' Specific objectives emanating from this broad hypothesis are

i. To test the predictions from the crystal structures that the general binding of Hsc70 and Hsp90 to the TPR1 and TPR2A domains of Hop each involves a network of electrostatic interactions between residues in the TPR grooves and the C-terminal peptides of the chaperones.

ii. To test the predictions from the crystal structures that Hop TPR domains discriminate between Hsc70 and Hsp90 via hydrophobic interactions between the side chains of residues in the TPR grooves and the C-terminal peptides of the chaperones.

ii. To characterize the binding of Hop to Hsc70 and Hsp90 *in vivo*.

For this study, the murine homologue of STI1, mSTI1, was used.

Chapter Two

Characterization of the electrostatic interactions required for successful mSTI1 binding to Hsc70 and Hsp90

2.1 Introduction

Experimental evidence and crystal structures suggest that conserved basic residues that project into the grooves of the TPR domains of proteins that interact with Hsp70 and Hsp90 are important for binding to these molecular chaperones (Russell *et al.*, 1999; Scheufler *et al.*, 2000). The crystal structures of TPR1 and TPR2A domains of Hop in complexes with the C-terminal peptides of Hsp70 and Hsp90 (Figures 2.1 and 2.2) predict that binding involves a network of electrostatic interactions between charged amino acid residues in the TPR domains and the C-terminal EEVD motifs of the molecular chaperones (Scheufler *et al.*, 2000). Recently, it has been shown that while Asp 0 and Val -1 act as general anchor residues, the highly conserved glutamates of the EEVD motif, which appear to be critical in Hsp90 binding by TPR2A, do not contribute appreciably to the interaction of Hsp70 with TPR1 (Brinker *et al.*, 2002). It was therefore hypothesized that the general binding of Hsp70 and Hsp90 to their respective TPR domains in mSTI1 occur by a similar but not identical mechanism. The objective of this study was to experimentally test the predictions from the crystal structures and to test the hypothesis above by characterizing the contacts between the TPR grooves of mSTI1 and the EEVD residues of Hsp70 and Hsp90 using site-directed mutagenesis and protein binding assays. The following amino acids were substituted in mSTI1 by alanine: Lys^{8}, Asn^{12}, Asn^{43}, Lys^{73}, Lys^{229}, and Lys^{301}. The modified mSTI1 proteins were tested for their ability to bind to Hsc70.

2.2 Experimental Procedures

2.2.1 Generation and analysis of modified plasmids

Modified plasmids were generated from either pGEX3X2000 or pQE30-2000, which contain the cDNAs coding for unmodified full-length gluathione-*S*-transferase-mSTI1 fusion protein, (GST-543), or 6 x histidine-tagged mSTI1, $(His)_6$-543, respectively. Silent mutations were engineered in oligonucleotide primers to create restriction sites for screening purposes except where the desired codon changes automatically generated or deleted restriction sites (Table 2.1). All mutations were carried out by site-directed mutagenesis based on double-stranded whole plasmid linear amplification, using the Stratagene QuikChange mutagenesis protocols (Stratagene, La Jolla, U.S.A), with modifications necessary to optimise the reaction (Table A.1, Appendix A). The plasmid pGEX3X2000(Δ37-47) (encoding GST fusion protein in which residues 37-47 have been deleted, GST-543(Δ37-47)) was generated before this study (van der Spuy *et al.*, 2000). Plasmids were used to transform competent *Escherichia coli* (*E. coli*) XL1 Blue cells (Appendix A, sections A.1 and A.2). Plasmids were isolated after transformation based on alkaline lysis of bacterial cells either by conventional method (Birnboim, 1983) or by using commercially available kits (Appendix A, sections A.4 and A.5). Mutations were confirmed both by restriction enzyme analysis (Appendix A, section A.7) and by automated DNA sequencing (Appendix A, section A.12), using the ABI PRISM 3100 Genetic Analyser (*PE* Biosystems, Foster City, U.S.A).

Table 2.1: Generation of modified plasmids from pGEX3X2000 used for general binding studies

Modified plasmid	Codon changes	Forward primers used for mutagenesis	Diagnostic restriction endonuclease
pGEX3X2000 (K8A)	aag : gcg	gtgaatgagctagcggagaagggc	*Nhe* I
pGEX3X2000 (N12A)	aat : gcc	gctaaaggagaagggcgccaaggccctgagtgc	*Nar* I
pGEX3X2000 (K8A, N12A)	aag : gcg aat : gcc	gaatgagctagcggagaagggcgccaaggccctgag	*Nhe* I, *Nar* I
pGEX3X2000 (N43A)	aat : gct	gtgctctacagcgctcgctctgcag	*Eco* 47 III
pGEX3X2000 (Δ37-47, K8A)	aag : gcg	gtgaatgagctagcggagaagggc	*Nhe* I
pGEX3X2000 (Δ37-47, N12A)	aat : gcc	gctaaaggagaagggcgccaaggccctgagtgc	*Nar* I
pGEX3X2000 (K301A)	caa : cgc agc : cgc	gcagatcgccgccgcttatgcccg	*Hind* III

2.2.2 Heterologous production and purification of recombinant GST-mSTI1 fusion proteins for general binding studies

Generally, before large-scale production of recombinant protein, the solubility of the protein was determined using a small-scale culture as described in Appendix A, section A.13. Over-production of recombinant GST-mSTI1 fusion proteins was induced in *E. coli* XLI Blue cells carrying pGEX3X derived plasmid constructs with isopropyl-1-thio-β-D-galactopyranoside (IPTG). The over-produced GST-mSTI1 proteins were purified using *S*-hexyl glutathione agarose affinity chromatography as described in Appendix A, section A.14. Protein content was determined using the Folin-phenol reagent as described by Lowry *et al* (1951).

2.2.3 Glutathione agarose pull down assays

S-hexyl glutathione agarose affinity of the GST-mSTI1 proteins was used to characterize their interaction with Hsc70 and/or Hsp90 (Apendix A, section A.18) using a protocol that has been optimised previously (van der Spuy *et al.*, 2000). Generally, the assays were carried out at room temperature and 137 mM NaCl concentration except where otherwise stated. Briefly, GST-mSTI1 fusion proteins were coupled to glutathione agarose beads after which binding was allowed to occur

with either Hsc70 from crude extracts of NIH3T3 mouse fibroblasts or purified Hsp90. Lysates from NIH3T3 mouse fibroblasts were used because previous study showed that the use of purified Hsc70 resulted in high background binding of Hsc70 to GST (van der Spuy *et al.*, 2000). The beads were washed extensively to remove unbound proteins and the proteins were resolved by electrophoresis on a 0.1 % sodium dodecyl sulphate (SDS), 12 % polyacrylamide gel (PAGE) (Appendix A, sections A.14 and A.19). After transferring onto nitrocellulose membrane, co-precipitation of Hsc70 and/or Hsp90 with the GST-mSTI1 fusion proteins was revealed by chemiluminescence-based immunodetection using the monoclonal primary antibodies H5147 (Sigma) and H9010 (kind gift from Drs Toft and Smith) specific for Hsc70/Hsp70 and Hsp90 respectively (AppendixA, sections A.20 and A.21).

2.2.4 Bioinformatic analysis and homology modeling

Co-ordinates used to draw Figures 2.1B and 2.2B were generated by the computer software programme WHAT IF (Vriend, 1990), using the crystal structures of the TPR1 (PDB code: 1ELW, Scheufler *et al.*, 2000) and TPR2A (PDB code: 1ELR, Scheufler *et al.*, 2000) domains of Hop as templates. Both figures 2.1 and 2.2 were visualised and drawn with the computer software programme MOLSCRIPT (Kraulis, 1991). All protein sequence alignments were generated using the computer software programme, PepTools (Wishart, *et al.*, 1997).

2.2.5 Biophysical analysis of $(His)_6$-543 and $(His)_6$-543(K8A, N12A) proteins

The plasmid pQE30-2000(K8A, N12A) was generated from pQE30-2000 containing the cDNA coding for the full length $(His)_6$-tagged mSTI1 protein. Over-production and purification of the protein was done as described in Appendix A, section A.15. Steady-state fluorescence and circular dichroism spectroscopies were used to determine the conformational stability of the modified protein using the unmodified $(His)_6$-543 as control (with technical assistance from Dr Judith Hornby). Fluorescence emission spectra and other fluorescence measurements were made at 25^0C in 20 mM sodium phosphate, 1 mM EDTA, pH 7.5. The intrinsic fluorescence of the lone trytophan (excitation at 295 nm) in mSTI1 was measured for 2 μM protein between

300 and 400 nm in a Perkin-Elmer fluorescence spectrophotometer. Circular dichroism measurements were made using 8 μM of each protein sample in a Jasco J-710 spectropolarimeter. Ellipticity values were collected (average of 10 runs) in both the near-UV (350-250 nm) and far-UV (250-200 nm) regions.

2.3 Results

2.3.1 Bioinformatic analysis and homology modeling of mSTI1 TPR domains

In Figures 2.1A and 2.2A, basic amino residues shown in sticks are predicted to make electrostatic interactions with the C-terminal aspartate (D0) in both Hsp70 and Hsp90, forming a so-called two-carboxylate clamp. Homology modeling, using co-ordinates generated from Hop, revealed that the structures of the N-terminal and the central TPR domains of mSTI1 are similar to that of Hop (Figures 2.1B and 2.2B). This was not unexpected since the homologues share 97 % amino acid identity (Blatch *et al.*, 1997). A sequence alignment of Hsp70-interacting TPR domains of STI1 homologues was constructed (Figure 2.3, first alignment). The alignment revealed that the charged residues in the TPR1 domains predicted to form the so-called two-carboxylate clamp with the EEVD motif of Hsp70 are strictly conserved among homologous STI1 proteins. Figure 2.4 (first alignment) reveals that a similar trend occurs in the Hsp90-binding TPR2A domains of STI1 homologues except at position equivalent to Lys^{301} in Hop. In another alignment (Figure 2.3, second alignment), the same basic residues in the Hsp70-binding TPR domains of non-homologous Hsp70-interacting proteins were compared. Conservation of the basic TPR groove residues was found to be less strict in these proteins, especially at positions equivalent to Lys^{73} and Arg^{77} in Hop. Similarly, conservation of these residues was much less strict in the TPR2A of non-homologous Hsp90-interacting proteins (Figure 2.4, second alignment).

2.3.2 Modified pGEX3X derived plasmids were successfully generated

Complementary mutagenic oligonucleotide primers were used to amplify the entire pGEX3X2000 plasmid to generate the following modified plasmids: pGEX3X2000(K8A), pGEX3X2000(N12A), pGEX3X2000(K8A, N12A),

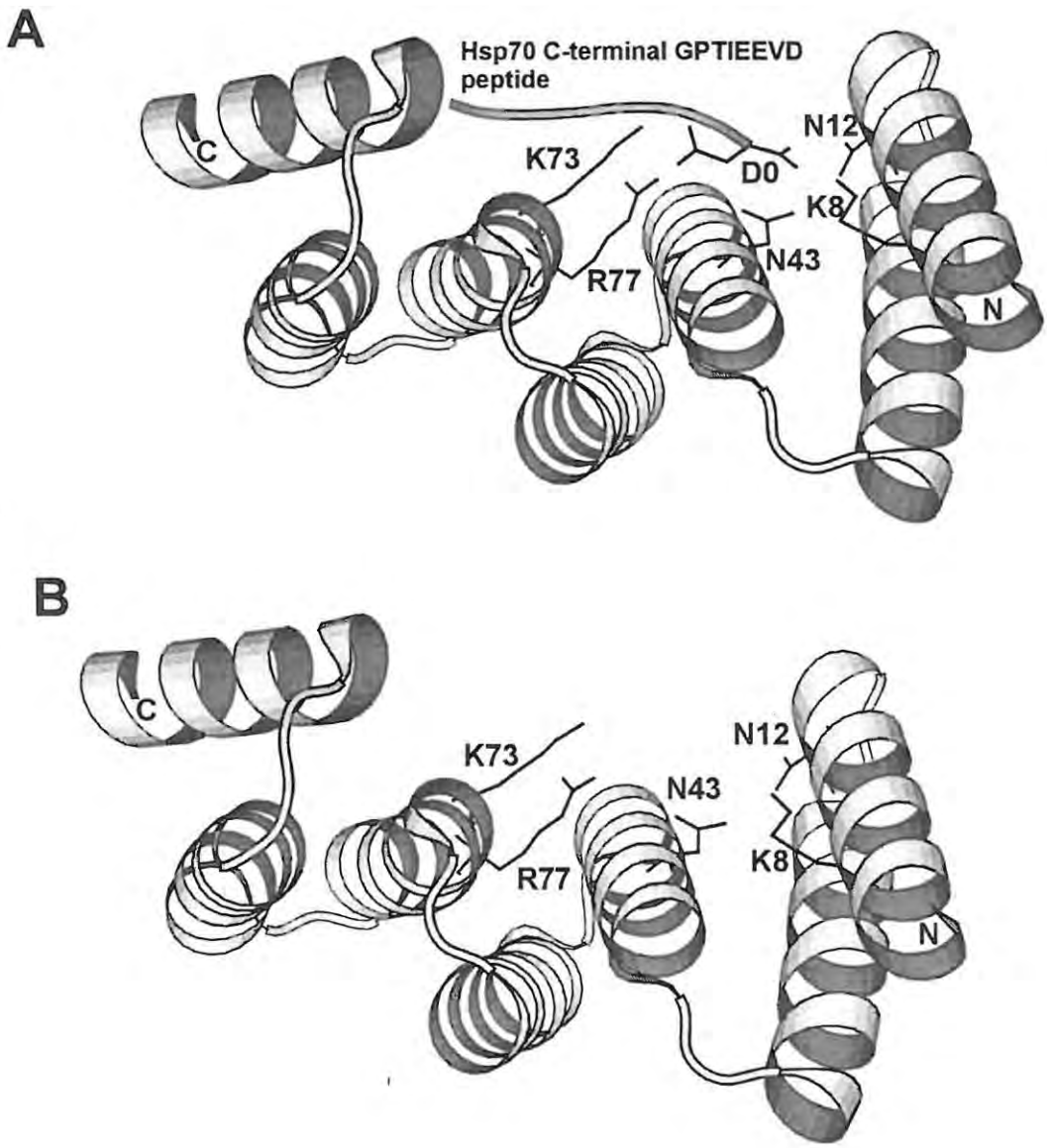

Figure 2.1: Hop N-terminal TPR domain in complex with the C-terminal Hsp70 heptapeptide. **A:** Ribbon representation of the crystal structure of the N-terminal TPR domain (TPR1; PDB code 1ELW, Scheufler, *et al.*, 2000) of Hop in complex with the C-terminal heptapeptide of Hsp70. **B:** Ribbon representation of the N-terminal TPR domain of mSTI1 modeled on the crystal structure of Hop. TPR domains are shown as ribbons, peptides as rods and amino acid residues as sticks. The TPR residue is labeled by the single letter code and a number that relates to its position in the primary amino acid sequence. N and C indicate N- and C-terminal ends of the polypeptides respectively. The co-ordinates of figure 2.1B were generated using WHAT IF (Vriend, 1990), and both figures were drawn with MOLSCRIPT (Kraulis, 1991).

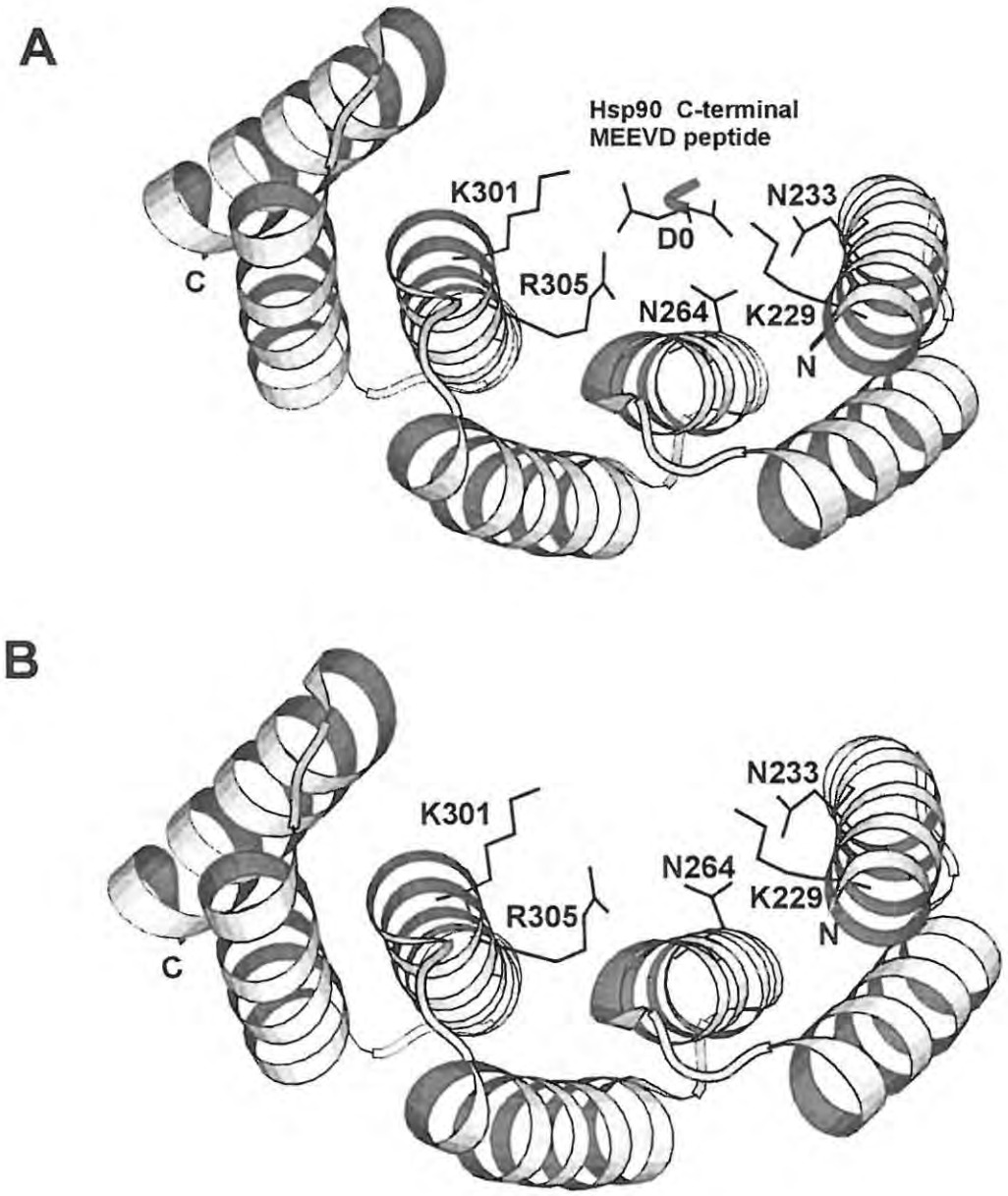

Figure 2.2: Hop central TPR domain in complex with the C-terminal Hsp90 pentapeptide.
A: Ribbon representation of the crystal structure of the central TPR domain (TPR2A; PDB code 1ELR, Scheufler *et al.*, 2000) of Hop in complex with the C-terminal pentapeptide of Hsp90. **B:** Ribbon representation of the central TPR domain of mSTI1 modeled on the crystal structure of Hop. TPR domains are shown as ribbons, peptides as rods and amino acid residues as sticks. The TPR residue is labeled by the single letter code and a number that relates to its position in the primary amino acid sequence. N and C indicate N- and C-terminal ends of the polypeptide respectively. The co-ordinates for figure 2.2B were generated using WHAT IF (Vriend, 1990) and both figures were drawn with MOLSCRIPT (Kraulis, 1991).

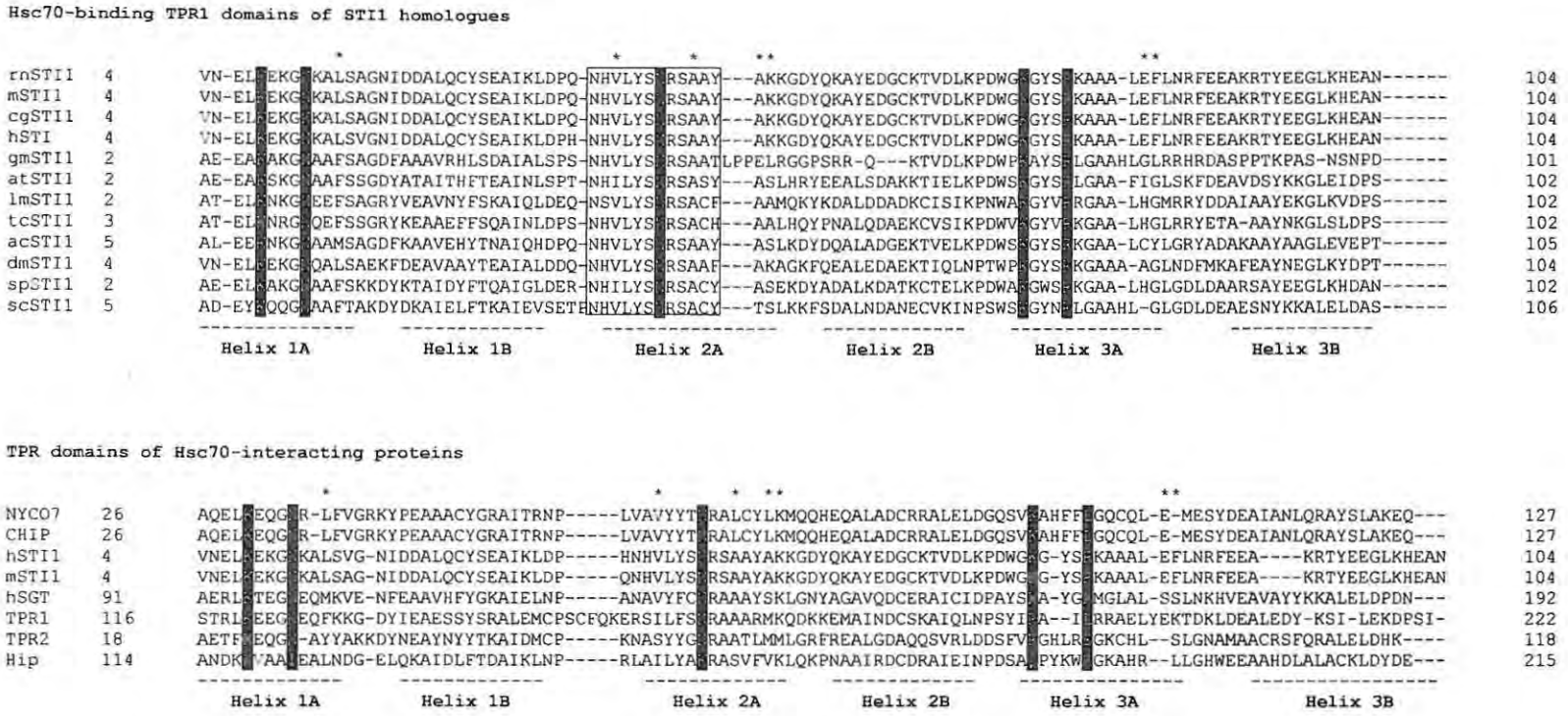

Figure 2.3: Multiple sequence alignments of Hsc70-interacting TPR1 domains of stress-inducible protein 1 homologues and other Hsp70-interacting proteins. Residues that are predicted to form a two-carboxylate clamp with the C-terminal aspartate in Hsp70 are shaded in black while asterisk (*) indicates positions of residues predicted to determine specificity of binding. A highly conserved region in the second TPR motif is shown in unfilled box. Hsp70-binding TPR1 domains of STI1 homologues: rn; (*Rattus norvegicus*, CAA75351.1), m; (*Mus musculus*, AAC53267.1), cg; (*Cricetulus griseus*, AAB94760.1), h; (*Homo sapiens*, AAA58682.1), tc; (*Trypanosoma cruzi*, AAC97378.1), ac; (*Achantamoeba castellanii*, AAB49720), at; (*Arabidopsis thaliana*, CAB45987.1), gm; (*Glycine max*, S56658), dm; (*Drosophila melanogaster*, AAC12945.1), lm; (*Leishmania major*, AAB37318), sp; (*Schizosaccharomyces pombe*, CAB39910.1), sc; (*Saccharomyces cerevisiae*, CAA60743.1). Hsp70-interacting TPR domains of other proteins: NY-CO-7; (colon cancer antigen 7, AAC18038), CHIP; (carboxyl terminus of Hsc70-interacting protein, AAK61242), hSTI1; (human STI1 or Hop, AAA58682.1), mSTI1; (murine STI1 or extendin, AAC53267.1), hSGT; (human small glutamine-rich protein, NP_003012), TPR1; (tetratricopeptide repeat domain 1, NP_003305), TPR2; (tetratricopeptide repeat domain 2, NP_003306), and Hip; (Hsc70-interacting protein, P50502). Dashed lines represent the extent of each TPR helix, based on the crystal structures of hSTI1 (Hop) (Scheufler *et al.*, 2000). Each TPR helix is named by a number and an alphabet showing its position within the motif. The sequence alignments were generated using PepTools (Wishart *et al.*, 1997).

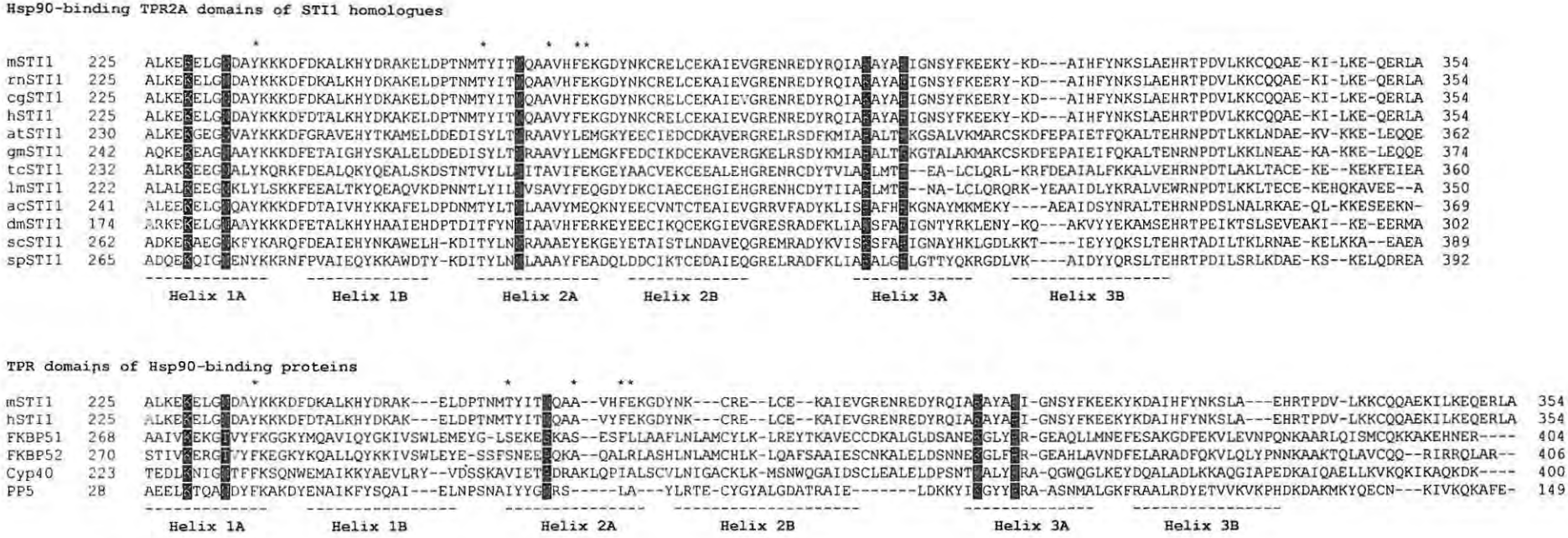

Figure 2.4: Multiple sequence alignments of Hsp90-interacting TPR2A domains of stress-inducible protein 1 homologues and other Hsp90-interacting proteins.
Residues that are predicted to form a two-carboxylate clamp with the terminal aspartate in Hsp90 are shaded in black while asterisk (*) indicates positions of residues predicted to determine specificity of binding. Hsp90-binding TPR2A domains of STI1 homologues: m; (*Mus musculus*, AAC53267.1), rn; (*Rattus norvegicus*, CAA75351.1), cg; (*Cricetulus griseus*, AAB94760.1), h; (*Homo sapiens*, AAA58682.1), at; (*Arabidopsis thaliana*, CAB45987.1), gm; (*Glycine max*, S56658), tc; (*Trypanosoma cruzi*, AAC97378.1), lm; (*Leishmania major*, AAB37318), ac; (*Achantamoeba castellanii*, AAB49720), dm; (*Drosophila melanogaster*, AAC12945.1), sc; (*Saccharomyces cerevisiae*, CAA60743.1), sp; (*Schizosaccharomyces pombe*, CAB39910.1). Hsp90-interacting domains of other proteins: mSTI1; (murine STI1 or extendin, AAC53267.1), hSTI1; (human STI1 or Hop, AAA58682.1), FKBP51; (Hsp90-binding immunophilin, Q13451), FKBP52; (Hsp90-binding immunophilin, Q02790), CyP40; (Cyclophilin-40, Q08752), PP5; (Protein phosphatase 5, NP_006238). Dashed lines represent the extent of each TPR helix, based on the crystal structures of hSTI1 (Hop) (Scheufler *et al.*, 2000). Each TPR helix is named by a number and an alphabet showing its position within the motif. The sequence alignments were generated using PepTools (Wishart *et al.*, 1997).

pGEX3X2000(N43A), pGEX3X2000(Δ37-47, K8A), pGEX3X2000(Δ37-47, N12A), and pGEX3X2000(K301A). The linear amplification products were digested with *Dpn* 1 after which 15 µl was resolved on a 1 % agarose gel stained with ethidium bromide. Generally, the putative mutants were observed to resolve as linearized bands corresponding to the size of the parental plasmid, pGEX3X2000. 1 µl of the amplification product was used to transform *E. coli* XLI Blue. Modified plasmids isolated from *E. coli* harbouring them were digested with their respective diagnostic restriction endonucleases (Table 2.1) to confirm mutations engineered therein. In addition, mutations were confirmed by automated DNA sequencing.

2.3.2.1 Analysis of pGEX3X2000(K8A) and pGEX3X2000(N12A) modified plasmids

pGEX3X2000(K8A) was generated from pGEX3X2000 by inserting a double base pair change (Table 2.1), which introduced a unique *Nhe* I site. DNA fragments resulting from the digestion of pGEX3X2000(K8A) with *Nhe* I were resolved on a 1 % agarose gel (Figure 2.5A). As expected, digestion with *Nhe* I linearized the modified plasmid pGEX3X2000(K8A) running at approximately 7000 bp, whereas the parental plasmid still remained undigested (Figure 2.5A, lanes 4 and 5). Both parental and modified plasmids were digested with *Pst* I, each releasing two fragments of equal sizes, to verify the size of the modified plasmid (Figure 2.5A, lanes 8 and 9).

A complete codon change (aat to gcc) in pGEX3X2000 generated the plasmid pGEX3X2000(N12A) with the introduction of a second *Nar* I site using a pair of complimentary primers (Table 2.1). Both the parental and modified plasmids were digested with *Nar* I to confirm the mutations. The restricted DNA fragments were resolved on a 1 % agarose gel. The parental plasmid was linearized with *Nar* I yielding a fragment of approximately 7000 bp, while the modified plasmid yielded two expected fragments of 5362 bp and 1655 bp in size (Figure 2.5B, lanes 6 and 7). It was observed that *Nar* I did not cut to completion as revealed by the uncut band in lane 6 and the linearized 7000 bp fragment in lane 7 of Figure 2.5B. Both parental and modified plasmids were further digested with *Pst* I, each releasing two fragments of equal sizes, to verify the size of the modified plasmid.

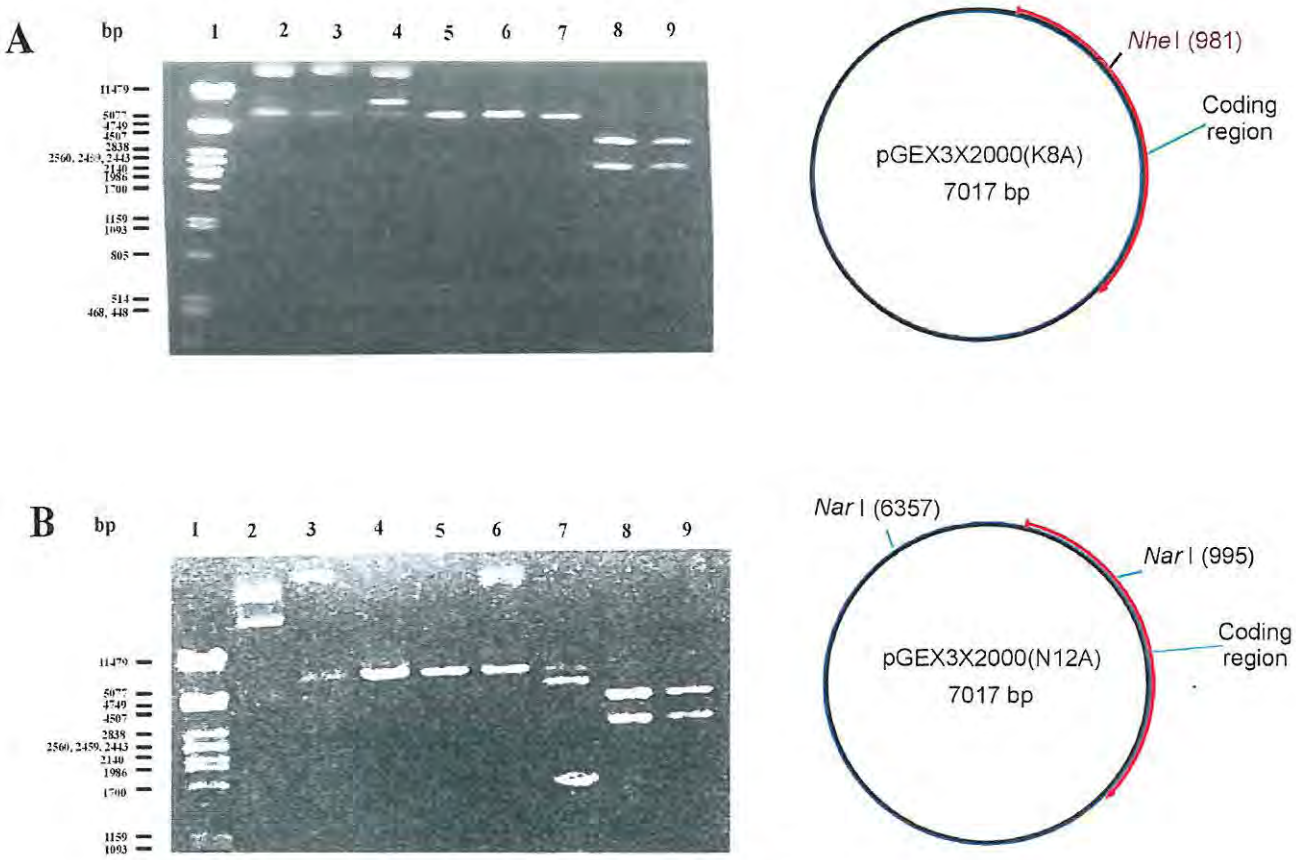

Figure 2.5: Diagnostic restriction endonuclease digestion of pGE3X2000(K8A) and pGEX3X2000(N12A) plasmids.
A: Ethidium bromide stain of 1 % agarose gel and restriction map of *Nhe* I-digested pGEX3X2000(K8A). Lane 1, *Pst* I-digested Lambda DNA molecular weight standards. Lanes 2 and 3, undigested pGEX3X2000 and pGEX3X2000(K8A) respectively. Lanes 4 and 5, *Nhe* I-digested pGEX3X2000 and pGEX3X2000(K8A) respectively. Lanes 6 and 7, *Hind* III-linearized pGEX3X2000 and pGEX3X2000(K8A) respectively. Lanes 8 and 9, *Pst* I-digested pGEX3X2000 and pGEX3X2000(K8A) respectively. **B:** Ethidium bromide stain of 1 % agarose gel and restriction map of *Nar* I-digested pGEX3X2000(N12A). Lane 1, *Pst* I-digested Lambda DNA molecular weight standards. Lanes 2 and 3, undigested pGEX3X2000 and pGEX3X2000(N12A) respectively. Lanes 4 and 5, *Hind* III-linearized pGEX3X2000 and pGEX3X2000(N12A) respectively. Lanes 6 and 7, *Nar* I-digested pGEX3X2000 and pGEX3X2000(N12A) respectively. Lanes 8 and 9, *Pst* I-digested pGEX3X2000 and pGEX3X2000(N12A) respectively. bp indicates DNA sizes in base pairs.

2.3.2.2 Analysis of pGEX3X2000(K8A, N12A) modified plasmid

Mutagenic oligonucleotide primers were used to introduce a double base pair change and a complete codon change (Table 2.1) into pGEX3X2000, to generate the plasmid pGEX3X2000(K8A, N12A). These mutations introduced both a unique *Nhe* I site and an additional *Nar* I site into the plasmid. Restriction endonuclease digestion, using both *Nhe* I and *Nar* I in separate reactions, was used to verify these mutations. *Nhe* I digestion of the modified plasmid yielded an expected linearized fragment of approximately 7000 bp, while the parental plasmid was undigested by *Nhe* I (Figure

2.6, lanes 6 and 7). As expected, *Nar* I digestion linearized pGEX3X2000 while it yielded two fragments of 5362 bp and 1655 bp in size for pGEX3X2000(K8A, N12A). *BamH* I digestion of both plasmids each generated equivalent fragment profiles of two DNA bands (Figure 2.6, lanes 10 and 11).

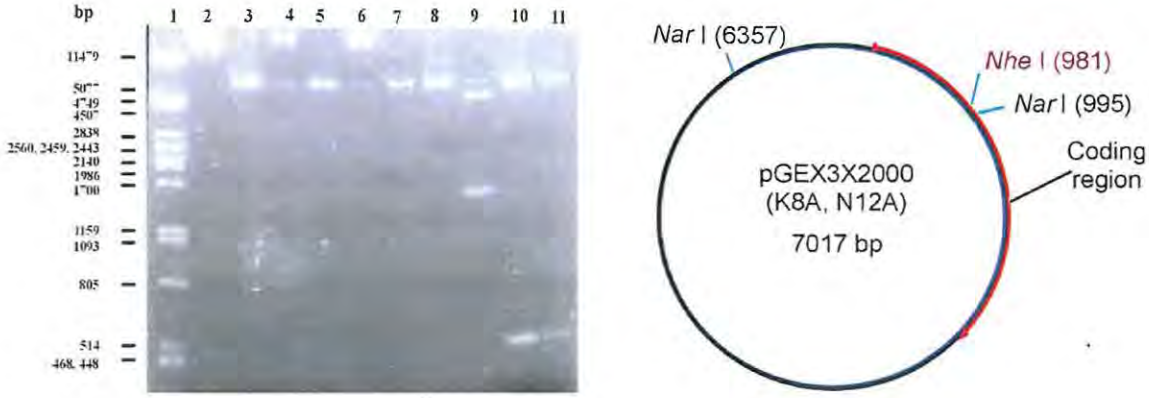

Figure 2.6: Diagnostic restriction endonuclease digestion of pGEX3X2000(K8A, N12A) plasmid. Ethidium bromide stain of 1 % agarose gel and restriction map of *Nhe* I and *Nar* I-digested pGEX3X2000(K8A, N12A). Lane 1, *Pst* I-digested Lambda DNA molecular weight standards. Lanes 2 and 3, undigested and *Hind* III-linearized pGEX3X2000 respectively. Lanes 4 and 5, undigested and *Hind* III-linearized pGEX3X2000(K8A, N12A) respectively. Lanes 6 and 7, *Nhe* I-digested pGEX3X2000 and pGEX3X2000(K8A, N12A) respectively. Lanes 8 and 9, *Nar* I-digested pGEX3X2000 and pGEX3X2000(K8A, N12A) respectively. Lanes 10 and 11, *BamH* I-digested pGEX3X2000 and pGEX3X2000(K8A, N12A) respectively. bp indicates DNA sizes in base pairs.

2.3.2.3 Analysis of pGEX3X2000(Δ37-47, K8A) and pGEX3X2000(Δ37-47, N12A) modified plasmids

The plasmid pGEX3X2000(Δ37-47) was previously generated as described by van der Spuy *et al* (2000). pGEX3X2000(Δ37-47, K8A) and pGEX3X2000(Δ37-47, N12A) were obtained from pGEX3X2000(Δ37-47) by doing the same mutations described in sections 2.3.2.1 respectively. Deletion of residues 37 to 47 from the cDNA encoding mSTI1 resulted in a slight reduction of the size of the pGEX3X2000 plasmid from 7017 bp to 6982 bp. Hence digestion of pGEX3X2000(Δ37-47, K8A) with *Nhe* I yielded a single fragment of approximately 7000 bp (Figure 2.7A, lane 7) while pGEX3X2000(Δ37-47) remained undigested. *Pvu* I digestion of both pGEX3X2000(Δ37-47) and pGEX3X2000(Δ37-47, K8A) yielded similar fragment patterns (Figure 2.7A, lanes 8 and 9), suggesting that the size of the modified plasmid

was correct. While *Nar* I linearized pGEX3X2000(Δ37-47) to yield a fragment of approximately 7000 bp, it partially digested pGEX3X2000(Δ37-47, N12A) into two expected fragments of 5329 bp and 1655 bp (Figure 2.7B, lanes 8 and 9). Similarly, *Pvu* I digestion of both pGEX3X2000(Δ37-47) and pGEX3X2000(Δ37-47, N12A) yielded fragments of equal sizes (Figure 2.7B, lanes 10 and 11), thus confirming the correct size of the modified plasmid.

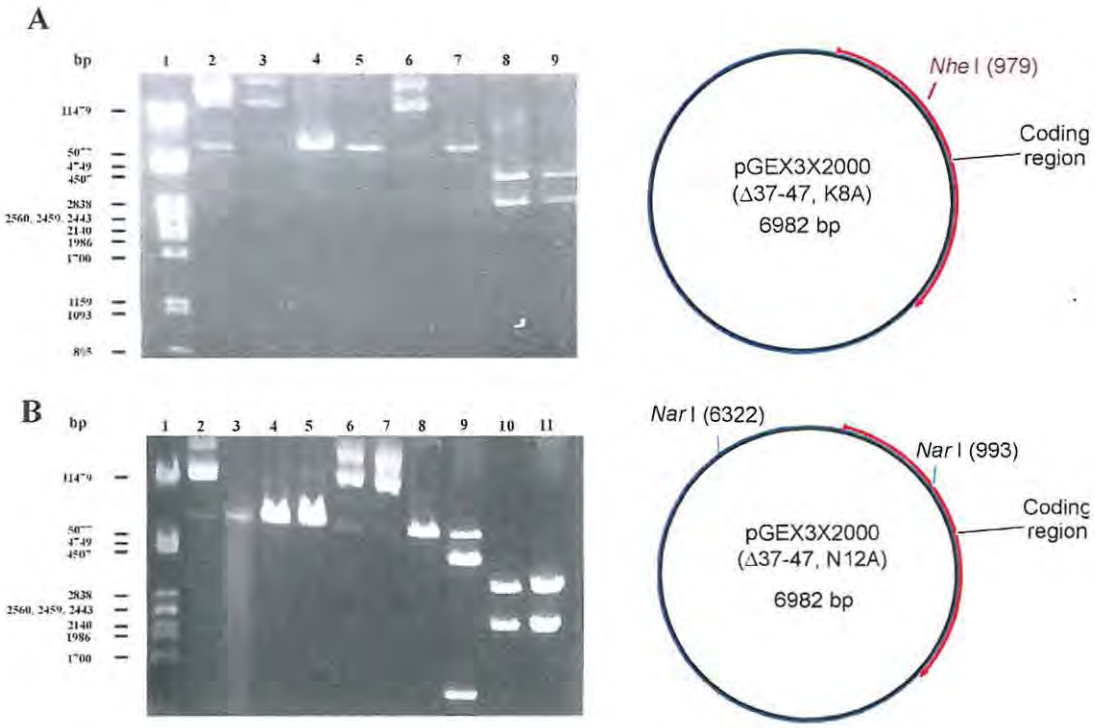

Figure 2.7: Diagnostic restriction endonuclease digestion of pGEX3X2000(Δ37-47, K8A) and pGEX3X2000(Δ37-47, N12A) plasmids.
A: Ethidium bromide stain of 1 % agarose gel and restriction map of *Nhe* I-digested pGEX3X2000(Δ37-47, K8A). Lane 1, *Pst* I-digested Lambda DNA molecular weight standards. Lanes 2 and 3, undigested pGEX3X2000(Δ37-47) and pGEX3X2000(Δ37-47, K8A) respectively. Lanes 4 and 5, *Hind* III-linearized pGEX3X2000(Δ37-47) and pGEX3X2000(Δ37-47, K8A) respectively. Lanes 6 and 7, *Nhe* I-digested pGEX3X2000(Δ37-47) and pGEX3X2000(Δ37-47, K8A) respectively. Lanes 8 and 9, *Pvu* I-digested pGEX3X2000(Δ37-47) and pGEX3X2000(Δ37-47, K8A) respectively. **B:** Ethidium bromide stain of 1 % agarose gel and restriction map of *Nar* I-digested pGEX3X2000(Δ37-47, N12A). Lane 1, *Pst* I-digested Lambda DNA molecular weight standards. Lanes 2 and 3, undigested pGEX3X2000(Δ37-47) and pGEX3X2000(Δ37-47, N12A) respectively. Lanes 4 and 5, *Hind* III-linearized pGEX3X2000(Δ37-47) and pGEX3X2000(Δ37-47, N12A) respectively. Lanes 6 and 7, *Nhe* I-digested pGEX3X2000(Δ37-47) and pGEX3X2000(Δ37-47, N12A) respectively. Lanes 8 and 9, *Nar* I-digested pGEX3X2000(Δ37-47) and pGEX3X2000(Δ37-47, N12A) respectively. Lanes 10 and 11, *Pvu* I-digested pGEX3X2000(Δ37-47) and pGEX3X2000(Δ37-47, N12A) respectively. bp indicates DNA sizes in base pairs. Red arc represents the coding region of GST-mSTI1.

2.3.2.4 Analysis of pGEX3X2000(N43A) and pGEX3X2000(K301A) modified plasmids

To generate pGEX3X2000(N43A) plasmid, a double base pair change (Table 2.1) was made in pGEX3X2000, yielding an additional *Eco* 47 III site. To distinguish between the parental plasmid and the modified plasmid, small scale preparations of both plasmids were digested with *Eco* 47 III (Figure 2.8A).

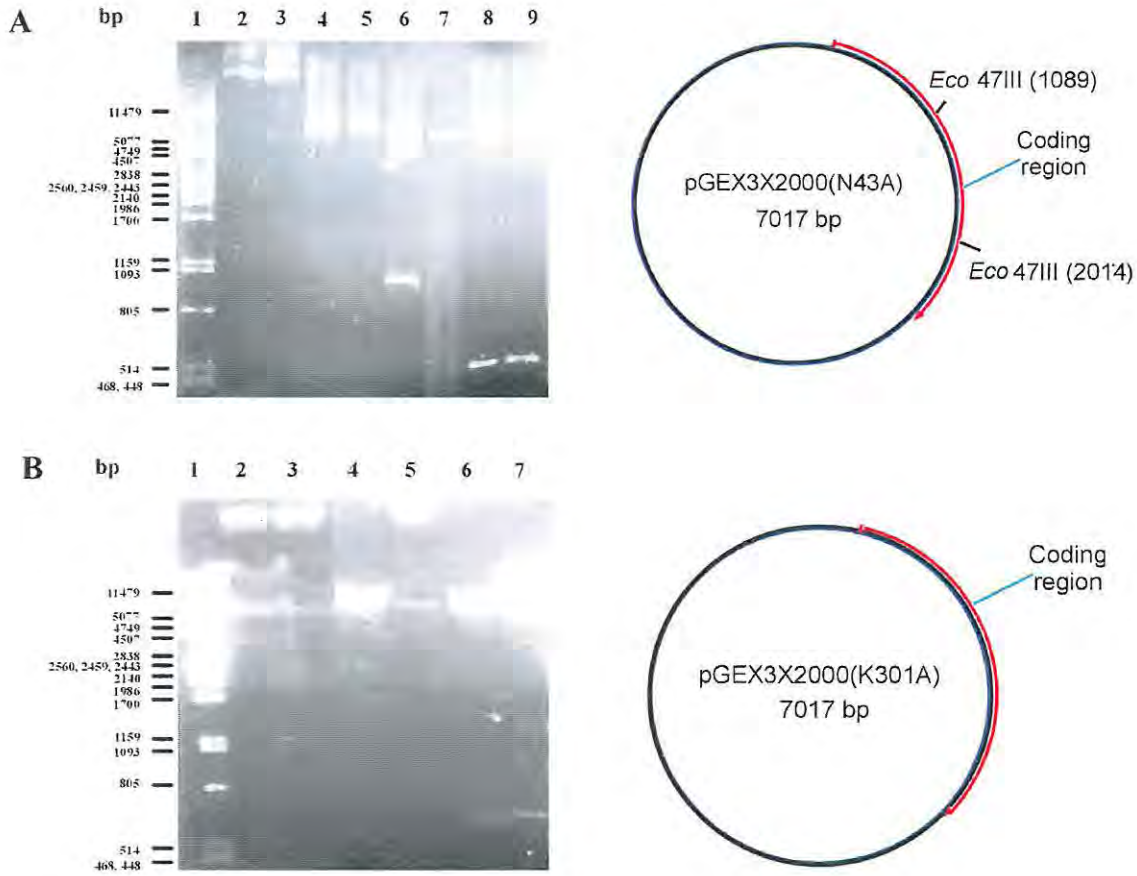

Figure 2.8: Diagnostic restriction endonuclease digestion of pGEX3X2000(N43A) and pGEX3X2000(K301A) plasmids.
A: Ethidium bromide stain of 1 % agarose gel and restriction map of *Eco* 47 III-digested pGEX3X2000(N43A). Lane 1, *Pst* I-digested Lambda DNA molecular weight standards. Lanes 2 and 3, undigested pGEX3X2000 and pGEX3X2000(N43A) respectively. Lanes 4 and 5, *Hind* III-linearized pGEX3X2000 and pGEX3X2000(N43A) respectively. Lanes 6 and 7, *Eco* 47 III-digested pGEX3X2000(N43A) and pGEX3X2000 respectively. Lanes 8 and 9, *BamH* I-digested pGEX3X2000 and pGEX3X2000(N43A) respectively. **B:** Ethidium bromide stain of 1 % agarose gel and restriction map of *Hind* III-digested pGEX3X2000(K301A). Lane 1, *Pst* I-digested Lambda DNA molecular weight standards. Lanes 2 and 3, undigested pGEX3X2000 and pGEX3X2000(K301A) respectively. Lanes 4 and 5, *Hind* III-linearized pGEX3X2000 and pGEX3X2000(K301A) respectively. Lanes 6 and 7, *BamH* I-digested pGE3X2000 and pGEX3X2000(K301A) respectively. bp indicates DNA sizes in base pairs.

As expected, the enzyme cut the parental plasmid once to generate a linear fragment of approximately 7000 bp, whereas digestion of the modified plasmid yielded two fragments of 6092 bp and 925 bp (Figure 2.8A, lanes 6 and 7). Comparison of the *BamH* I digestion products of both plasmids showed that the modified plasmid was of the right size (Figure 2.8A, lanes 8 and 9). A double codon mutation in pGEX3X2000 (Table 2.1) yielded the modified plasmid pGEX3X2000(K301A) and resulted in the loss of the only *Hind* III restriction site in the parental plasmid. Thus, *Hind* III could not digest the modified plasmid whereas it linearized the parental plasmid (Figure 2.8B, lanes 4 and 5).

2.3.3 Heterologous production and purification of GST-543 protein and its derivatives

GST-mSTI1 and its derivatives were heterologously over-produced in *E. coli* XLI Blue cells carrying pGEX3X derived plasmid constructs (Figure 2.9A) using IPTG, and the proteins were purified by *S*-hexyl glutathione agarose affinity chromatography. Generally, optimal expression was observed 5 hours after induction. Much of the protein was recovered in the soluble fractions after clarification of the extracts of the induced cells in the presence of PMSF. A significant amount of protein was eluted from the agarose beads compared to the clarified *E. coli* XLI Blue cell extracts. Thus, the proteins were highly enriched for by glutathione agarose affinity chromatography. Aliquots of the purified proteins were resolved on a 0.1 % SDS-12 % PAGE gel to determine subunit molecular weight and to estimate levels of purity. In some cases, proteins were filtered to remove aggregates before using them for binding assays. Significant amounts of proteins corresponding to the expected molecular masses were visible on the gel, with a purity of at least 85 % (Figure 2.9B).

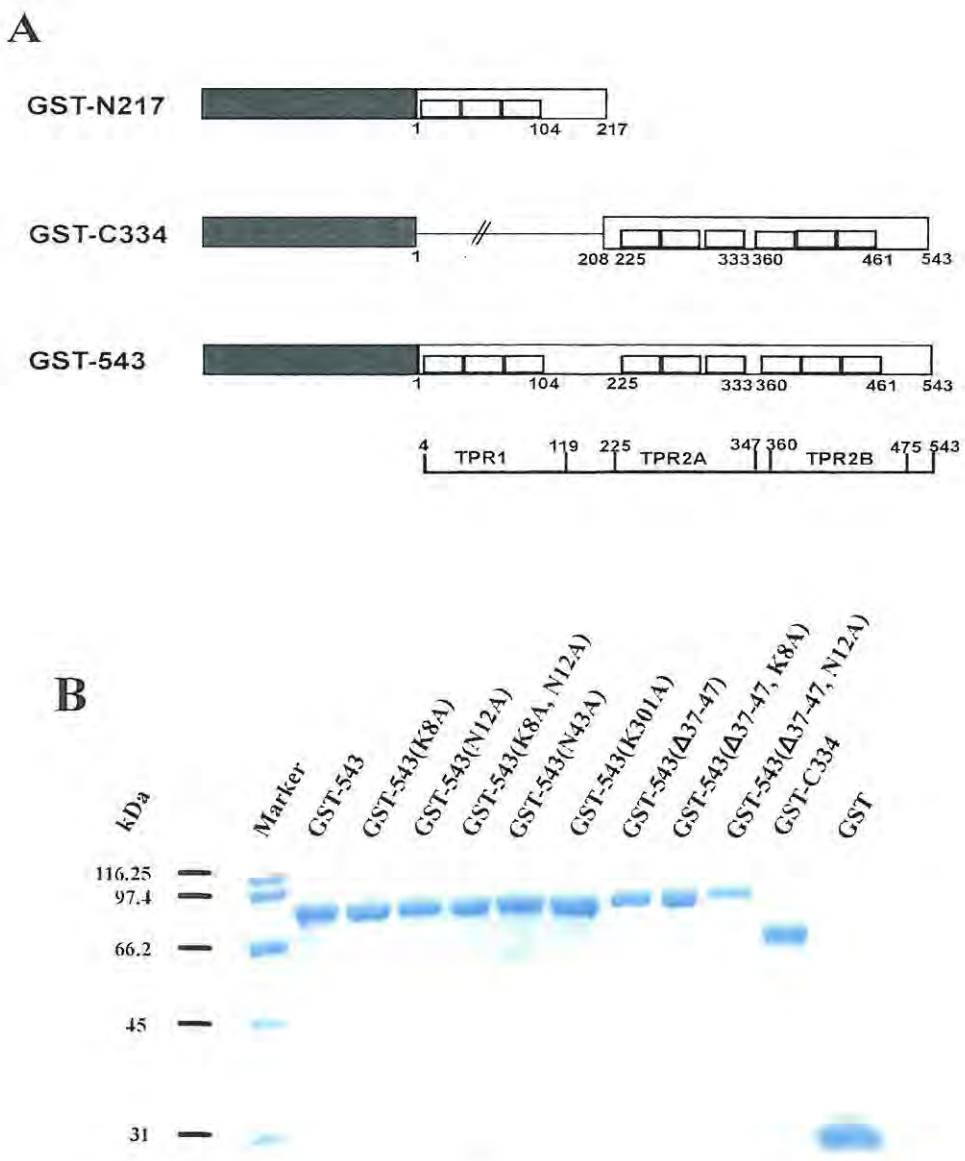

Figure 2.9: Purification of GST and GST-mSTI1 fusion proteins by glutathione agarose affinity chromatography.
A: Schematic representations of GST-mSTI1 derivatives showing the GST tag (large solid bars), mSTI1 sequence (large open bars), TPR motifs (small open bars). The numbering refers to amino acid positions in mSTI1. Extent of each TPR domain is represented on the grid. **B:** Coomassie-stained SDS-PAGE gels of GST and GST-mSTI1 fusion proteins recovered after purification by glutathione agarose affinity chromatography. Marker: Protein molecular mass standards in kiloDaltons (kDa).

2.3.4 Interactions of GST-543 protein and its mutant derivatives with Hsc70 and Hsp90

Basic residues in the TPR1 domain of mSTI1 predicted to make electrostatic interactions with the C-terminal aspartate in Hsp70 were substituted for by alanine by charged-to-alanine scanning mutagenesis. Single mutants generated included GST-543(K8A), GST-543(N12A), GST-543(N43A), GST-543(K301A), GST-543(Δ37-47,

K8A), and GST-543(Δ37-47, N12A); and the only double mutant was GST-543(K8A, N12A). GST-543(K73A), GST-543(R77A), GST-543(K229A) and GST-543(N233A) could not be produced successfully, possibly due to deleterious structural effects of the amino acid substitutions on the protein. The various GST fusion proteins were tested for their ability to bind to either Hsc70 from NIH3T3 mouse fibroblast cell extracts or to purified Hsp90. After transferring onto nitrocellulose paper, the presence of Hsc70 or Hsp90 binding to the GST-mSTI1 fusion proteins was revealed by chemiluminescence-based immunodetection using antibodies specific for Hsc70/Hsp70 or Hsp90. Previously published data indicated that the use of purified Hsc70 for the pull down assays resulted in high level of non-specific binding of Hsc70 to GST and non-Hsc70 binding GST-mSTI1 derivatives (van der Spuy *et al.*, 2000). GST-543(K301A) was tested for its ability to bind to purified Hsp90.

2.3.4.1 K8A or N12A single substitution in the TPR1 domain of mSTI1 did not affect its specific binding to Hsc70 significantly.

Results showed that GST-543(K8A) and GST-543(N12A) modified proteins were able to interact with native Hsc70 from the lysates of NIH3T3 mouse fibroblast cells at levels comparable to that of the unmodified protein (Figure 2.10). GST alone did not interact with Hsc70 to a detectable level (Figure 2.10). Therefore single mutation of Lys^{8} or Asn^{12} in mSTI1 had no major effect on its specific binding to Hsc70. It should be noted that both Lys^{8} and Asn^{12} are located in the helix A (helix 1A) of the first TPR motif in mSTI1.

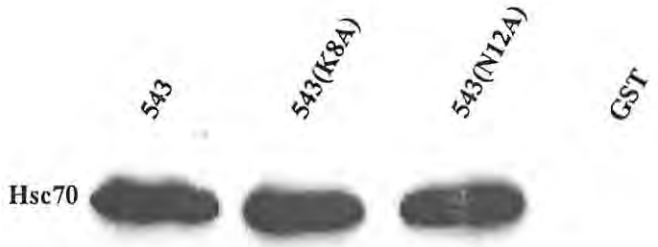

Figure 2.10: GST-543(K8A) and GST-543(N12A) modified proteins were able to interact with native Hsc70.
Autoradiogram of chemiluminescence-based immunodetection of native Hsc70 from NIH3T3 mouse fibroblast cell extracts after binding to GST-mSTI1 fusion proteins indicated above each lane. 543 is equivalent to GST-543. Information in brackets indicate substitutions carried out in the proteins.

2.3.4.2 The interactions of GST-543, GST-543(K8A) and GST-543(N12A) with native Hsc70 were specific

Doing binding assays at increasing ionic concentrations confirmed the specificity of the interaction of Hsc70 with GST-mSTI1 proteins. The interaction of GST-543 appeared to be specific as binding of the unmodified protein was found to decrease with increasing ionic concentrations (Figure 2.11A). The binding of GST-543(K8A), and GST-543(N12A) followed the same pattern at increasing ionic concentrations, though with higher sensitivity to salt (Figure 2.11, B and C, respectively). These results provided evidence that the binding of Hsc70 to the GST-mSTI1 derivatives was specific and not the recognition of misfolded proteins by Hsc70 molecular chaperone.

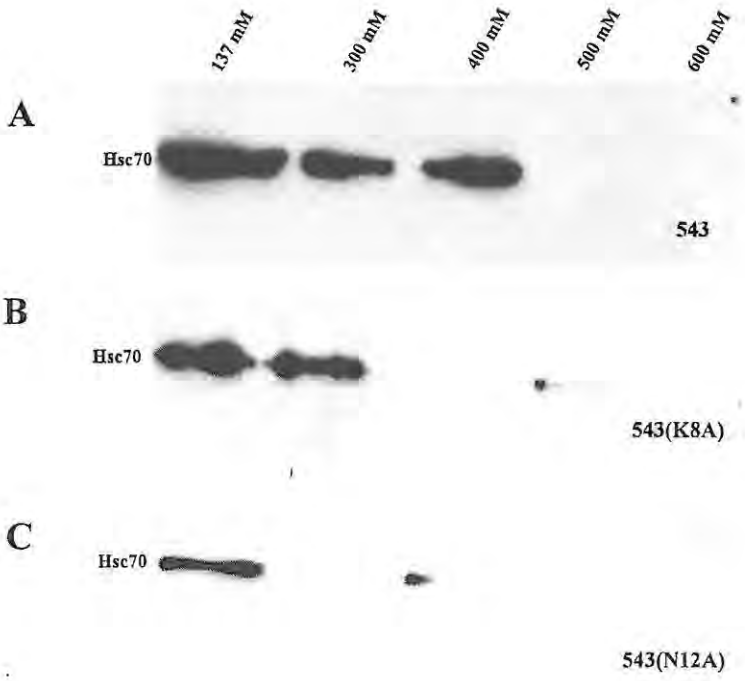

Figure 2.11: The interactions of GST-543, GST-543(K8A) and GST-543(N12A) proteins with native Hsc70 were specific.
Autoradiograms of chemiluminescence-based immunodetection of native Hsc70 from NIH3T3 mouse fibroblast cell extracts after binding with GST-543 (A), GST-543(K8A) (B) and GST-543(N12A) (C), in the presence of increasing concentrations of NaCl (137 mM to 600 mM). 543 is equivalent to GST-543. Information in brackets indicate substitutions carried out in the proteins.

2.3.4.3 K8A, N12A double substitutions in the TPR1 domain of mSTI1 abrogated its binding to Hsc70 while N43A substitution lowered but did not abrogate binding

Having shown that the single mutation of Lys^{8} or Asn^{12} in mSTI1 had no significant effect on its interaction with Hsc70, the effect of a double substitution of these amino acid residues was tested. Whereas GST-543, GST-543(K8A) and GST-543(N12A) were able to bind to Hsc70 as expected, the double mutant was found not to interact with Hsc70 at detectable level (Figure 2.12) It appeared therefore that double substitution of Lys^{8} and Asn^{12} in helix A of the first TPR motif in mSTI1 was required to cause an abrogation of its interaction with Hsc70. GST-543(N43A) modified protein was able to bind to Hsc70 but at a very reduced level (Figure 2.12). Hence, mutation of Asn^{43} in helix A of the second TPR motif resulted in a significant decrease in the affinity of mSTI1 for Hsc70 but not abrogation of interaction. As an additional negative control, a modified fusion protein, GST-543(Y27A), which has been shown not to bind to Hsc70 (van der Spuy *et al.*, 2000) was used. As expected, GST alone did not bind to Hsc70.

Figure 2.12: GST-543(K8A, N12A) protein did not interact with native Hsp70 while GST-543(N43A) bound only at low levels.
Autoradiogram of chemiluminescence-based immunodetection of native Hsc70 from NIH3T3 mouse fibroblast cell extracts after binding to GST-mSTI1 proteins indicated above each lane. 543 is equivalent to GST-543. Information in brackets indicate substitutions carried out in the proteins.

2.3.4.4 Δ37-47, K8A or Δ37-47, N12A mutations in the TPR1 domain of mSTI1 significantly lowered but did not abrogate its specific binding to Hsc70

K8A or N12A mutation was introduced into GST-543(Δ37-47) to generate GST-543(Δ37-47, K8A) or GST-543(Δ37-47, N12A) proteins respectively. Results of pull down assays showed that these proteins were able to bind to native Hsc70 with similar affinity compared to GST-543(Δ37-47), all at relatively low levels (Figure 2.13 A and B). It was therefore concluded that partial deletion of the highly conserved helix A of the second TPR motif in mSTI1 coupled with K8A or N12A mutation was not sufficient to cause abrogation of its interaction with Hsc70.

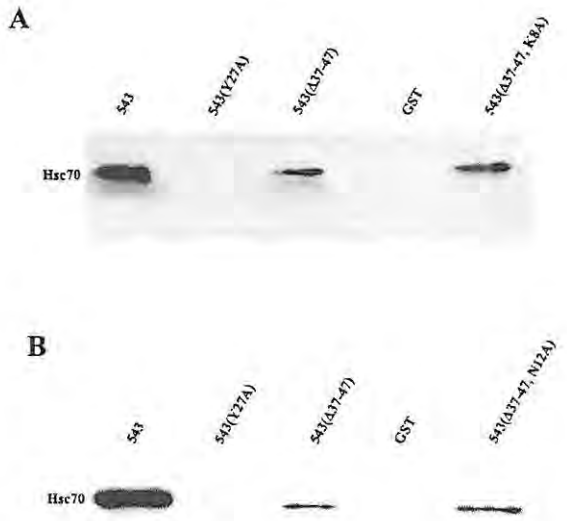

Figure 2.13: GST-543(Δ36-47, K8A) and GST-543(Δ37-47, N12A) proteins were able to interact with Hsc70 only at low levels
Autoradiograms of chemiluminescence-based immunodetection of native Hsc70 from NIH3T3 mouse fibroblast cell extracts after binding to GST-mSTI1 fusion proteins indicated above each lane. **A:** Effect of (Δ37-47, K8A) mutations in mSTI1 on its interaction with Hsc70. **B:** Effect of (Δ37-47, N12A) mutations in mSTI1 on its interaction with Hsc70. 543 is equivalent to GST-543. Information in brackets indicate mutations carried out in the proteins. (Δ37-47) represents the deletion of residues 37 to 47 in mSTI1.

2.3.4.5 K301A single substitution in the TPR2A domain of mSTI1 was sufficient to abrogate its binding to Hsp90

The ability of GST-543, GST-C334, GST-543(K301A) and GST to interact with Hsp90 was tested using purified rat αHsp90. GST-543 and GST-C334 were found to

bind to Hsp90 at comparable levels (Figure 2.14). Interestingly, GST-543(K301A) was unable to bind to Hsp90 at detectable level (Figure 2.14). No detectable background binding of GST to purified Hsp90 was observed (Figure 2.14). Thus, it seemed that single mutation of Lys^{301} to alanine in the TPR2A domain of mSTI1 was sufficient to abrogate its interaction with Hsp90.

Figure 2.14: GST-543(K301A) protein was not able to interact with Hsp90
Autoradiogram of chemiluminescence-based immunodetection of purified Hsp90 after binding to GST-mSTI1 proteins indicated above each lane. 543 and C334 are equivalent to GST-543 and GST-C334 respectively. Information in brackets indicate substitutions carried out in the proteins.

2.3.5 K8A, N12A double substitutions disrupted interactions of TPR1 with other domains in mSTI1

Steady-state fluorescence and circular dichroism spectroscopies were used to analyse the effects of the double K8A and N12A mutations on both the secondary (far- and near-UV) and tertiary structures (steady-state fluorescence) of mSTI1 using the $(His)_6$- tagged variant of the modified protein, $(His)_6$-543(K8A, N12A). The intrinsic fluorescence of the lone tryptophan in mSTI1 (Trp^{71}) was monitored. This trytophan is located in helix B of the second TPR motif, a position in relatively close proximity to the regions of the mutations, and therefore could serve effectively as a local probe of the tertiary structure of TPR1 domain. The fluorescence profile of the wild type protein, $(His)_6$-543, showed a characteristic peak at 345 nm (Figure 2.15), indicative of a partially buried residue. Completely exposed residues give a wavelength peak in the vicinity of 357 nm. The fluorescence profile of the $(His)_6$-543(K8A, N12A) mutant revealed an identical peak wavelength at 345 nm with a slight increase in intensity (Figure 2.15). This indicated a similar environment surrounding the

tryptophan residue in both proteins and suggested that there was no significant change in the tertiary structure of the TPR domain due to the double mutations.

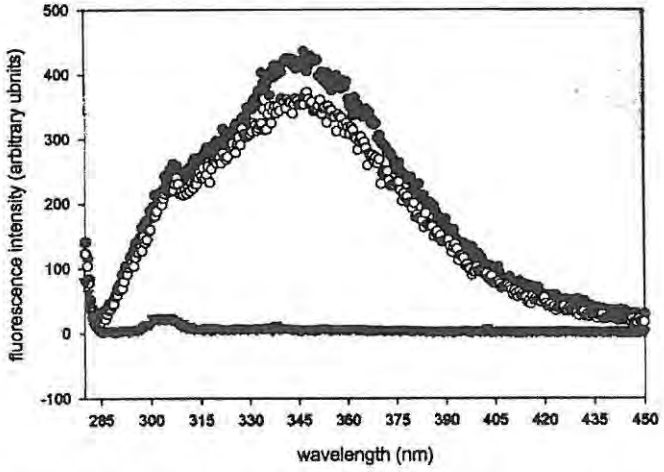

Figure 2.15: K8A, N12A double substitutions did not cause any significant change in the tertiary structure of the TPR1 domain in mSTI1.
Steady-state fluorescence using the lone tryptophan (Trp^{71}) in $(His)_6$-543 (open circles) and $(His)_6$-543 (K8A, N12A) (closed circles). $(His)_6$-543 is equivalent to $(His)_6$-tagged full-length mSTI1 protein.

However, both far- and near-UV circular dichroisms revealed an apparent loss of helical content in the $(His)_6$-543 (K8A, N12A) variant protein, to about 25 %. This was illustrated by the decrease in ellipticity observed in the spectra of the double mutant protein (Figure 2.16). These data suggested that K8A, N12A double substitutions had disrupted interactions outside the TPR1 domain.

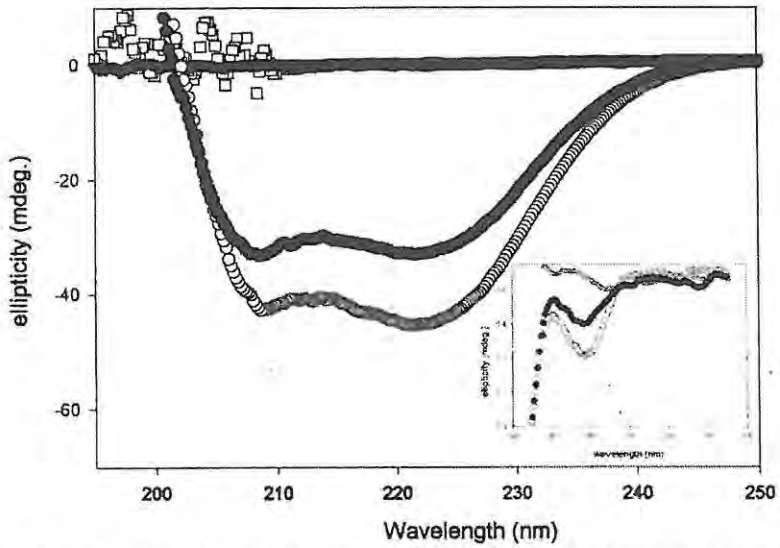

Figure 2.16: Far- and near-UV circular dichroisms revealed an apparent loss of helical content in the $(His)_6$-543 (K8A, N12A) modified protein.
Far-UV circular dichroism spectra of $(His)_6$-543 (open circles) and $(His)_6$-543(K8A, N12A) (closed circles) in 20 mM sodium phosphate buffer, pH 7.5. Spectra are an average of 10 runs. The insert describes the near-UV dichroism spectra of $(His)_6$-543 (open circles) and $(His)_6$-543(K8A, N12A) (closed circles) in the same buffer. The horizontal line in both figures represents buffer control.

2.4 Discussions

Prior to the generation of crystal structures of the TPR domains of Hop, hypotheses were based on sequence alignments and the crystal structure of the only TPR domain in protein phosphatase 5 (Das *et al.*, 1998). Using mutational analysis, the Hsp70 and Hsp90 interacting domains of Hop and mSTI1 were mapped to the N- terminal and central TPR domains respectively (Chen *et al.*, 1997; Lassle *et al.*, 1997; van der Spuy *et al.*, 2000). In addition, it has been shown that the amino acid residues 1 to 109 in the N-terminal TPR domain in mSTI1, without extensive flanking regions are necessary and sufficient for its interaction with Hsc70 (van der Spuy *et al.*, 2000). Furthermore, previous data suggested that the TPR consensus residue Tyr^{27} in the first TPR motif of mSTI1 might play a crucial structural role by holding charged residues in the first TPR motif in proper position for interaction with complementary charged groups in Hsc70 (van der Spuy *et al.*, 2000).

The crystal structures of the TPR domains of Hop in complexes with C-terminal Hsp70 heptapeptide and Hsp90 pentapeptide (Scheufler *et al.*, 2000) corroborated previous data in predicting that certain basic residues protruding into the TPR groove were required for TPR domain-mediated interaction of Hop with both Hsp70 and Hsp90 (Das *et al.*, 1998; Russell *et al.*, 1999; Scheufler *et al.*, 2000). Among the residues in the TPR1 domain of Hop predicted to be required for the formation of the so-called two-carboxylate clamp with the C-terminal aspartate in Hsp70 are Lsy^{8}, Asn^{12}, Asn^{43}, Lys^{73} and Arg^{77} (Scheufler *et al.*, 2000). In the TPR2A domain, the topologically equivalent residues are Lys^{229}, Asn^{233} Asn^{264}, Lys^{301} and Arg^{305} (Scheufler *et al.*, 2000).

Multiple sequence alignment revealed that these charged residues are strictly conserved among homologous STI1 proteins. In another alignment, the same basic residues were compared in the Hsc70-binding TPR domains of non-homologous Hsc70-interacting proteins of colon cancer antigen 7 (NY-CO-7; Liu *et al.*, 1999), carboxyl terminus of Hsc70-interacting protein (CHIP; Ballinger *et al.*, 1999), Hop (Honore *et al.*, 1992), mSTI1 (Blatch *et al.*, 1997), human small glutamine-rich protein (hSGT; Liu *et al.*, 1999), tetratricopeptide repeat domain 1 (TPR1; Liu *et al.*, 1999), tetratricopeptide repeat domain 2 (TPR2; Liu *et al.*, 1999) and Hsc70-

interacting protein (Hip; Hohfeld *et al.*, 1995). Conservation was found to be less strict in these proteins, especially at positions equivalent to Lys^{73} and Arg^{77} in Hop. Except for Hip, all these proteins interact with Hsc70 via its C-terminal EEVD motif. Similar trends of conservation were observed from multiple sequence alignments of TPR2A domains except that in non-homologous Hsp90-binding proteins, residues at positions equivalent to Asn^{233} and Asn^{264} in Hop were less conserved.

Based on sequence alignments of the TPR domains of various Hsp70- and/or Hsp90-interacting proteins and Hop's crystal structures, it was hypothesized that these basic residues in the TPR1 and TPR2A domains of mSTI1 formed a network of electrostatic interactions with the C-terminal aspartate (Asp 0) in Hsp70 and Hsp90 respectively; and that these interactions were necessary for the general binding of these molecular chaperones to mSTI1. To test this hypothesis, a charged-to-alanine scanning mutagenesis of these residues in both TPR domains was done. The results showed that K8A or N12A single mutation in the TPR1 domain of mSTI1 did not affect its interaction with native Hsc70 significantly. It could not be ascertained whether the observed higher sensitivity of the two mutants to increase in salt concentration was significant or not. Overall, this result was in line with our hypothesis that a network of electrostatic interactions was involved in the general binding of mSTI1 to Hsp70. The side chains of Lys^{8} and Asn^{12} were proposed to form direct hydrogen bonds with the C-terminal main chain carboxylate of aspartate in Hsp70 (Scheufler, *et al.*, 2000). It required a double knockout of Lys^{8} and Asn^{12} to sufficiently abrogate interaction of mSTI1 with Hsc70. This result suggested that the collective electrostatic contacts made by Lys^{8} and Asn^{12} in the TPR1 domain of mSTI1 are necessary for successful binding to Hsc70. A highly sensitive and quantitative approach, surface plasmon resonance spectroscopy, was used to quantitate the affinities of the interactions, as discussed in latter chapters.

On the other hand, single mutation of Lys^{301} in the TPR2A domain of mSTI1 was sufficient to cause an abrogation of its interaction with Hsp90. From the crystal structure, TPR2A donates one hydrogen bond to the side chain of Asp 0 via Lys^{301} (Scheufler *et al.*, 2000). Based on the data from this study, it seems that a higher level of complexity may be involved in the interaction of TPR1 domain with Hsp70 than in

the interaction of TPR2A with Hsp90. Effects of mutations of topologically equivalent residues such as Lys^{73} and Lys^{301} would have provided a more appropriate comparison of data. Recently, the sequence motifs for TPR1 and TPR2A binding were defined by alanine scanning of the C-terminal octapeptides of Hsp70 and Hsp90 and by screening of combinatorial peptide libraries (Brinker *et al.*, 2002). It was concluded that the formation of the Hsp70-Hop complex depended not only on recognition of the C-terminal Hsp70 heptapeptide but also on additional contacts between Hsp70 and Hop (Brinker *et al.*, 2002). In addition to this, the interaction of TPR2A with the C-terminal pentapeptide was identified as the core and sufficient contact for successful binding of Hop to Hsp90.

Results from steady state fluorescence spectroscopy suggested that there was no significant disruption in the overall tertiary structure of the TPR1 domain. However, data from circular dichroism spectroscopy indicated that these mutations caused apparent loss of helicity in the protein. It could not be deduced from the CD data exactly what part of the protein was affected. mSTI1/Hop is very rich in helical structures, and has a unique arrangement of these secondary structures across its entire length. In fact, secondary structure predictions suggested that mSTI1 was composed mainly of α-helices and coils with no tendency to form β sheets. The crystal structures in part, confirmed these predictions. One may conclude that the overall loss of helical content was not localized; rather it was a cumulative effect within the entire protein. On the other hand, one may conclude that some perturbations occurred in specific domains of the protein outside the TPR1 domain that make contact with TPR1, resulting in the loss of helical content. Hence, the observed abrogation of binding to Hsc70 due to the double substitution might have occurred primarily as a result of loss of important electrostatic contacts with the TPR domain and secondarily as a result of disruption of contacts with other domains required for complete and tight interaction with Hsc70.

Support for this hypothesis comes from earlier observations that mutation of the C-terminal DPEV motif of Hop or its DPAM to APAV and APAM respectively caused a reduction in Hop's ability to bind to Hsc70 (Chen and Smith, 1998). This is a very interesting phenomenon since truncation of this region in Hop caused only a partial

loss of Hsp70 binding (Chen *et al.*, 1996). In a helix-rich protein such as mSTI1, it is most likely that this C-terminal region of the protein folds into a helical structure. Of interest however, is the observation that binding of Hop to Hsp90 was unaffected by mutations in this region of the protein (Chen and Smith, 1998).

Mutation of Asn^{43} to alanine significantly lowered but did not abrogate mSTI1-Hsc70 interaction. Asn^{43} occurs within helix A of the second TPR motif (helix 2A), a region that is highly conserved in homologous STI1 TPR domains. Deletion of this highly conserved block of amino acid residues coupled with the mutation of Lys^{8} or Asn^{12} to alanine significantly lowered but did not abrogate binding of mSTI1 to Hsc70. This result is consistent with and extends earlier report that removal of the highly conserved part of helix 2A lowered but did not abolish binding of mSTI1 to Hsc70 (van der Spuy *et al.*, 2000). It is possible that there was a shift of the helices to compensate for the partial deletion of helix 2A. The side chain carbonyl of Asn^{43} makes a direct hydrogen bond contact with the backbone amide of Asp 0 of Hsc70, and an indirect contact with the side chain carboxylate of the same residue that is mediated by a tightly bound water molecule. The interactions of Asn^{43} and other helix 2A residues appear not to be as important for Hsc70 binding as the electrostatic contacts made collectively by Lys^{8} and Asn^{12} with Asp 0. These results, which are partially consistent with crystallographic predictions for the Hop-Hsp70 peptide complex, further provide evidence that a network of electrostatic interactions was necessary for the binding of mSTI1 to Hsc70.

Therefore we conclude that the collective electrostatic contacts made by Lys^{8} and Asn^{12} in the TPR1 domain of mSTI1 define part of the minimum critical contacts necessary for successful binding to Hsc70, but for complete and tight ligand binding other contacts outside the TPR domain are required.

Chapter Three

Characterization of the interactions involved in determining specificity of binding of mSTI1 to Hsc70 and Hsp90

3.1 Introduction

There is ample experimental evidence that demonstrate the involvement of hydrophobic contacts in TPR-mediated protein-protein interactions (Gounalaki *et al.*, 2000; Scheufler *et al.*, 2000 and Brinker *et al.*, 2002). Data from Hop's crystal structures in complexes with C-terminal peptides of Hsp70 and Hsp90 suggested that discrimination between the C-termini of the two molecular chaperones depended largely on hydrophobic and van der Waals interactions between residues in Hop's TPR domains and residues upstream of the EEVD motif (Scheufler *et al.*, 2000). For example, Ala^{46}, Ala^{49} and Lys^{50}, all in helix A of the second TPR motif (helix 2A) in TPR1 of Hop make hydrophobic contacts with the isoleucine (Ile -4) of the IEEVD sequence in Hsp70 while Tyr^{236} and Glu^{271} in helix A of the first TPR motif (helix 1A) and helix A of the second TPR motif (helix 2A) of TPR2A, respectively, make important hydrophobic contacts with the methionine (Met -4) of the MEEVD sequence in Hsp90. Pro -6 which is further upstream of the EEVD motif in Hsp70 exists in a hydrophobic cavity formed by Glu^{83} and Phe^{84} of helix A of the third TPR motif (helix 3A) in TPR1. Val -1 in the EEVD motif of Hsp70 makes hydrophobic contacts with Asn^{12} and Leu^{15} in helix 1A and with Asn^{43} in helix 2A of TPR1. In the TPR2A complex, Val -1 in the EEVD motif of Hsp90 is in hydrophobic contacts with Asn^{233}, Asn^{264} and Ala^{267}.

Based on the predictions from the three-dimensional structure of the TPR domains of Hop in complex with their respective peptides (Scheufler *et al.*, 2000), topologically equivalent residues involved in specificity determination were identified in TPR1 versus TPR2A, that differed greatly in the nature of their contacts with residues upstream of the EEVD motif of their respective Hsps. It was observed that Tyr^{236},

Phe^{270} and Glu^{271} in TPR2A were significantly different from but topologically equivalent to Leu^{15}, Ala^{49} and Lys^{50} respectively, in TPR1 (Figure 3.1). It was reasoned that by doing simple amino acid substitutions of L15Y, A49F, K50E, and Y236L, F270A, E271K, it would be possible to swap the binding specificity of TPR1 and TPR2A domains respectively. Theoretically, these substitutions should allow TPR1 to accommodate Met -4 of Hsp90 and TPR2A to accommodate Ile -4 of Hsc70, respectively. Therefore, the hypothesis proposed was firstly, that L15Y, A49F and K50E substitutions in TPR1 domain of mSTI1 would result in loss of ability to bind Hsc70 and gain of capacity to bind Hsp90 and secondly, that Y236L, F270A, and E271K substitutions in TPR2A would result in loss of ability to bind Hsp90 and gain of capacity to bind Hsc70. In the first part of the hypothesis, single, double and triple mutants were generated using a C-terminal truncated mSTI1 protein, GST-N217 (with TPR2A and TPR2B domains removed) as follows: GST-N217(L15Y), GST-N217(A49F, K50E), and GST-N217(L15Y, A49F, K50E). In addition, a triple mutant of the full-length GST-543 protein, GST-543(L15Y, A49F, F50E) was generated. These modified proteins were tested for their ability to bind both Hsc70 and Hsp90. Conversely, an N-terminal truncated mutant protein GST-C334, incapable of binding to Hsc70, was used to generate the following modified proteins: GST-C334(Y236L), GST-C334(F270A, E271K), and GST-C334(Y236L, F270A, E271K) and the proteins were also tested for their ability to bind to both Hsp90 and Hsc70.

3.2 Experimental procedures

3.2.1 Generation and analysis of modified plasmids

For this study, modified plasmids were generated from the parental plasmid, pGEX3X2000. The plasmids pGEX3X1400 (encoding mutant GST-543 with TPR1 domain removed) and pGEX3X700 (encoding mutant GST-543 with TPR2A and TPR2B domains removed) were generated prior to this study (Lassle *et al.*, 1997). Mutations were carried out and confirmed as described in section 2.2.1. To obtain pGEX3X700(L15Y, A49F, K50E) and pGEX3X2000(L15Y, A49F, K50E), either the single mutant or double mutant was first generated and then used as template for the triple mutant. Similar procedure was used to generate pGEX3X1400(Y236L, F270A, E271K) (Table 3.1).

Table 3.1: Generation of modified plasmids used for specificity studies

Modified plasmid	Codon change(s)	Forward primers used for mutagenesis	Diagnostic restriction endonuclease
pGEX3X700 (L15Y)	ctg : tat aag : aaa	gaagggcaataaagcctatagtgctgggaac	*Dra* II
pGEX3X700 (A49F, K50E)	gcc : ttc aag : gag gca : gcg	caatcgctctgcggcctacttcgagaaaggagac	*Pst* I
pGEX3X700 (L15Y, A49F, K50E)	As in rows 2 and 3 above	As in rows 2 and 3 above	As in rows 2 and 3 above
pGEX3X2000 (L15Y, A49F, K50E)	As in rows 2 and 3 above	As in rows 2 and 3 above	As in rows 2 and 3 above
pGEX3X1400 (Y236L)	tac : ctt	ggaaatgatgcccttaagaagaaag	*Afl* II
pGEX3X1400 (F270A, E271K)	ttt : gct gag : aag cac : cat	gctgtgcatgctaagaagggcgac	*ApaL* I
pGEX3X1400 (Y236L, F270A, E271K)	As in rows 6 and 7 above	As in rows 6 and 7 above	As in rows 6 and 7 above

3.2.2 Heterologous production and purification of recombinant GST-N217, GST-C334 and their modified derivatives

As described in section 2.2.2, solubility of proteins was determined before large scale production and purification. Similar procedures were used as described in section 2.2.2.

3.2.3 Glutathione agarose pull down assays

In separate reactions, equal final concentrations of GST-N217, GST-C334 and their modified derivatives were adsorbed onto GSH beads before adding either cytosolic fractions of NIH3T3 cells or purified Hsp90. Binding was allowed to occur for 2 hours at 4^0C before the beads were washed extensively to remove unbound proteins. Further steps were as described in section 2.2.3.

3.2.4 Bioinformatic analysis and homology modeling

All protein sequence alignments were generated using PepTools (Wishart *et al.*, 1997). The co-ordinates used to draw figures 3.1B and 3.2B were generated using WHAT IF (Vriend, 1990). Both figures 3.1 and 3.2 were visualised and drawn with MOLSCRIPT (Kraulis, 1991).

3.3 Results

3.3.1 The TPR1 and TPR2B domains of Hop/mSTI1 have similar specificity determinants

Figures 3.1 A and B show the amino acid residues in the TPR1 domain of mSTI1/Hop that are predicted by crystal structures to be important in determining specificity of binding of Hop to Hsp70. Similarly, Figures 3.2 A and B show topologically equivalent residues in the TPR2A that are predicted by crystal structures to be important in determining specificity of binding of Hop to Hsp90. Multiple sequence alignment (Figure 3.3) revealed that the residues that determine specificity of binding of TPR1 domain in mSTI1 to Hsc70 are conserved in TPR2B domain. This suggests that TPR2B may be a second Hsc70-binding domain in Hop/mSTI1. Recent quantitative analysis of Hsp70-Hop-Hsp90 interactions revealed that TPR2B domain had a very low affinity for Hsp70, whereas it did not interact at all with Hsp90 (Brinker *et al.*, 2002). Other evidence in support of this observation comes from binding and dissociation data that revealed complex multiphasic binding curves for the interaction of Hop with Hsc70, whereas with Hsp90, it was monophasic (Brinker *et al.*, 2002). Multiphasic binding curves imply conformational flexibility of the interacting molecules and the existence of high- and low-affinity binding sites. Put together, the evidence mentioned above, and other results from this study that are discussed later (Chapter 4), suggest that Hop/mSTI1 possesses two Hsp70-binding sites, a high affinity site (TPR1 domain) and a low affinity site (TPR2B domain). However, this claim is yet to be experimentally verified.

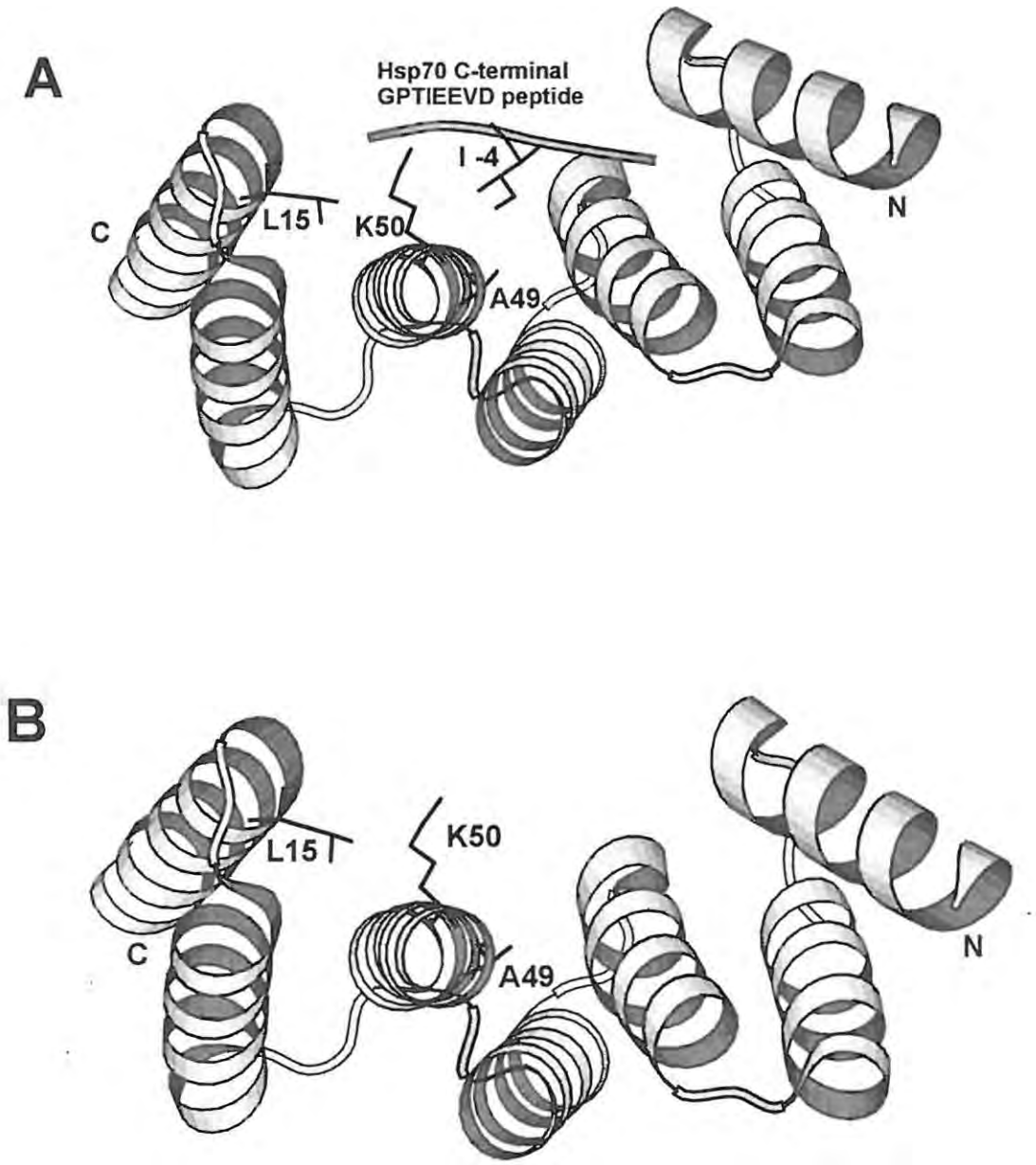

Figure 3.1: Hop N-terminal TPR domain in complex with the C-terminal Hsp70 heptapeptide showing residues predicted to determine specificity of binding.

A: Ribbon representation of the crystal structure of the N-terminal (TPR1; PDB code 1ELW, Scheufler *et al.*, 2000) domain of Hop in complex with the C-terminal heptapeptide of Hsp70. **B:** Ribbon representation of the N-terminal TPR domain of mSTI1 modeled on the crystal structure of Hop.

TPR domains are shown as ribbons, peptides as rods and amino acid residues as sticks. The TPR residue is labeled by the single letter code and a number that relates to its position in the primary amino acid sequence. N and C indicate N-terminal and C-terminal ends of the polypeptide respectively. Residues shown are predicted to make hydrophobic contacts with Isoleucine -4 (I -4), and that these contacts are critical in determining specificity of binding. The co-ordinates for mSTI1 model were generated using WHAT IF (Vriend, 1990), and both figures were drawn with MOLSCRIPT (Kraulis, 1991).

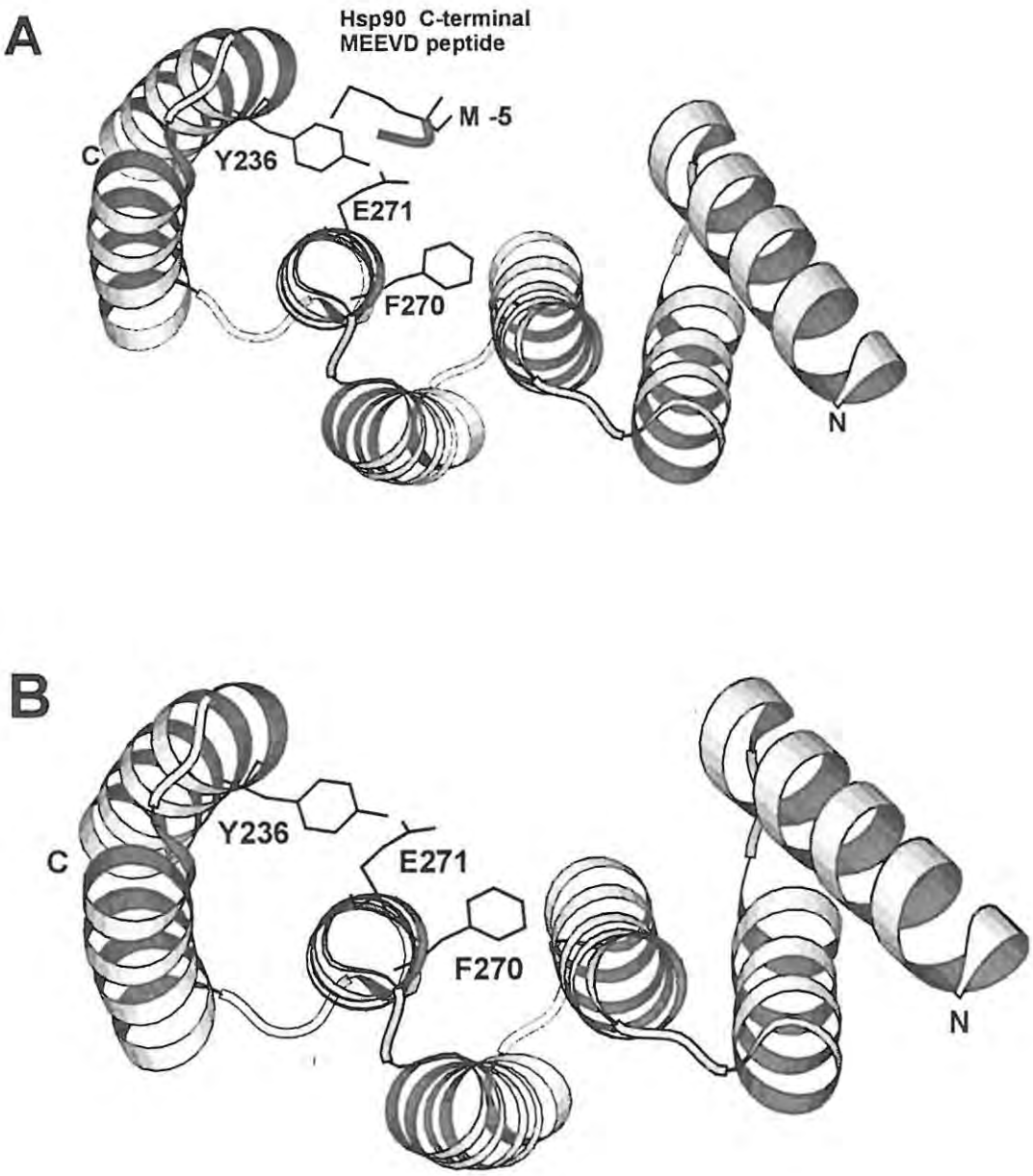

Figure 3.2: Hop central TPR domain in complex with the C-terminal Hsp90 pentapeptide showing residues predicted to determine specificity of binding.
A: Ribbon representation of the crystal structure of the central TPR (TPR2A; PDB code 1ELR, Scheufler *et al.*, 2000) domain of Hop in complex with the C-terminal pentapeptide of Hsp90.
B: Ribbon representation of the central TPR domain of mSTI1 modeled on the crystal structure of Hop. TPR domains are shown as ribbons, peptides as rods and amino acid residues as sticks. The TPR residue is labeled by the single letter code and a number that relates to its position in the primary amino acid sequence. N and C indicate N-terminal and C-terminal ends of the polypeptide respectively. Residues shown are predicted to make hydrophobic contacts with Methionine -5 (M -5), and that these contacts are critical in determining specificity of binding. The co-ordinates for mSTI1 model were generated using WHAT IF (Vriend, 1990), and both figures were drawn with MOLSCRIPT (Kraulis, 1991).

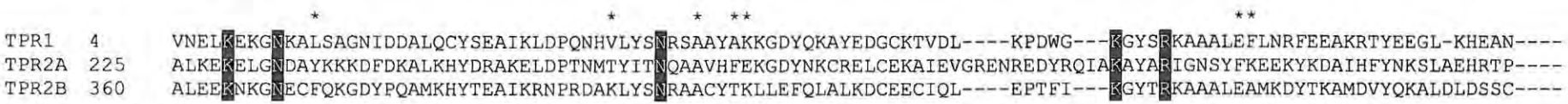

Figure 3.3: Multiple sequence alignment of the TPR1, TPR2A and TPR2B domains of mSTI1.

Residues that are predicted to form a two-carboxylate clamp with the terminal aspartate in Hsp70 are shaded in black while asterisk (*) indicates positions of residues predicted to determine specificity of binding. TPR1; N-terminal TPR domain of mSTI1, TPR2A; first central TPR domain of mSTI1, and TPR2B; C-terminal TPR domain of mSTI1. The alignment was generated using PepTools (Wishart *et al.*, 1997).

3.3.2 pGEX3X700 and pGEX3X1400 modified plasmids were successfully generated

Complementary mutagenic oligonucleotide primers were used to amplify the plasmids pGEX3X700 and pGEX3X1400 to generate the following modified plasmids, pGEX3X700(L15Y), pGEX3X700(A49F, K50E), pGEX3X700(L15Y, A49F, K50E), pGEX3X1400(Y236L), pGEX3X1400(F270A, E271K) and pGEX3X1400(Y236L, F270A, E271K). The modified plasmid pGEX3X2000(L15Y, A49F, K50E) was generated from pGEX3X2000. The linear amplification products were digested with *Dpn* I after which 15 µl was resolved on a 1 % agarose gel stained with ethidium bromide. 1 µl of the amplification product was used to transform *E. coli* XLI Blue. Modified plasmids isolated from *E. coli* harbouring them were digested with their respective diagnostic restriction endonucleases to confirm mutations engineered therein. In addition, automated DNA sequencing using primers confirmed the mutations.

3.3.2.1 Analysis of pGEX3X700(L15Y) and pGEX3X700(A49F, K50E) plasmids

pGEX3X700(L15Y) modified plasmid was generated from the parental plasmid, pGEX3X700, by a single codon change (Table 3.1). A silent mutation of "aag" codon to "aaa" resulted in the deletion of a *Dra* II site (Table 3.1). Small scale DNA preparations of both parental and modified plasmids were digested with *Dra* II to confirm mutations. Digestion of the unmutated plasmid yielded three fragments while the modified plasmid yielded only two fragments due to the loss of a *Dra* II site (Figure 3.4A, lanes 6 and 7). *BamH* I digestion of both plasmids confirmed that their sizes were the same (Figure 3.4A, lanes 8 and 9). To generate the plasmid pGEX3X700(A49F, K50E), two codon changes were made in pGEX3X700 (Table 3.1). An additional single base change (Table 3.1) resulted in the loss of a *Pst* I site, and this was used for diagnostic purpose. Digestion of pGEX3X700 with *Pst* I was expected to release four fragments. As shown in Figure 3.4B (lane 6), two small fragments could not be retained in a 1 % agarose gel, however the other two fragments were visible. In the pGEX3X700(A49F, K50E) plasmid, the loss of a *Pst* I site yielded a larger fragment of 493 bp, which could be seen visibly on the gel

(Figure 3.4B, lane 7). Similarly, *BamH* I digestion was used to confirm the sizes of the two plasmids (Figure 3.4B, lanes 8 and 9).

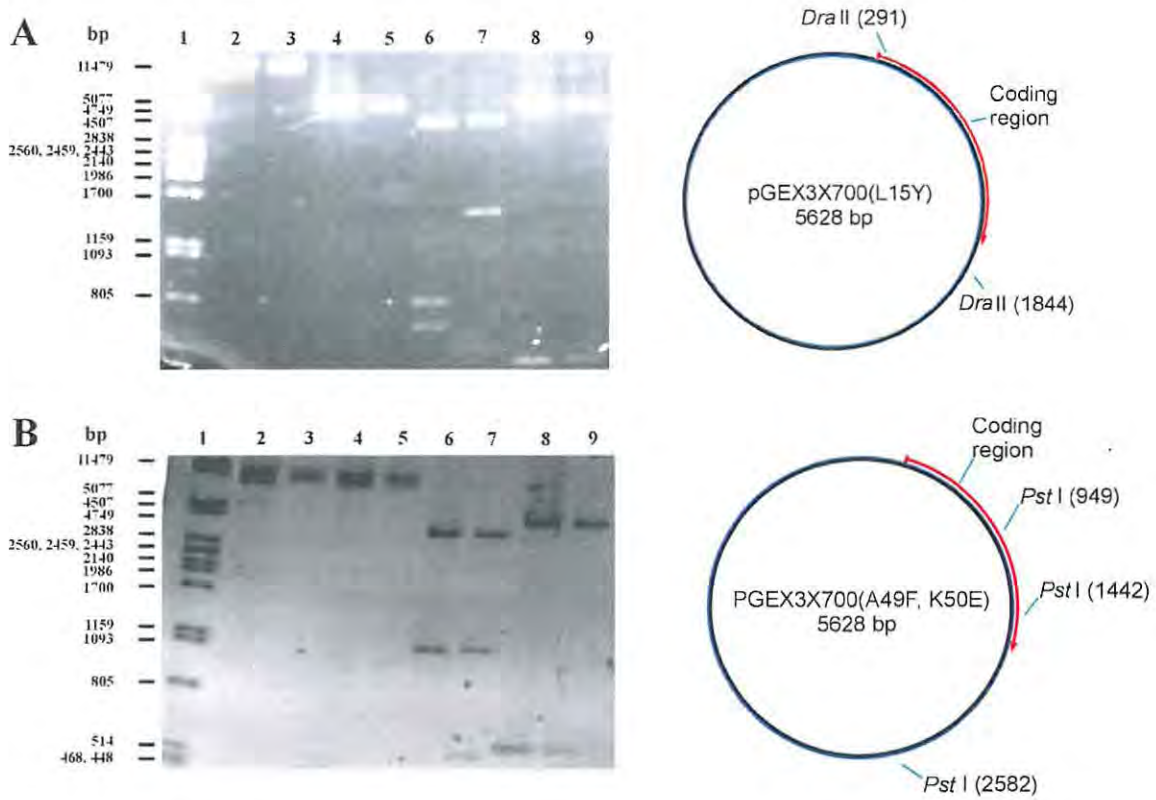

Figure 3.4: Diagnostic restriction endonuclease digestion of pGEX3X700(L15Y) and pGEX3X700(A49F, K50E) plasmids.
A: Ethidium bromide stain of a 1 % agarose gel and restriction map of *Dra* II-digested pGEX3X700(L15Y). Lane 1, *Pst* I-digested Lambda DNA molecular weight standards. Lanes 2 and 3, undigested pGEX3X700 and pGEX3X700(L15Y) respectively. Lanes 4 and 5, *Hind* III-digested pGEX3X700 and pGEX3X700(L15Y) respectively. Lanes 6 and 7, *Dra* II-digested pGEX3X700 and pGEX3X700(L15Y) respectively. Lanes 8 and 9, *BamH* I-digested pGEX3X700 and pGEX3X700(L15Y) respectively. **B:** Ethidium bromide stain of a 1 % agarose gel and restriction map of *Pst* I-digested pGEX3X700(A49F, K50E). Lane 1, *Pst* I-digested Lambda DNA molecular weight standards. Lanes 2 and 3, undigested pGEX3X700 and pGEX3X700(A49F, K50E) respectively. Lanes 4 and 5, *Hind* III-digested pGEX3X700 and pGEX3X700(A49F, K50E) respectively. Lanes 6 and 7, *Pst* I-digested pGEX3X700 and pGEX3X700(A49F, K50E) respectively. Lanes 8 and 9, *BamH* I-digested pGEX3X700 and pGEX3X700(A49F, K50E) respectively. bp indicates DNA sizes in base pairs.

3.3.2.2 Analysis of pGEX3X700(L15Y, A49F, K50E) plasmid

To generate the plasmid, pGEX3X700(L15Y, A49F, K50E), previously confirmed modified plasmid pGEX3X700(L15Y) was entirely amplified using complementary primers containing the mutations A49F and K50E. All the mutations were confirmed as described in section 3.3.2.1 (Figure 3.5, lanes 6 and 7, 8 and 9, 10 and 11).

Figure 3.5: Diagnostic restriction endonuclease digestion of pGEX3X700(L15Y, A49F, K50E) plasmid.
Ethidium bromide stain of a 1 % agarose gel and restriction map of *Pst* I and *Dra II*-digested pGEX3X700(L15Y, A49F, K50E). Lane I, *Pst* I-digested Lambda DNA molecular weight standards. Lanes 2 and 3, undigested pGEX3X700 and pGEX3X700(L15Y, A49F, K50E) respectively. Lanes 4 and 5, *Nco* I-linearized pGEX3X700 and pGEX3X700(L15Y, A49F, K50E) respectively. Lanes 6 and 7, *Pst* I-digested pGEX3X700 and pGEX3X700(L15Y, A49F, K50E) respectively. Lanes 8 and 9, *Dra* II-digested pGEX3X700 and pGEX3X700(L15Y, A49F, K50E) respectively. Lanes 10 and 11, *BamH* I-digested pGEX3X700 and pGEX3X700(L15Y, A49F, K50E) respectively. bp indicates DNA sizes in base pairs.

3.3.2.3 Analysis of pGEX3X1400(Y236L) and pGEX3X1400(F270A, E271K) plasmids

Changing a "tac" codon to "ctt" in the template plasmid DNA, pGEX3X1400, introduced a unique *Afl* II site and formation of a modified plasmid, pGEX3X1400(Y236L) (Table 3.1). Hence, while *Afl* II does not cut the parental plasmid, it linearizes the modified plasmid (Figure 3.6A, lanes 6 and 7). To generate the plasmid pGEX3X1400(F270A, E271K), two codon changes and a base pair change were made as described in Table 3.1. The single base pair change resulted in the loss of an *ApaL* I restriction site. Digestion of pGEX3X1400 with *ApaL* I should yield five fragments of 1776 bp, 1339 bp, 1246 bp, 1118 bp and 910 bp while pGEX1400(F270A, E271K) should yield four fragments of 2894 bp, 1339 bp, 1246, bp and 910 bp (Figure 3.6B, lanes 6 and 7). However, *ApaL* I did not cut the plasmids to completion, hence the presence of an additional fragment running close to 4 kb in lane 6 and another fragment of approximately 2140 bp in lane 7. However, the mutations were further confirmed by automated DNA sequencing.

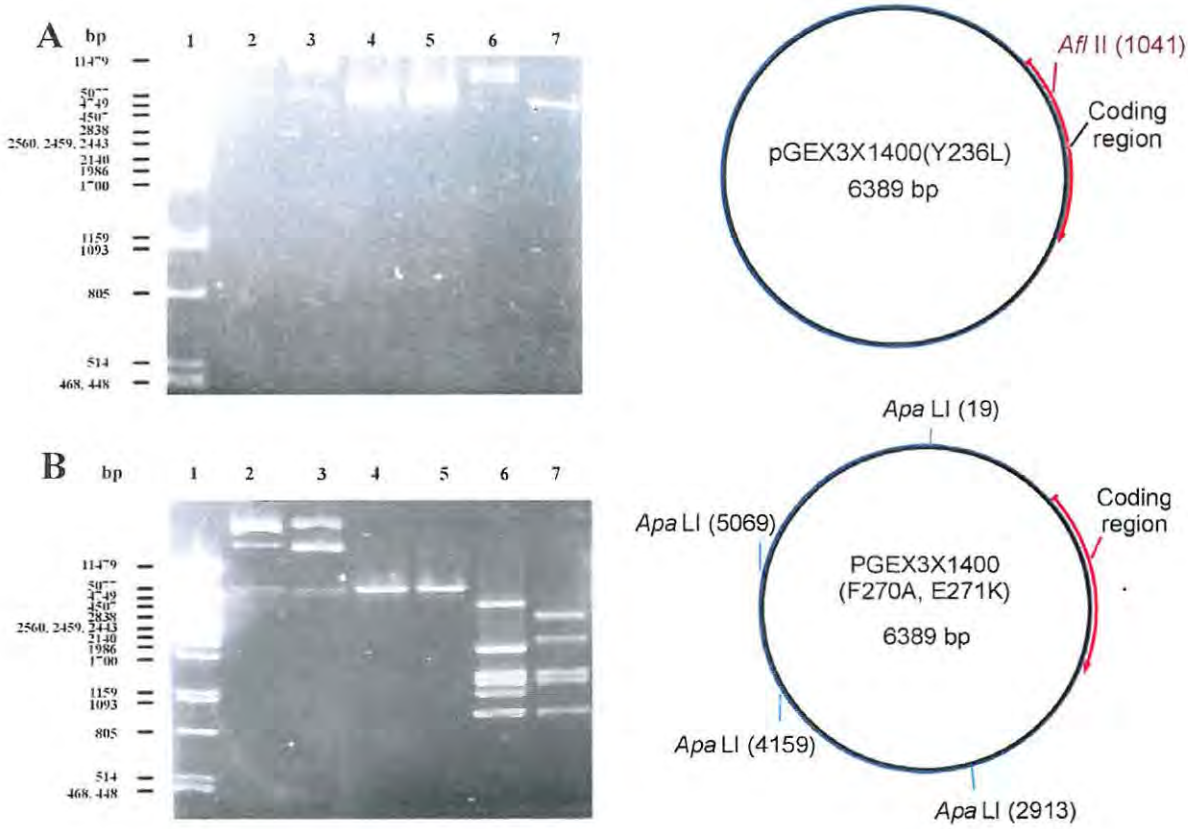

Figure 3.6: Diagnostic restriction endonuclease digestion of pGEX3X1400(Y236L) and pGEX3X1400(F270A, E271K) plasmids.
A: Ethidium bromide stain of a 1 % agarose gel and restriction map of *Afl* II-digested pGEX3X1400(Y236L). Lane 1, *Pst* I-digested Lambda DNA molecular weight standards. Lanes 2 and 3, undigested pGEX3X1400 and pGEX3X1400(Y236L) respectively. Lanes 4 and 5, *Hind* III-linearized pGEX3X1400 and pGEX3X1400(Y236L) respectively. Lanes 6 and 7, *Afl* II-digested pGEX3X1400 and pGEX3X1400(Y236L) respectively. **B:** Ethidium bromide stain of a 1 % agarose gel and restriction map of *ApaL* I-digested pGEX3X1400(F270A, E271K). Lane 1, *Pst* I-digested Lambda DNA molecular weight standards. Lanes 2 and 3, undigested pGEX3X1400 and pGEX3X1400(F270A, E271K) respectively. Lanes 4 and 5, *Hind* III-linearized pGEX3X1400 and pGEX3X1400(F270A, E271K) respectively. Lanes 6 and 7, *ApaL* I-digested pGEX3X1400 and pGEX3X1400(F270A, E271K) respectively. bp indicates DNA sizes in base pairs.

3.3.2.4 Analysis of pGEX3X1400(Y236L, F270A, E271K) modified plasmid

To generate the plasmid, pGEX3X1400(Y236L, F270A, E271K), previously confirmed modified plasmid pGEX3X1400(F270A, E271K) was entirely amplified using complementary primers containing the mutation Y236L. All the mutations were confirmed as described in section 3.3.2.3 using *Afl* II (Figure 3.7, lanes 6 and 7) and *ApaL* I (Figure 3.7, lanes 8 and 9). Again, *ApaL* I did not cut the plasmids to completion.

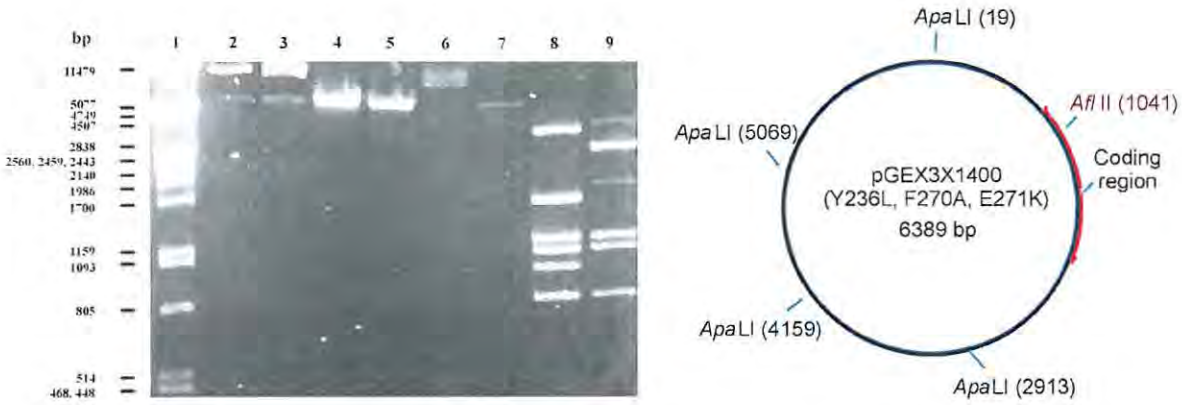

Figure 3.7: Diagnostic restriction endonuclease digestion of pGEX3X1400(Y236L, F270A, E271K) plasmid.
Ethidium bromide stain of a 1 % agarose gel and restriction map of *Afl* II and *ApaL* I-digested pGEX3X1400(Y236L, F270A, E271K). Lane 1, *Pst* I-digested Lambda DNA molecular standards. Lanes 2 and 3, undigested pGEX3X1400 and pGEX3X1400(Y236L, F270A, E271K) respectively. Lanes 4 and 5, *Hind* III-linearized pGEX3X1400 and pGEX3X1400(Y236L, F270A, E271K) respectively. Lanes 6 and 7, *Afl* II-digested pGEX3X1400 and pGEX3X1400(Y236L, F270A, E271K) respectively. Lanes 8 and 9, *ApaL* I-digested pGEX3X1400 and pGEX3X1400(Y236L, F270A, E271K) respectively.

3.3.3 Heterologous production and purification of GST-N217, GST-C334 proteins and their derivatives for specificity studies

GST-N217, GST-C334 and their derivatives were heterologously over-produced in *E. coli* XLI Blue cells harbouring pGEX3X derived plasmid constructs using IPTG, and the proteins were purified by *S*-hexyl glutathione agarose affinity chromatography. Significant amounts of the proteins were recovered from the beads by elution with reduced glutathione solution. Aliquots of the purified proteins were resolved on a 0.1 % SDS- 12 % PAGE gel to determine subunit molecular weight and to estimate levels of purity. Significant amounts of proteins corresponding to the expected molecular masses were visible on the gel (Figures 3.8).

3.3.4 Interactions of GST-N217, GST-C334 proteins and their mutant derivatives with Hsc70 and Hsp90

Topologically equivalent residues involved in specificity determination were identified in TPR1 domain versus TPR2A domain that differed greatly in the nature of their contacts with residues upstream of the EEVD motif of their respective Hsps. Using site-directed mutagenesis, these residues were swapped between the domains. The following modified proteins were generated: GST-N217(L15Y), GST-N217(A49F, K50E), GST-N217(L15Y, A49F, K50E), GST-C334(Y236L), GST-

C334(F270A, E271K) and GST-C334(Y236L, F270A, E271K). The proteins were then tested for their ability to bind to either Hsc70 or Hsp90 as described in Appendix A, section A.19.

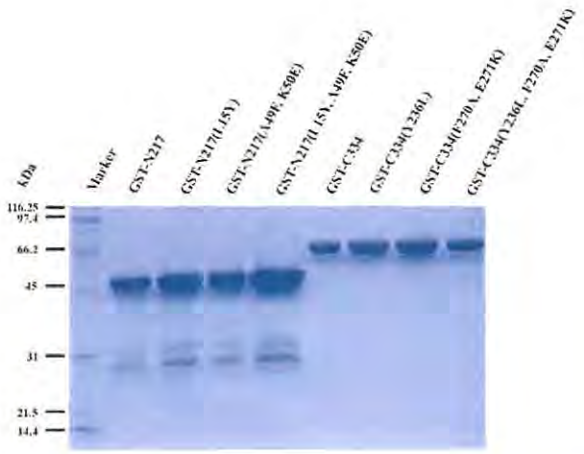

Figure 3.8: Purification of GST-mSTI1 fusion proteins by glutathione agarose affinity chromatography.
Coomassie-stained SDS-PAGE gel of GST-mSTI1 fusion proteins recovered after purification by glutathione agarose affinity chromatography. Marker: Protein molecular weight standards in kiloDaltons (kDa).

3.3.4.1 Double substitution of Ala^{49} and Lys^{50} to Phe and Glu, respectively, significantly lowered the affinity of TPR1 domain for Hsc70

Using the C-terminal truncated mutant protein GST-N217 (with TPR2A and TPR2B domains removed), double and triple modified derivatives were generated as follows: GST-N217(L15Y), GST-N217(A49F, K50E), and GST-N217(L15Y, A49F, K50E). These modified proteins were tested for their ability to bind both Hsc70 and Hsp90. In the Hsc70 co-precipitation assays, GST-N217 was found to associate with Hsc70 at levels that compared favourably with the full-length protein, GST-543 (Figure 3.9, lanes 1 and 3). As expected, both GST-543(Y27A) and GST did not bind to Hsc70 (Figure 3.9, lanes 2 and 4). The single mutant GST-N217(L15Y) bound to Hsc70 at a slightly lower level compared to GST-N217, while binding affinity was significantly lowered using the double mutant GST-N217(A49F, K50E) (Figure 3.9, lanes 5 and 6). No binding to Hsc70 was observed in the triple mutants GST-N217(L15Y, A49F, K50E) and GST-543(L15Y, A49F, K50E) (Figure 3.9, lanes 7 and 8). It appeared that

double substitution of Ala[49] and Lys[50] in mSTI1 drastically reduced binding to Hsc70 while triple substitution of Leu[15], Ala[49] and Lys[50] abolished binding.

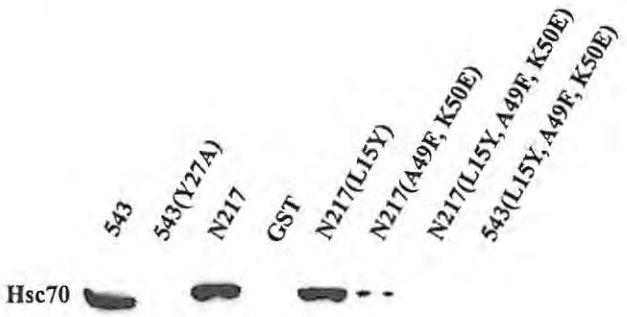

Figure 3.9: N217(A49F, K50E) and N217(L15Y, A49F, K50E) were unable to bind to Hsc70. Autoradiogram of chemiluminescence-based immunodetection of native Hsc70 from NIH3T3 mouse fibroblast cell extracts after binding to GST-mSTI1 fusion proteins indicated above each lane. 543 and N217 are equivalent to GST-543 and GST-N217 respectively. Information in brackets indicate substitutions carried out in the proteins.

3.3.4.2 Hsp90-binding capacity was engineered on the Hsp70-binding TPR1 domain of mSTI1

After pull down assays with Hsc70, the next step was to test whether the mutants in section 3.3.4.1 could interact with Hsp90. In this experiment, purified Hsp90 was used instead of cell lysates. As expected, full-length unmodified protein, GST-543, and N-terminal truncated protein GST-C334 (with TPR1 domain deleted) bound to purified Hsp90 at equivalent levels (Figure 3.10, lanes 3 and 5). The C-terminal truncated protein, GST-N217, its mutant derivative, GST-N217(L15Y), and GST alone did not bind to Hsp90 (Figure 3.10, lanes 4, 6 and 8). The double mutant GST-N217(A49F, K50E) was found to bind to Hsp90 at levels comparable to both GST-543 and GST-C334 (Figure 3.10, lanes 3, 5 and 7). No Hsp90-binding was observed with the triple mutant GST-N217(L15Y, A49F, K50E) (Figure 3.10, lane 9). Put together, these results suggested that double substitution of Ala[49] and Lys[50] by Phe and Glu respectively, was sufficient to confer the ability to bind Hsp90 on the Hsc70-binding TPR1 domain of mSTI1.

3.3.4.3 Y236L, F270A or E271K substitution in the TPR2A domain of mSTI1 abrogated binding to Hsp90.

The N-terminal truncated mutant protein, GST-C334, incapable of binding to Hsc70 was used to generate the following modified proteins: GST-C334(Y236L), GST-

C334(F270A, E271K), and GST-C334(Y236L, F270A, E271K); the proteins were tested for their ability to bind to Hsp90. Both GST-543 and GST-C334 were found to

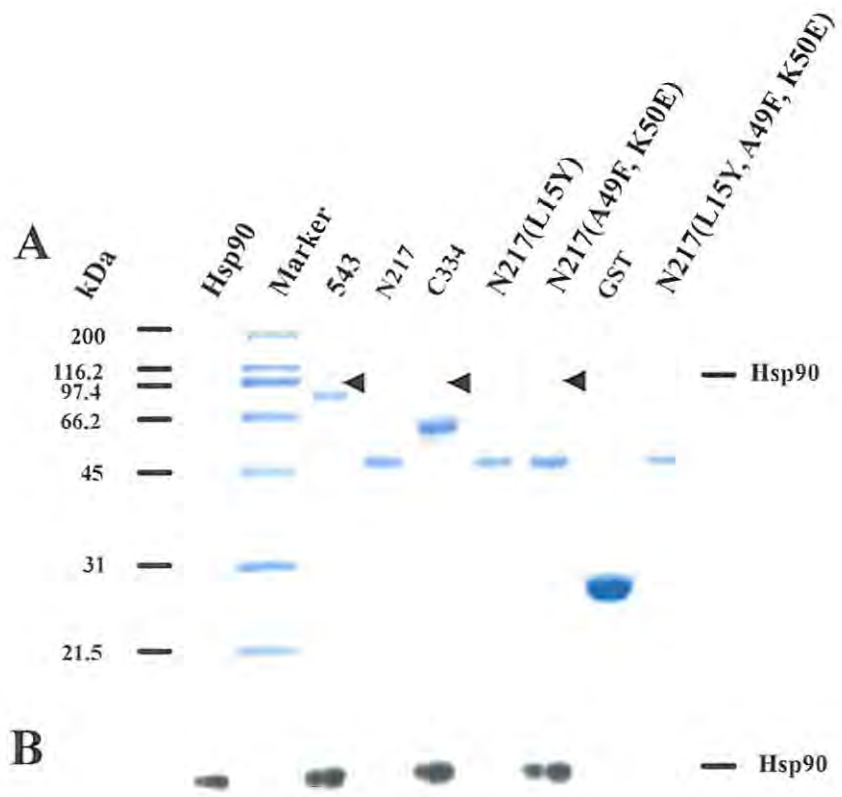

Figure 3.10: GST-N217(A49F, K50E) successfully bound to Hsp90.
A: Coomassie-stained SDS-PAGE gel of co-precipitation assays showing differential binding of various mutant derivatives of GST-mSTI1 to purified Hsp90. **B:** Autoradiogram of chemiluminescence-based immunodetection of purified Hsp90 after binding to GST-mSTI1 proteins. Lane 1, purified Hsp90. Lanes 2-9, co-precipitating GST-mSTI1 proteins with Hsp90. 543, N217 and C334 are equivalent to GST-543, GST-N217 and GST-C334 respectively. Information in brackets indicate substitutions carried out in the proteins. Marker: Protein molecular weight standards in kiloDaltons (kDa).

bind Hsp90 as expected (Figure 3.11, lanes 1 and 6). As expected, GST did not bind to Hsp90 (Figure 3.11, lane 2). The single, double and triple mutant proteins, GST-C334(Y236L), GST-C334(F270A, E271K), and GST-C334(Y236L, F270A, E271K), respectively, lost their ability to bind to Hsp90 (Figure 3.11, lanes 3, 4 and 5). These results suggested that these mutations, either single or multiple, abrogated binding of mSTI1 to Hsp90.

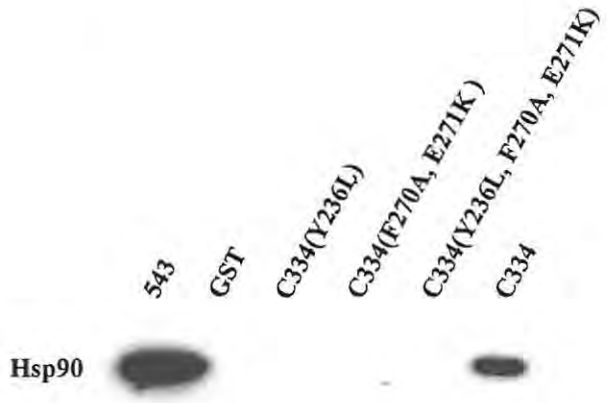

Figure 3.11:GST-C334 modified proteins could not bind to Hsp90.
Autoradiogram of chemiluminescence-based immunodetection of purified Hsp90 after co-precipitation with GST-mSTI1 proteins indicated above each lane. 543 and C334 are equivalent to GST-543 and GST-C334 respectively. Information in brackets indicate substitutions carried out in the proteins.

3.3.4.4 Hsc70-binding capacity could not be engineered onto the TPR2A domain of mSTI1

Next, the proteins (section 3.3.4.3), were tested for their ability to bind to native Hsc70 from the lysates of NIH3T3 mouse fibroblast cells. GST-543 was found to bind to Hsc70 successfully while GST did not (Figure 3.12, lanes 1 and 2). Neither GST-C334 nor any of its derivatives was able to bind to Hsc70 (Figure 3.12, lanes 3-6). Hence, engineering Hsc70-binding capacity on TPR2A was not possible by simple swapping of topologically equivalent residues.

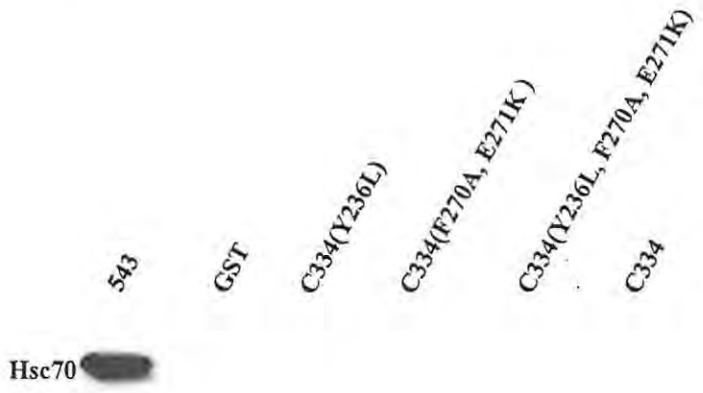

Figure 3.12: GST-C334 protein and its derivatives could not bind to Hsc70
Autoradiogram of chemiluminescence-based immunodetection of native Hsc70 from NIH3T3 mouse fibroblast extracts after co-precipitation with GST-mSTI1 fusion proteins indicated above each lane. 543 and C334 are equivalent to GST-543 and GST-C334 respectively. Information in brackets indicate substitutions carried out in the proteins.

3.4 Discussions

The crystal structures of the Hop TPR domains in complex with Hsc70 and Hsp90 peptides predict that certain residues in Hop make hydrophobic and van der Waals contacts with residues in the peptides, and that these interactions are used to discriminate between the C-termini of Hsc70 and Hsp90. Based on these data and sequence alignments, it was hypothesized that by doing L15Y, A49F and K50E substitutions, TPR1 could be engineered to accommodate the Met -4 upstream of the Hsp90 C-terminal EEVD motif and hence bind Hsp90 with high affinity. Conversely, by doing Y236L, F270A, and E271K substitutions in TPR2A, it was hypothesized that this domain could be engineered to bind to Hsc70. For the first hypothesis, a C-terminal truncated GST fusion derivative of mSTI1, (GST-N217), that lacks the Hsp90-binding TPR domain, was used. As expected, the L15Y substitution alone only slightly lowered the affinity of mSTI1 for Hsc70. From the crystal structure, Figure 3.1A, it is obvious that the hydrophobic pocket accommodating the C-terminal isoleucine in Hsp70 (I -4) is mainly formed by the side chains/groups of Lys^{50} and Ala^{49}. It appears that Leu^{15} does not contribute significantly to these hydrophobic and /or van der Waals interactions since its side groups and those of I -4 may not be in sufficiently close proximity. On the other hand, GST-N217(L15Y) did not bind to Hsp90. This observation may be due to the fact that substituting Tyr for Leu did not provide enough hydrophobic contacts for the modified mSTI1 to interact successfully with Hsp90. The substitution could not be regarded as "disruptive" since both amino acids are bulky and the modified protein was found to express quite readily.

Interestingly, the double mutant GST-N217(A49F, K50E) bound to Hsc70 with low affinity. The close proximity of both Lys^{50} and Ala^{49} to I -4 implies that the side chains/groups of these amino acids collectively form strong hydrophobic and/or van der Waals interactions that are important in determining the specificity of interaction of Hop with Hsp70. It is proposed that mutations of these residues will severely disrupt the specific interaction of Hop with Hsp70. Support for this proposition comes from data that showed that partial deletion of helix 2A (residues 37 to 47) coupled with K8A substitution was not sufficient to abrogate binding of Hop to Hsc70 (see section 2.3.4.5). The effect of single mutation of Lys^{50} or Ala^{49} on the interaction of Hop with Hsc70 could have been investigated to further verify this hypothesis.

Conversely, the modified protein, GST-N217(A49F, K50E), successfully bound to Hsp90 at an affinity even higher than that of the full-length unmodified protein as indicated by SPR spectroscopy (Chapter 4). This result suggests that the double mutations provide sufficient amount of hydrophobic contacts for the modified protein to interact successfully with Hsp90. Therefore, substitution of Ala^{49} and Lys^{50} to Phe and Glu, respectively, in mSTI1 resulted in severe loss of affinity for Hsc70 but gain of affinity for Hsp90. Furthermore, these data provide evidence that hydrophobic contacts in the second TPR motif of TPR1 domains are important in determining specificity of mSTI1 interaction with Hsc70. Surprisingly, the triple mutant GST-N217(L15Y, A49F, K50E) lost the ability to bind to both Hsc70 and Hsp90. While Leu^{15} may be involved in specificity, its proximity to Lys^{8} and Asn^{12} may suggest that any changes in this region will disturb the two-carboxylate clamp sufficiently to cause the triple mutant GST-N217(L15Y, A49F, K50E) to lose its capacity to bind to Hsp90.

For the second hypothesis, an N-terminal truncated GST fusion derivative of mSTI1, (GST-C334), that lacks the Hsc70-binding TPR1 domain was used. All the three modified proteins GST-C334(Y236L), GST-C334(F270A, E271K) and GST-C334 (Y236L, F270A, E271K) could not bind to either Hsc70 or Hsp90. From the crystal structure, Figure 3.2A, it appears that the side chain of Met -5 is in close proximity to Tyr^{236} and Glu^{271} while Phe^{270} may not be within reacting distance from Met -5. One can conclude therefore that the side chains/groups of these two residues contribute significantly to the hydrophobic contacts made with Met -5. In the Hop-Hsp90 specific interaction, it seems that helix 1A of TPR2A is contributing significantly to the network of hydrophobic contacts compared to helix 1A in TPR1 domain (Leu^{15}) for Hop-Hsc70 interaction. The obvious similarity between the two domains is the significance of the topologically equivalent residues Lys^{50} and Glu^{271}. Interestingly, these residues are highly charged and opposite in charge. Again, the effect of single mutation of Glu^{271} or Phe^{270} on the interaction of Hop with Hsp90 could have been investigated. Results from these experiments could have provided insight into the significance of each of these residues to the network of hydrophobic contacts.

Together, these results do suggest that binding of Hsc70 to mSTI1 or Hop is more specific than the binding of Hsp90. In conclusion, firstly, evidence has been provided

to show that hydrophobic contacts in the second TPR motif (Ala^{49} and Lys^{50}) of TPR1 may be more important than other regions of this domain in determining specificity of mSTI1 interaction with Hsc70. Secondly, Hsp90 binding capacity has been successfully engineered on the Hsc70-binding TPR1 domain of mSTI1 by doing simple amino acid substitution without elaborate domain swapping.

Chapter Four

Quantitation of the affinities of binding of mSTI1 proteins to Hsc70 and Hsp90 using surface plasmon resonance spectroscopy

4.1 Introduction

Results from pull down assays using glutathione affinity chromatography suggested that the basic TPR groove residues of the TPR1 domain of mSTI1 contributed differentially to the Hsc70-mSTI1 interaction (Chapters 2 and 3). One limitation of protein pull down methods, including the GST affinity pull down assay, is that they detect only relatively high affinity (micromolar concentrations) protein interactions. Furthermore, inconsistent binding affinities (K_D) have been reported for Hsp70-Hop-Hsp90 interactions (Mayr *et al.*, 2000; Brinker *et al*, 2002; Hernández *et al.*, 2002). Therefore, the objective of this study was to use a more sensitive and quantitative technique to detect protein interactions undetectable by the GST affinity pull down assays and to collect kinetic data for specific interactions of Hsc70 or Hsp90 with mSTI1 and its modified derivatives.

The Biacore surface plasmon resonance (SPR) spectroscopy system was used to analyse biomolecular interactions. The system allows for collection of real time kinetic data independent of the properties of the sample. Continuous gathering of information in the form of the sensorgram provides information on all steps in multi-step analysis. No labelling of the sample is required and there is minimal loss of sample during the analytical process. Analysis can be performed on tissue culture media or bacterial broth with minimal purification of the analyte stream. One of the disadvantages is the effect of mass transport of molecules, which may give results that inaccurately depict the kinetics of the interaction. Also, during the regeneration step, when analyte bound to the immobilized ligand is removed, it is possible to denature the ligand. In some cases, immobilization of the ligand, especially proteins could

generate steric effect on its interaction with the analyte. Non-specific binding to the surface of the chip is reduced by the use of inert molecules such as dextran.

4.2 Experimental procedures

In this experiment, purified proteins were dialysed to exchange the Tris-HCl buffer used to prepare glutathione elution buffer for PBS, before using them for SPR spectroscopy studies. Biomolecular interactions in real time were monitored using the Biacore X apparatus machine (Biacore, Uppsala, Sweden). All experiments were performed at 25^0C in buffer A (PBS containing 0.005% P20 surfactant; Biacore, Uppsala, Sweden). GST and GST-mSTI1 fusion proteins (ligands) were bound in separate flow cells to anti-GST antibody (Biacore, Uppsala, Sweden) immobilized on a sensor chip to give approximately the same number of response units. Increasing concentrations of purified Hsc70 (kind gift from Dr Mike Cheetam) or Hsp90 (kind gift from Dr David Smith) were passed over the bound proteins, and interactions were monitored for a period of time. For competition experiments, a mixture of full-length Hsc70 and Hsp90 (analytes) was pre-incubated at 25^0C before passing it over the immobilised GST-mSTI1 proteins. Background binding to GST was subtracted from each signal to account for non-specific binding to GST (See Appendix A, section A.23 for details on Biacore SPR).

4.3 Results

4.3.1 Quantitation of the affinities of binding of mSTI1 proteins to Hsc70 and Hsp90

To determine the contribution of each individual amino acid residue to the binding of Hsc70 by mSTI1, surface plasmon resonance spectroscopy was used to monitor bimolecular interactions. Concentration-dependent SPR signals were recorded for specific protein interactions, and thermodynamic dissociation constants (K_D values) were determined and taken as apparent affinities of binding. The K_D of binding of the full-length unmodified mSTI1 to full-length Hsc70 was calculated to be approximately 2 μM (Figure 4.1A). The value compares favourably with K_D values reported in literature (2 μM, Brinker *et al.*, 2002), and (1.3 μM, Hernández *et al.*, 2002). For GST-543(K8A) modified protein, the K_D was calculated to be approximately 3 μM (Figure 4.1B).

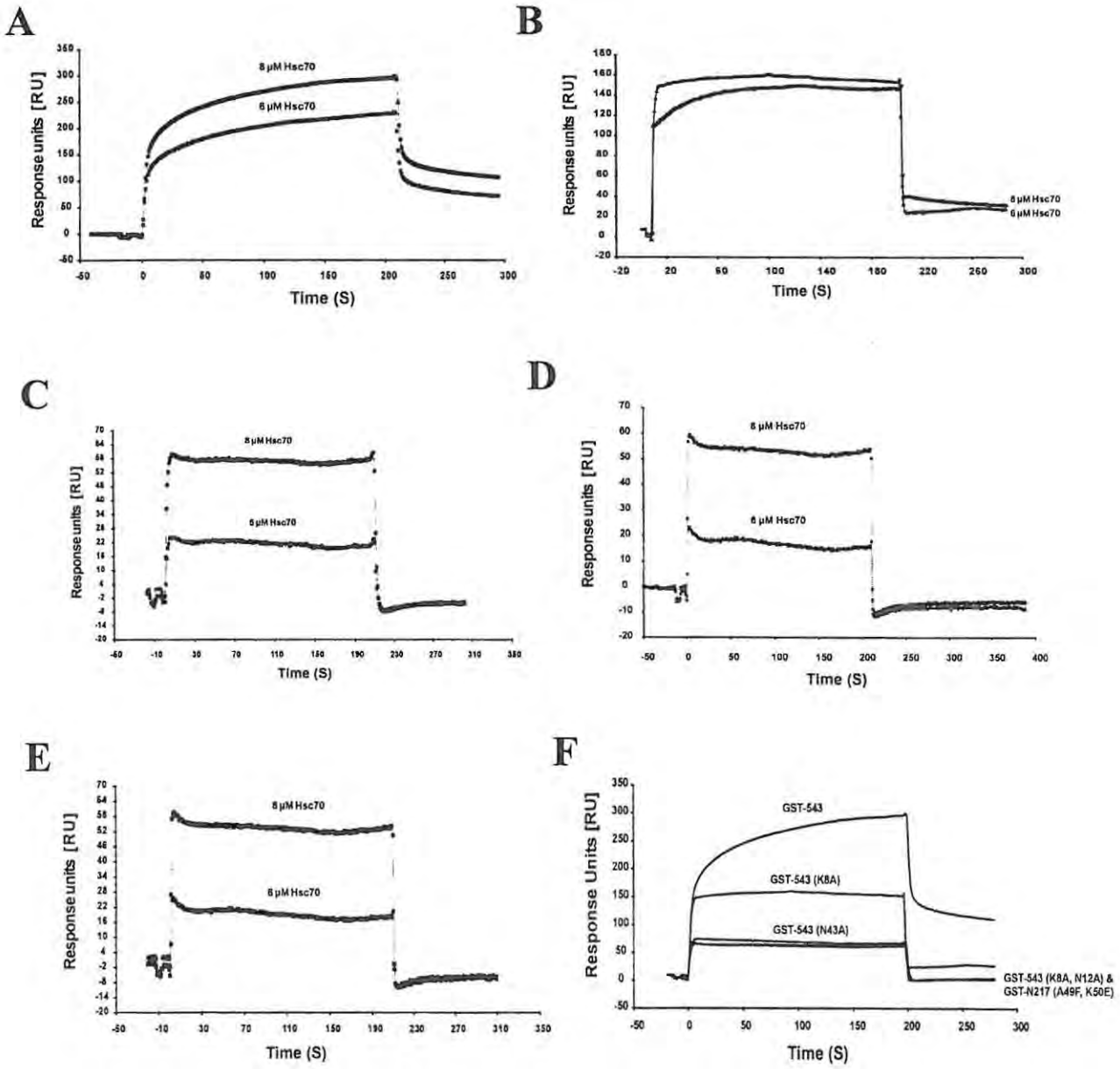

Figure 4.1: Binding curves of the interactions of GST-543 protein and its derivatives with Hsc70 using surface plasmon resonance spectroscopy.
Increasing concentrations of purified Hsc70 were passed over GST-mSTI1 proteins immobilized on a sensor chip CM5. **A:** GST-543 interaction with Hsc70; K_D was calculated to be 2 µM. **B:** GST-543 (K8A) interaction with Hsc70; K_D was calculated to be 3 µM. **C:** GST-543(K8A, N12A) interaction with Hsc70. **D:** GST-543(N43A) interaction with Hsc70. **E:** GST-N217(A49F, K50E) interaction with Hsc70. **F:** Relative binding response curves of GST-543 and its modified derivatives to Hsc70. Concentration of Hsc70 used was 8 µ M.

Compared to the unmodified full-length mSTI1, the kinetics of the interactions of the GST-543(K8A, N12A), GST-543(N43A) and GST-N217(A49F, K50E) modified proteins with full-length Hsc70 was different (Figures 4.1C, 4.1D and 4.1E respectively). The binding curves could not be perfectly fitted to a 1:1 Langmuir

binding model. It was notable that the effect of the buffer on the kinetics of binding to Hsc70 was more pronounced in the modified proteins compared to the unmodified full-length protein. In addition, the modified proteins displayed reduced response to Hsc70 binding when compared to the unmodified protein (Figure 4.1F).

In the Hsp90 binding assays, the unmodified full-length mSTI1, (GST-543) displayed kinetics similar to its interaction with Hsc70 (Figure 4.2A); the K_D was calculated to be approximately 1.5 μM. Again, similar K_D value for Hop-Hsp90 binding has been reported in literature (Brinker *et al.*, 2002). However, a number of investigators have reported higher binding affinity for Hop interaction with full-length Hsp90 (90 nM, Hernández *et al.*, 2002), and (32 nM, Mayr *et al.*, 2000). A very interesting observation was the higher affinity of the GST-N217 (A49F, K50E) modified protein; K_D of 0.15 μM, (150 nM) compared to the full-length unmodified protein (Figure 4.2B). Interestingly, even in the presence of Hsc70, GST-N217(A49F, K50E) protein was still able to bind to Hsp90 with the same affinity (Figure 4.2C). It is clear from these results that mutation of any of the residues in the TPR1 domain of mSTI1 that form the so-called two-carboxylate clamp disrupted its interaction with Hsc70 and that the individual amino acid residues contribute differentially to the network of electrostatic contacts. In addition, double mutation of A49F and K50E in the TPR1 domain of mSTI1 was found to confer increased Hsp90-binding affinity on the protein.

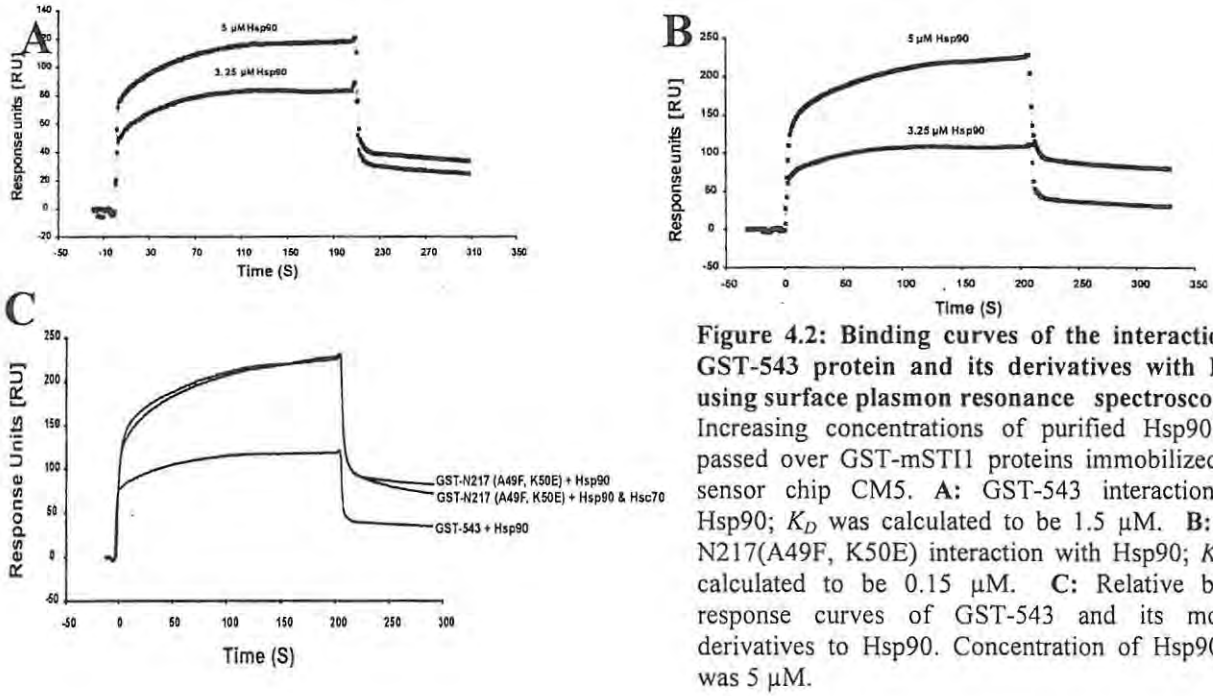

Figure 4.2: Binding curves of the interactions of GST-543 protein and its derivatives with Hsp90 using surface plasmon resonance spectroscopy. Increasing concentrations of purified Hsp90 were passed over GST-mSTI1 proteins immobilized on a sensor chip CM5. **A:** GST-543 interaction with Hsp90; K_D was calculated to be 1.5 μM. **B:** GST-N217(A49F, K50E) interaction with Hsp90; K_D was calculated to be 0.15 μM. **C:** Relative binding response curves of GST-543 and its modified derivatives to Hsp90. Concentration of Hsp90 used was 5 μM.

4.4 Discussions

Quantitative analysis using SPR spectroscopy revealed that mutations, either single or double, in the TPR1 domain of mSTI1 affected the kinetics of its binding to either Hsc70 or Hsp90. In general, interactions of the modified mSTI1 proteins with either Hsc70 or Hsp90, exhibited monophasic binding and dissociation curves. Monophasic binding curve implies that the interacting species are monovalent. Interestingly, similar binding curves have been reported in which isolated TPR domains were used in binding studies with either fragments of Hsp70/Hsp90 or full-length Hsp70/Hsp90 (Brinker *et al.*, 2002). On the contrary, interactions between unmodified full-length mSTI1 and full-length Hsc70 and/or Hsp90 displayed multiphasic kinetics. This kind of kinetics suggests conformational rearrangement or flexibility of the interacting proteins and possibly the existence of high- and low-affinity states in dynamic equilibrium.

Though there exist some discrepancies in the affinities reported for the binding of Hop to Hsp90, all the figures do suggest that Hop binds to Hsp90 with a higher affinity than to Hsc70 (Mayr *et al.*, 2000; Brinker *et al.*, 2002; Hernández *et al.*, 2002). Support for this data comes from observation that majority of the Hop in rabbit reticulocyte lysate is bound to Hsp90 (Silverstein *et al.*, 1999; Murphy *et al.*, 2001). It is interesting to note that in this study a higher affinity of binding (150 nM) of the modified protein GST-N217(A49F, K50E) to Hsp90 was obtained compared to the full-length protein. This value does not differ significantly from the value reported by Hernández *et al* (2002), 90 nM, for the interaction of full-length Hop with full-length Hsp90. In their study, they calculated the binding affinity of Hop to Hsp90 in the presence of the full complement of Hsp70-Hsp40 chaperoning system. In our study, a direct binding of Hop to Hsp90 without other competing partner proteins was monitored. The former seems to be a more appropriate approach to obtaining accurate affinity values, not only because it is dynamic but also because it "mimics" the *in vivo* situation. In addition, other data obtained in this study, which are discussed in Chapter 5 of this thesis, do suggest that a dynamic equilibrium exists in the sequential interaction of Hop with Hsc70 and Hsp90 *in vivo*.

Many investigators have reported data suggesting the existence of high- and low-affinity binding sites in the interactions of Hop with both Hsc70 and Hsp90. These data were explained in terms of Hop interacting with Hsc70 and/or Hsp90 at more than one site, or in terms of conformational rearrangement in one or both of the interacting proteins (Brinker *et al.*, 2002; Hernández *et al.*, 2002). For instance, it has been reported that Hsp90 reduces the number of Hsp70 binding sites on the Hop dimer (Hernández *et al.*, 2002).

Data from sequence alignments revealed that the residues that determine specificity of binding of TPR1 domain in mSTI1/Hop to Hsp70 show high homology to the topologically equivalent residues in the TPR2B domain, suggesting that this region of the protein might be a second Hsp70-binding TPR domain. Recently, using SPR spectroscopy, it was shown that whereas TPR2B domain of Hop bound Hsp70 with a very low affinity, it did not interact with Hsp90 at all (Brinker *et al.*, 2002). Results of competition assays using ^{35}S-Met Hsp70 and ^{35}S-Met Hsp90 suggested that the binding of Hsp90 to Hop increased the affinity of Hop to bind to Hsp70 but not *vice versa* (Hernández *et al.*, 2002). Furthermore, they predicted that in the cell, all of Hop might be in a complex with Hsp90, more so since Hsp90 is more abundant than Hop (Hernández *et al.*, 2000). Therefore, it seems logical to think that the only species of Hop that Hsp70 may interact with is a pre-existing Hsp90-Hop complex. However, data from this and other studies (Brinker *et al.*, 2002; Hernández *et al.*, 2002) did indicate that Hsp70 could interact with Hop in the absence of Hsp90, though with much lower affinity.

Putting all these data together, one can predict that the TPR2B domain of mSTI1/Hop binds to Hsp70 in its ATP-bound state with low affinity whereas TPR1 domain interacts more tightly with the ADP-bound Hsp70. If the predominant form of Hsp70 in the cell is Hsp70-ATP as predicted (Hernández *et al.*, 2002), then the proposed interaction of Hsp70-ATP with TPR2B of mSTI1/Hop could be part of a cytoplasmic retention mechanism for Hsp70 in the cell. In the presence of the progesterone receptor substrate, Hsp40 will stimulate Hsp70's ATP hydrolysis to generate ADP-bound Hsp70 while the binding of Hsp90 to TPR2A of Hop will cause a conformational rearrangement which will result in the opening of TPR1 domain for a tight binding of Hsp70.

Evidence to support these predictions comes from observation that ATP influences the interaction of Hsp70 with Hop but not of Hsp90 with Hop (Hernández *et al.*, 2002). They observed that at high concentrations of ATP and no Hsp40, the binding of Hsp70 to Hop was decreased. This inhibitory effect of ATP was reversed when Hsp40 was present, presumably through ATP hydrolysis to produce Hsp70-ADP. However these predictions must be confirmed experimentally. Evidently, there is a need to do more experiments to be able to clearly define the role of TPR2B domain. For example, the TPR2B domain could be used as bait in yeast two-hybrid system to identify TPR2B-interacting proteins. It is possible that TPR2B domain interacts with an entirely different protein.

Chapter 5

Characterization of the binding of mSTI1 to Hsc70 and Hsp90 *in vivo*

5.1 Introduction

Chang *et al* (1997) provided the first evidence to show the direct interaction of STI1 and Hsp90 *in vivo*. Combined mutations in *Saccharomyces cerevisiae* that eliminated STI1 or reduced intracellular concentrations of Hsp90 were found to greatly reduce or eliminate growth at normal temperatures. In a semi *in vivo* experiment, Lässle *et al* (1997) used a set of GST-STI1 fusion proteins comprising different parts of mSTI1 to pull down STI1-interacting proteins from metabolically labelled M27 cell extracts. They found proteins of 70 and 90 kDa binding to the GST fusion protein that contained the complete mSTI1 sequence. Using fusion proteins representing discrete regions of the mSTI1 proteins, they found differential binding of the 70 and 90 kDa proteins to the N- and C-terminal domains of mSTI1 respectively.

Using complementation experiments, Dolinski *et al* (1998) showed that cyclophilin seven suppressor (Cns1) encoded an essential Stil homologue in *Saccharomyces cerevisiae* that suppressed cyclophilin 40 mutations and interacted with Hsp90. Using a yeast two-hybrid system with Hsc70 or its C-terminal 30-kDa domain as bait, Liu *et al* (1999) isolated several proteins interacting with Hsc70, including Hop. In addition, they demonstrated by both *in vitro* and *in vivo* experiments that the TPR domains of these proteins were necessary and sufficient for mediating their interactions with Hsc70. All these data show that STIl does interact with both Hsp90 and Hsc70 *in vivo*.

The objective of this study therefore, was to characterize *in vivo* the interactions of unmodified mSTI1 and its modified derivatives, especially N217(A49F, K50E), with Hsp90 and Hsc70. For these experiments, pCEP4 mammalian plasmids (See Appendix B, Figure B.3 for plasmid map) carrying cDNAs encoding $(His)_6$-tagged mSTI1 proteins were used to transiently transfect NIH3T3 mouse fibroblast cells.

Complexes containing $(His)_6$-tagged mSTI1 proteins were co-precipitated from cell lysates using nickel-chelating sepharose beads (Amersham Pharmacia Biotech, Uppsala, Sweden). After transferring onto nitrocellulose membranes, $(His)_6$-tagged mSTI1 proteins, Hsc70 or Hsp90 was immunodetected using specific antibodies.

5.2 Experimental procedures

5.2.1 Insertion of cDNAs encoding $(His)_6$-tagged mSTI1 proteins into pCEP4 mammalian plasmid

Oligonucleotide primers were designed to amplify cDNAs encoding $(His)_6$-tagged full-length mSTI1, $(His)_6$-543, C-terminal deletion modified mSTI1 protein, $(His)_6$-N217, and N-terminal deletion modified protein, $(His)_6$-C334, with and without mutations. The forward primers were designed to include, from the 5' end, a *Kpn* I restriction site, a eukaryotic Kozak sequence, and a $(His)_6$ tag coding sequence. The reverse primers contained, at the 5' end, a stop codon, and terminates with an *Xho* I restriction site. Polymerase chain reaction (PCR) was carried out as described in Appendix A, section A.10. PCR products were resolved on a 1 % agarose gel. The band of interest was carefully excised from the gel and the DNA purified using the GFX Gel Band purification kit (Amersham Pharmacia Biotech, Uppsala, Sweden). The purified cDNA was ligated into the pGEMT cloning vector (See Appendix B, Figure B.2 for plasmid map) as described in Appendix A, section A.11. The ligation product was used to transform *E. coli* XLI Blue cells.

Plasmid DNA was isolated from the *E. coli* cells harbouring plasmids. Thereafter, the pGEMT clone was digested with *Kpn* I and *Xho* I restriction endonucleases to release the cDNA insert. The cDNA insert was purified from agarose gel, and finally ligated into pCEP4 mammalian expression vector, which had been previously digested with *Kpn* I and *Xho* I restriction endonucleases. Plasmid DNA preparations of the pCEP4 clones were digested with *Kpn* I and *Xho* I restriction endonucleases to confirm the sizes of the cDNA inserts. In addition, mutations were further confirmed by automated DNA sequencing.

Table 5.1: Design of primers for PCR amplification of mSTI1 cDNAs from pGEX3X plasmids

Restriction endonuclease sites are indicated in bold letters, Kozak sequences are underlined, and $(His)_6$ tag sequences are in italics.

Name of insert	Forward primer	Reverse primer	Size of insert
His-2000, encoding full-length mSTI1	5' **ggtacc**agaatggga*catcatcatcatcatcat*ggaatggagcaggtgaatgag 3'	5' **ctcgag**ttatcattatcaccgaattgcgatgag 3'	1629 bp
His-700, encoding N217 protein	5' **ggtacc**agaatggga*catcatcatcatcatcat*ggaatggagcaggtgaatgag 3'	5' **ctcgag**ttatcagatcttcttccattgg 3'	652 bp
His-1400, encoding C334 protein	5' **ggtacc**agaatggga*catcatcatcatcatcat*gaacccaagccagaaccaatg 3'	5' **ctcgag**ttatcattatcaccgaattgcgatgag 3'	1006 bp

5.2.2 Transfection of NIH3T3 mouse fibroblast cells with pCEP4 plasmids carrying mSTI1 cDNAs

Ultra-pure pCEP4 plasmids carrying mSTI1 cDNAs were prepared using the QIAprep Spin Miniprep kit (QIAGEN, Hilden, Germany). The plasmid DNA preparations were then used to transiently transfect actively growing cultures of NIH3T3 mouse fibroblast cells by calcium phosphate mediation (See Appendix A, section A.17). As controls, pCEP4 vector and pBCMGNeo-mSTI1-EGFP plasmids (encoding EGFP-tagged mSTI1, from Vicky Longshaw) were used in separate transfections. The cells were harvested 48 hours after transfection and lysed. In this study, only three pCEP4 clones were used for transfection: pCEP4His-2000 (encoding $(His)_6$-543), pCEP4His-700 (encoding $(His)_6$-N217), and pCEP4His-700(A49F, K50E) (encoding (His)6-N217(A49F, K50E)).

5.2.3 Detection of Hsc70-mSTI1-Hsp90 complexes using immobilized metal ion affinity chromatography

For each transfection event, cells were pooled from ten 75-cm^2 tissue culture flasks and lysed in 2 ml of lysis buffer (See Appendix A, section A.16 for details on lysis). The lysates were clarified by centrifugation at 12,000 x g for 30 minutes at 4^0C. 500 µl of the clarified lysate was removed before adding 500 µl of 50 % slurry of chelating sepharose beads, previously charged with $NiSO_4$ (nickel sulphate). Binding to the nickel chelating sepharose beads continued for 3 hours after which the beads were washed extensively with ample amounts of ice-cold PBS to remove unbound proteins. The beads were then resuspended in 100 µl of SDS-PAGE sample buffer and

heated for 5 minutes at 95^{0}C. The mixture was centrifuged briefly to pellet the beads before loading 25 µl of the supernatant on a 0.1 % SDS-10 % PAGE gel (See Appendix A, section A.19 for details). After transferring onto nitrocellulose membranes, $(His)_6$-tagged mSTI1 proteins, Hsc70 or Hsp90 was immunodetected using specific antibodies (See Appendix A, sections A.20 and A.21 for details).

5.3 Results

5.3.1 $(His)_6$-mSTI1 encoding cDNAs were successfully ligated into pCEP4 mammalian expression vector.

PCR amplification of the cDNAs encoding various $(His)_6$-tagged mSTI1 proteins was successful. DNA bands of the correct sizes were obtained (see section 5.2.2), with little or no contaminating non-specific DNA bands. Nonetheless, before ligating into pGEMT cloning vector, correct bands were excised from low-temperature agarose gels and purified. Insert DNA of the right sizes were successfully cloned into pCEP4 mammalian expression vector (results not shown).

5.3.2 $(His)_6$-tagged mSTI1 proteins were successfully expressed transiently in NIH3T3 mouse fibroblast cells.

The presence of $(His)_6$-tagged mSTI1 proteins in the lysates of transiently transfected NIH3T3 cells was revealed by immunodetection using anti-$(His)_6$ antibody, prior to chelating with nickel sepharose. Bands corresponding to $(His)_6$-543 (~ 64 kDa), $(His)_6$-N217 (~ 27 kDa), and $(His)_6$-N217(A49F, K50E) (~ 27 kDa) were observed (Figure 5.1). Additional bands observed could be due to cross-reactivity of the primary antibody with other proteins.

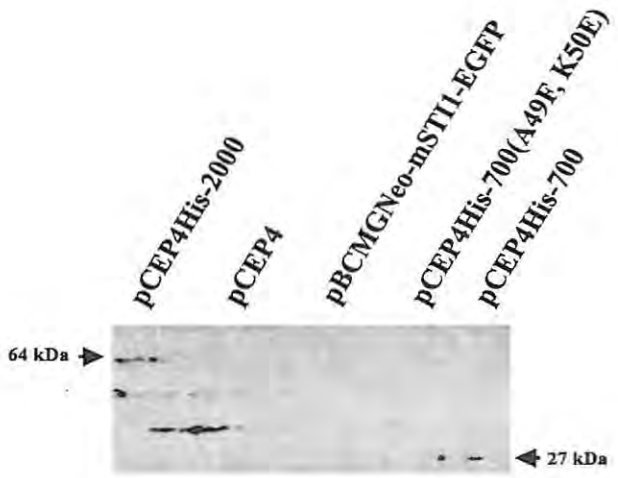

Figure 5.1: Transient expression of $(His)_6$-tagged mSTI1 proteins in NIH3T3 mouse fibroblast cells.
Autoradiogram of chemiluminescence-based immunodetection of $(His)_6$-543 (~ 64 kDa), $(His)_6$-N217 (~ 27 kDa) and $(His)_6$-N217(A49F, K50E) (~ 27 kDa) proteins encoded by the respective pCEP4 plasmids indicated above each lane, after their expression in NIH3T3 mouse fibroblast cells. Controls used were pCEP4 plasmid vector and pBCMGNeo-mSTI1-EGFP mammalian plasmid, which encodes full-length EGFP-tagged mSTI1 (EGFP-543). 543 and N217 represent full-length and C-terminal truncated mSTI1 proteins respectively. EGFP: enhanced green fluorescent protein.

5.3.3 $(His)_6$-N217 and $(His)_6$-N217(A49F, K50E) proteins interacted with both Hsc70 and Hsp90 *in vivo*.

Chemiluminescence-based immunodetection analysis revealed that all the three mSTI1 proteins, $(His)_6$-543, $(His)_6$-N217 and $(His)_6$-N217(A49F, K50E) were able to bind to Hsc70 *in vivo* (Figure 5.2A). The strong binding of $(His)_6$-N217(A49F, K50E) to Hsc70 *in vivo* was however unexpected since *in vitro* binding assays revealed that this modified mSTI1 protein had a very low capacity to bind to native Hsc70 from the lysates of NIH3T3 mouse fibroblast cells (see Figure 3.9). Similarly, all the three proteins were found in complex with Hsp90 *in vivo* (Figure 5.2B). While the strong interactions of $(His)_6$-543 and $(His)_6$-N217(A49F, K50E) with native Hsp90 corroborated results obtained from *in vitro* binding assays, binding of $(His)_6$-N217 to Hsp90 was contrary to *in vitro* results (see Figure 3.10). Transfection with both pCEP4 vector and pBCMGNeo-mSTI1-EGFP plasmids produced no chemiluminescence detection with anti-$(His)_6$ antibody, suggesting that there was no background reactivity with the antibody.

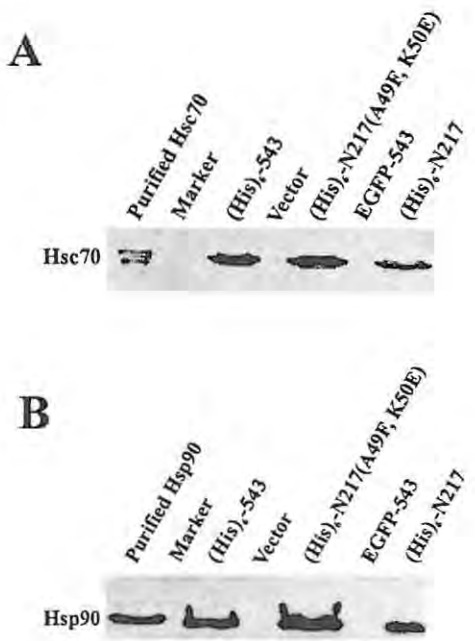

Figure 5.2: $(His)_6$-543, $(His)_6$-N217 and $(His)_6$-N217(A49F, K50E) proteins interacted with both Hsc70 and Hsp90 *in vivo*.
A: Autoradiogram of chemiluminescence-based immunodetection of Hsc70 in complex with mSTI1 proteins indicated above each lane, after their expression in NIH3T3 mouse fibroblast cells. **B:** Autoradiogram of chemiluminescence-based immunodetection of Hsp90 in complex with mSTI1 proteins indicated above each lane, after their expression in NIH3T3 mouse fibroblast cells. 543 and N217 represent full-length and C-terminal truncated mSTI1 proteins respectively. EGFP: enhanced green fluorescent protein.

5.4 Discussions

The objectives of this study were to (i) verify the *in vitro* binding assay results and (ii) further characterize the interactions of mSTI1 protein and its various derivatives with Hsc70 and Hsp90 *in vivo*. To eliminate the possibility of endogenous glutathione-*S*-transferase enzyme interference with protein-protein interactions, the mSTI1 proteins were tagged with a small tag, 6 x histidine, $(His)_6$. The pCEP4 mammalian expression vectors carrying cDNAs of various mSTI1 protein derivatives were used to transiently transfect NIH3T3 cells. Complexes containing $(His)_6$-tagged mSTI1 proteins were precipitated from the cell lysates using nickel-chelating sepharose, and the presence of Hsc70 and/or Hsp90 in the co-precipitating complexes was detected using specific antibodies against these chaperones. The most interesting findings were the fact that $(His)_6$-N217 and $(His)_6$-N217(A49F, K50E) were able to interact significantly with Hsp90 and Hsc70, respectively. The GST-tagged N217 protein was found not to bind to Hsp90 *in vitro*, since the Hsp90-binding TPR2A had been deleted. Similarly,

results from *in vitro* binding assays indicated that GST-N217(A49F, K50E) had very low capacity to bind to Hsc70, whereas it was able to bind to Hsp90 very strongly. It seemed therefore that there was involvement of endogenous Hsc70-mSTI1-Hsp90 complex in the interactions. There are many possible explanations for this phenomenon. First, N217 interacts directly with Hsc70, which in turn interacts also directly with Hsp90. Some investigators have reported that purified Hsp70 and Hsp90 interact directly with each other to form weak Hsp90-Hsp70 complexes. (Murphy *et al.*, 2001 and Morishima *et al.*, 2001). Whether this direct interaction between Hsp70 and Hsp90 occurs in the cell, and its stoichiometry, is yet to be experimentally investigated.

A second explanation is the mediation of endogenous mSTI1 in bringing Hsc70 and Hsp90 together in close proximity. In this case, N217 displaces endogenous mSTI1 to bind to Hsc70, while Hsp90 maintains a weak interaction with Hsc70. Similarly, complex formed between N217(A49F, K50E) and Hsp90 *in vivo* could co-precipitate with Hsc70 either by direct Hsc70-Hsp90 interaction or by Hop mediated interaction of Hsc70 with Hsp90. Since N217(A49F, K50E) interacts very strongly with Hsp90, it is possible for the complex to precipitate more Hsc70/Hsp70 compared to the control N217. The other possibility is that N217 or N217(A49F, K50E) may dimerise with full-length mSTI1 in complex with both Hsc70 and Hsp90. This is only a speculation since the dimerization of mSTI1/Hop *in vivo* and the domains(s) involved, has not been shown experimentally.

Intriguing however is the fact that in *in vitro* binding assays, GST-N217 did not show any detectable interaction with Hsp90 (See Chapter Three, Figure 3.10), neither did GST-543(Y27A) (See Chapter 3, Figure 3.9) show any detectable interaction with Hsc70. One explanation for this is that, *in vitro*, exogenous recombinant mSTI1 is unable to displace native mSTI1 from the pre-existing complexes with Hsc70 or Hsp90 in the cell lysates. Therefore, it is only capable of binding to free Hsc70 or Hsp90 in the lysates. Whereas endogenously expressed recombinant mSTI1 not only binds to free Hsc70 and Hsp90, it seems to be able to compete with and probably displace native mSTI1 from complexes with Hsc70 and/or Hsp90. A better negative control for this *in vivo* experiment would be an mSTI1 protein derivative incapable of binding to both Hsc70 and Hsp90. Finally, it is possible that a mutant *in vivo* might be

in a more native state because of better chaperoning or the influence of post-translational modifications such as phosphorylation. Also, the *in vivo* complexes may contain more proteins that help keep everything together.

Chapter Six

Summary and Conclusions

The STI1 co-chaperones are associated with the dynamic Hsp70/Hsp90-dependent multi-chaperone complexes involved in the folding and functional maturation of some specific target substrates such as the steroid hormone receptors and cell cycle kinases. While STI1 has no measurable chaperone activity *in vitro*, it is important for the assembly of glucocorticoid receptor-chaperone complexes *in vivo*. In this study, a combination of techniques was used to characterize both qualitatively and quantitatively the contacts necessary for the N-terminal TPR domain of mSTI1 to bind to Hsc70. *In vitro* binding assays revealed that basic residues especially Lys^{8} and Asn^{12} in the helix A of the first TPR motif in mSTI1 are important in mediating its interaction with Hsc70.

While single mutation of either of these residues did not affect interaction of mSTI1 significantly, double substitution abrogated binding. This suggests that a network of electrostatic interactions is involved in the mSTI1-Hsc70 complex formation. On the other hand, mutations of any of the charged residues in helix A of the second TPR motif, could not abrogate binding of mSTI1 to Hsc70. Binding assay results showed that mSTI1 without the C-terminus was able to bind sufficiently with Hsc70. Combined results from steady state fluorescence and circular dichroism spectroscopy studies suggested the double substitution of Lys^{8} and Asn^{12} might have disrupted contacts made by TPR1 domain with other parts of mSTI1. Putting all these data together, it is therefore proposed that an additional domain exits in mSTI1, possibly at the C-terminus, which together with TPR1 domain is required for the complete binding of Hsc70 (Figure 6.1) (Odunuga *et al.*, 2003).

This model proposes two possible mechanisms for the binding of Hop to Hsc70. First, Hsc70 makes contacts with both the TPR1 domain and the proposed C-terminal domain (C domain) without any direct contacts between TPR1 and C domains themselves (Figure 6.1, pathway A). Second, TPR1 makes direct contacts with C domain, which together bind Hsc70 (Figure 6.1, pathway B). Data from this study support the latter hypothesis. While TPR1 domain alone can bind successfully to

Hsc70, C domain may not. But both domains are required for a complete and functional binding of Hop/mSTI1 to Hsc70. In addition to the above, it is further proposed that TPR2B binds to Hsp70, possibly in its ATP bound form. Possible experiments that could be carried out to test these hypotheses will include mutation of residues within the loop region between TPR2B and C domain. Mutations in this loop region will affect the interactions between TPR1 and C domains. In addition, further mutations other than those already done within the C domain of Hop/mSTI1, especially in identified motifs such as DPEV and DPAM (Chen and Smith, 1998) will be necessary to determine their effects on the proposed contacts between the TPR1 and C domains. The two domains can be isolated either by tryptic digestion or recombinant expression, and direct binding assays can be carried out in the presence and absence of Hsp70. Also, interaction between TPR1 and C domains can be monitored using fluorescence resonance energy transfer.

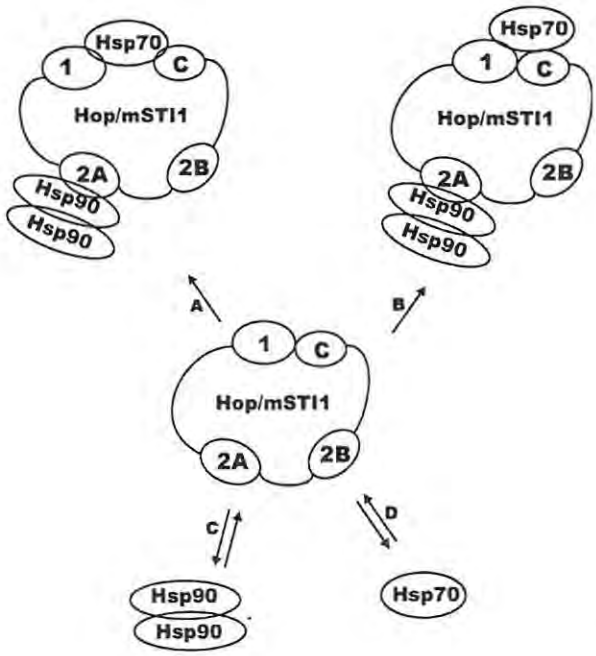

Figure 6.1:Proposed models for the interaction of Hop/mSTI1 with Hsp70 and Hsp90.
1: TPR1 domain; 2A: TPR2A; 2B: TPR2B; C: Proposed C-terminal domain.

In the second part of the study, interactions predicted by the crystal structures to mediate mSTI1 discrimination between Hsp70 and Hsp90 were characterized by a combination of site-directed mutagenesis, *in vitro* binding assays and surface plasmon resonance spectroscopy. Results from these experiments revealed that while Hsp90-binding capacity could be engineered on the Hsp70-binding N-terminal TPR domain of mSTI1, the reverse was not possible. In addition, this study reveals the importance of residues C-terminal of helix A of the second TPR motif in TPR1, in determining specificity of binding of mSTI1 to Hsp70 (Odunuga *et al.*, 2003).

In vivo characterization of these interactions was attempted. Histidine-tagged mSTI1 proteins were for the first time successfully expressed in cultured mouse fibroblasts using mammalian expression vector. One of the outcomes of the *in vivo* study was revealing the differences in the dynamics of interactions between Hop/mSTI1 and pre-existing complexes in *in vivo* and *in vitro* experiments. This study indicates that purified exogenous recombinant mSTI1 cannot displace native mSTI1 from complexes with Hsc70 and/or Hsp90 in cell lysates, rather it binds free Hsc70 and Hsp90. Whereas endogenously expressed recombinant mSTI1 can compete with and displace native mSTI1 from complexes with Hsc70 and/or Hsp90.

The experiments on the *in vivo* characterization of the TPR-mediated interactions of mSTI1/Hop need to be extended further to determine the effects of substitutions of other residues within both TPR1 and TPR2A domains. Other functional studies can be done by using the modified mSTI1 proteins in receptor complex reconstitution experiments. Additional experiments are needed to identify proteins that specifically interact with TPR2B.

References

Abbas-Terki, T., Donze, O., Briand, P. –A., Picard, D. (2001) Hsp104 interacts with Hsp90 cochaperones in respiring yeast. *Mol. Cell Biol.* **21**, 7569-7575

Abbas-Terki, T., Briand, P. -A., Donze, O., and Picard, D. (2002) The Hsp90 co-chaperones Cdc37 and Sti1 interact physically and genetically. *Biol. Chem.* **383**, 1335-1342

Agarraberes, F. A., and Dice, J. F. (2001) A molecular chaperone complex at the lysosomal membrane is required for protein translocation. *J. Cell Sci.* **114**, 2491-2499

Andrade, M. A., Ponting, C., Gibson, T., and Bork, P. (2000) Identification of protein repeats and statistical significance of sequence comparisons. *J. Mol. Biol.* **298**, 521-537

Anfisen, C. B. (1973) Principles that govern the folding of protein chains. *Science* **181**, 223-230

Argon, Y., and Simen, B. B. (1999) Grp94, an ER chaperone with protein and peptide binding properties. *Semin. Cell. Dev. Biol.* **10**, 495-505

Ballinger, C. A., Connell, P., Wu, Y., Hu, Z., Thompson, L. J., Yin, L.-Y., and Patterson, C. (1999) Identification of CHIP, a novel tetratricopeptide repeat-containing protein that interacts with heat shock proteins and negatively regulates chaperone functions. *Mol. Cell. Biol.* **19**, 4535-4545

Basso, D. A., Solit, D. B., Chiosis, G., Giri, B., Tsichlis, P., and Rosen, N. (2002) Akt forms an intracellular complex with heat shock protein 90 (Hsp90) and Cdc37 and is destabilized by inhibitors of Hsp90 function. *J. Biol. Chem.* **277**, 39858-39866

Baur, A., Schaaff-Gerstenschlager, I., Boles, E., Miosga, T., Rose, M., and Zimmermann, F. K. (1993) Sequence of a 4.8 kb fragment of *Saccharomyces cerevisiae* chromosome II including three essential open reading frames. *Yeast* **9**, 289-293

Beckman, R. P., Lovett, M., and Welch, W. J. (1992) Examining the function and regulation of Hsp70 in cells subjected to stress. *J. Cell Biol.* **117**, 1137-1150

Bell, D. R., and Poland, A. (2000) Binding of aryl hydrocarbon receptor (AhR) to AhR-interacting protein. *J. Biol. Chem.* **275**, 36407-36414

Bhattacharyya, T., Karneszis, A. N., Murphy, S. P., Hoang, T., Freeman, B. C., Philips, B., and Morimoto, R. I. (1995) Cloning and subcellular localization of human mitochondrial Hsp70. *J. Biol. Chem.* **270**, 1705-1710

Birnboim, H. C. (1983) A rapid alkaline extraction method for the isolation of plasmid DNA. *Methods Enzymol.* **100**, 243-255

Blake, C., and Serpell, L. (1996) Synchrotron X-ray studies suggest that the core of the transthyretin amyloid fibril is a continuous beta-sheet helix. *Structure* **4**, 989-98

Blatch, G. L., Lassle, M., Zetter, B. R., and Kundra, V. (1997) Isolation of a mouse cDNA encoding mSTI1, a stress-inducible protein containing the TPR motif. *Gene* **194**, 277-282

Blatch, G. L., and Lassle, M. (1999) The tetratricopeptide repeat, a structural motif mediating protein-protein interactions. *BioEssays* **21**, 932-939

Boguski, M. S., Sikorski, R. S., Hieter, P., and Goebl, M. (1990) Expanding family. *Nature* **346**, 114-116

Boguski, M. S., Murray, A. W., and Powers, S. (1992) Novel repetitive sequence motifs in the alpha and beta subunits of prenyl-protein transferases and homology of the subunit to the MAD2 gene product of yeast. *New Biol.* **4**, 408-411

Boltner, D., MacMahon, C., Pembroke, J. T., Strike, P., and Osborn, A. M. (2002) R391: a Conjugative Integrating Mosaic Comprised of Phage, Plasmid, and Transposon Elements. *J. Bacteriol.* **184,** 5158-5169

Bonnefoy, S., Attal, G., Lansgley, G., Tekaia, F., and Mercerean-Puijalon, O. (1994) Molecular characterization of the heat shock protein 90 gene of the human malarial parasite *Plasmodium falciparum. Parasitol.* **67**, 157-170

Brinker, A., Scheufler, C., von Der Mulbe, F., Fleckenstein, B., Herrmann, C., Jung, G., Moarefi, I., and Hartl, F. U. (2002) Ligand discrimination by TPR domain, relevance and selectivity of EEVD-recognition in Hsp70.Hop.Hsp90 complexes. *J. Biol. Chem.* **277**, 19265-19275

Bucciantini, M., Giannoni, E., Chiti, F., Baroni, F., Formigli, L., Zurdo, J., Taddei, N., Ramponi, G., Dobson, C. M., and Stefani, M. (2002) Inherent toxicity of aggregates implies a common mechanism for protein misfolding diseases. *Nature* **416**, 507-511

Buchner, J. (1999) Hsp90 & co. – a holding for folding. *Trends Biochem. Sci.* **24**, 136-141

Bukau, B., and Horwich, A. L. (1998) The Hsp70 and Hsp90 chaperone machines. *Cell* **92**, 351-366

Bult, C. J., White, O., Oslen, G. J., *et al.*, (1996) Complete genome sequence of the methanogenic archaeon, *Methanococcus jannaschii. Science* **273**, 1058-1073

Burkholder, W. F., Zhao, X., Zhu, X., and Hendrickson, W. A. (1996) Mutations in the C-terminal fragment of DnaK affecting peptide binding. *Proc. Natl. Acad. Sci.* USA **93**, 10632-10637

Carlton, J. M., Angiuoli, S. V., Suh, B. B., *et al.*, (2002) Genome sequence and comparative analysis of the model rodent malaria parasite *Plasmodium yoelii yoelii*. *Nature* **419**, 512-519

Caplan, A. J. (1999). Hsp90's secrets unfold: new insights from structural and functional studies. *Trends Cell Biol.* **9**, 262-268.

Carrello, A., Ingley, E., Minchin, R. F., Tsai, S., and Ratajczak, T. (1999) The common tetratricopeptide repeat acceptor site for steroid receptor-associated immunophilins and Hop is located in the dimerization domain of Hsp90. *J. Biol. Chem.* **274**, 2682-2689

Chang, H-C. J., Nathan, D. F., and Lindquist, S. (1997) *In vivo* analysis of the Hsp90 cochaperone Sti1. *Mol. Cell. Biol.* **17**, 318-325

Celis, J. E., Dejgaard, K., Madsen, P., Leffers, H., Gesser, B., Honore, B., Rasmussen, H. H., Olsen, E., Lauridsen, J. B., and Ratz, G. (1990). The MRC-5 human embryonal lung fibroblast two-dimensional gel cellular protein database: quantitative identification of polypeptides whose relative abundance differs between quiescent, proliferating and SV40 transformed cells. *Electrophoresis* **11**, 1072-1113

Chen, S., Prapapanich, V., Rimerman, R. A., Honore, B., and Smith, D. F. (1996) Interactions of p60, a mediator of progesterone receptor assembly, with heat shock proteins hsp90 and hsp70. *Mol. Endocrinol.* **10**, 682-693

Chen, S., and Smith, D. F. (1998) Hop as an adaptor in the heat shock protein 70 (hsp70) and hsp90 chaperone machinery. *J. Biol. Chem.* **273**, 35194-35200

Cheng, C. H., Liu, S. M., Chow, T. Y., Hsiao, Y. Y., Wang, D. P., Huang, J. J., and Chen, H. H. (2002) Analysis of the Complete Genome Sequence of the Hz-1 Virus Suggests that It Is Related to Members of the *Baculoviridae*. *J. Virol.* **76**, 9024-9034

Chomczynski, P., and Sacchi, N. (1987) Single-step method of RNA isolation by acid guanidinium thiocyanate-phenol-chloroform extraction. *Anal. Biochem.* **162**, 156-159

Cheung, J., and Smith, D. F. (2000). Molecular chaperone interactions with steroid receptors: an update. *Mol. Endocrinol.* **14**, 939-946.

Craig, E. A., Gambill, B. D., and Nelson, R. J. (1993) Heat shock proteins, molecular chaperones of protein synthesis. *Microbiol. Rev.* **57**, 402-414

Csaba, S., Racz, A., and Csermely, P. (2002) A nucleotide-dependent molecular switch controls ATP binding at the C-terminal domain of Hsp90. *J. Biol. Chem.* **277**, 7066-7075

Czar, M. J., Galigniana, M. D., Silverstein, A. M., and Pratt, W. B. (1997) Geldanamycin, a heat shock protein 90-binding benzoquinone ansamycin, inhibits steroid-dependent translocation of the glucocorticoid receptor from the cytoplasm to the nucleus. *Biochemistry* **36**, 7776-7785

Das, A. K., Cohen, P. T. W., and Barford, D. (1998) The structure of the tetratricopeptide repeats of protein phosphatase 5, implications for TPR-mediated protein-protein interactions. *EMBO J.* **17**, 1192-1199

Delling, U., Raymond, M., and Schurr, E. (1998) Identification of *Saccharomyces cerevisiae* genes conferring resistance to quinoline ring-containing antimalarial drugs. *Antimicrob. Agents Chemo.* **42**, 1034-1041

Demand, J., Luders, J., and Hohfeld, J. (1998) The carboxy-terminal domain of Hsc70 provides binding sites for a distinct set of chaperone cofactors. *Mol. Cell. Biol.* **18**, 2023-2028

Dey, B., Caplan, A. J., and Boschelli, F. (1996) The Ydj1 molecular chaperone facilitates formation of active p60v-src in yeast. *Mol. Biol. Cell* **7**, 91-100

Dill, K. A., and Chan, H. S. (1997) From Levinthal to pathways to funnels. *Nat. Struct. Biol.* **4**, 10-19

Dittmar, K. D., Hutchison, K. A., Owens-Grillo, J. K., and Pratt, W. B. (1996) Reconstitution of the steroid receptor-hsp90 heterocomplex assembly system of rabbit reticulocyte lysate. *J. Biol. Chem.* **271**, 12833-12839

Dittmar, K. D., and Pratt, W. B. (1997) Folding of the glucocortoid receptor by the reconstituted hsp90-based chaperone machinery The initial hsp90.p60.hsp70-dependent step is sufficient for creating the steroid binding conformation. *J. Biol. Chem.* **272**, 13047-13054

Dittmar, K. D., Demady, D. R., Stancato, L. F., Krishna, P., and Pratt, W. B. (1997) Folding of the glucocortoid receptor by heat shock protein (hsp) 90-based chaperone machinery The role of p23 is to stabilize receptor.hsp90 heterocomplexes formed by hsp90.p60.hsp70. *J. Biol. Chem.* **272**, 21213-21220

Dodt, G., Braverman, N., Wong, C., Moser, H. W., Watkins, P., Valle, D., and Gould, S. J. (1995) Mutations in the PTS1 receptor gene, PXR1, define complementation group 2 of the peroxisome biogenesis disorders. *Nat. Genet.* **9**, 115-125

Dutta, R., and Inouye, M. (2000) GHKL, an emergent ATPase/kinase superfamily. *Trends Biochem. Sci.* **25**, 24-28

Dolinski, K. J., Cardenas, M. E., and Heitman, J. (1998) *CNS1* encodes an essential p60/Stil1 homolog in *Saccharomyces cerevisiae* that suppresses cyclophilin 40 mutations and interacts with Hsp90. *Mol. Cell. Biol.* **18**, 7344-7352

Ellis, R. J. (1987) Proteins as molecular chaperones. *Nature* **328**, 378-379

Ellis, R. J., and Pinheiro, T. J. P. (2002) Medicine: Danger-misfolding proteins. *Nature* **416**, 483-484

Feldman, D. E., Thulasiraman, V., Ferreyra, R. G., and Frydman, J. (1999) Formation of the VHL-elongin BC tumor suppressor complex is mediated by the chaperonin TRiC. *Mol. Cell.* **4**, 1051-1061

Felts, S. J., Owen, B. A. L., Nguyen, P., Trepel, J., Donner, D. B., and Toft, D. O. (2000) The hsp90-related protein TRAP1 is a mitochondrial protein with distinct functional properties. *J. Biol. Chem.* **275**, 3305-3312

Flaherty, K. M., Deluca-Flaherty, C., and McKay, D. B. (1990) Three-dimensional structure of the ATPase fragment of a 70kD heat shock cognate protein. *Nature* **346**, 623-628

Freedman, R. B., Hirst, T. R., and Tuite, M. F. (1994) Protein disulphide isomerase: building bridges in protein folding. *Trends Biochem. Sci.* **19**, 331-336

Frydman, J. (2001) Folding of newly translated proteins *in vivo*: the role of molecular chaperones. *Annu. Rev. Biochem.* **70**, 603-647

Frydman, J., Nimmesgern, E., Ohtsuka, K., and Hartl, F. U. (1994) Folding of nascent polypeptide chains in a high molecular mass assembly with molecular chaperones. *Nature* **370**, 111-117

Frydman, J., and Hartl, F. U. (1996) Principles of chaperone-assisted protein folding, differences between *in vitro* and *in vivo* mechanisms. *Science.* **272**, 1497-1502

Frydman, J., and Hohfeld, J. (1997) Chaperones get in touch, the Hip-Hop connection. *Trends Biochem. Sci.* **22**, 87-92

Gale, M. Jr., Tan, S. L., Wambach, M., and Katze, M. G. (1996) Interaction of the interferon-induced PKR protein kinase with inhibitory proteins P581PK and vaccinia virus K3L is mediated by unique domains, implications for kinase regulation. *Mol. Cell Biol.* **16**, 4172-4181

GeneTools, version 1.0, BioTools Incorporated 2002 (Canada)

Georgopoulos, C. (1992) The emergence of the chaperone machines. *Trends Biochem. Sci.* **17**, 295-299

Gething, M. J., and Sambrook, J. F. (1992) Protein folding in the cell. *Nature* **355**, 33-45

Gindhart, J. G., Jr., and Goldstein, L. S. (1996) Tetratricopeptide repeats are present in the kinesin light chain. *Trends Biochem. Sci.* **21**, 52-53

Goebl, M., and Yanagida, M. (1991) The TPR snap helix: a novel protein repeat motif from mitosis to transcription. *Trends Biochem. Sci.* **16**, 173-177

Goffeau, A., Barrell, B. G., Bussey, H., Davis, R. W., Dujon, B., Feldmann, H., Galibert, F., Hoheisel, J. D., Jacq, C., Johnston, M., Louis, E. J., Mewes, H. W.,

Murakami, Y., Philippsen, P., Tettelin, H., and Oliver, S. G. (1996) Life with 6000 genes. *Science* **274**, 546, 563-567

Gounalaki, N., Tzamarias, D., and Vlassi, M. (2000) Identification of residues in the TPR domain of Ssn6 responsible for interaction with the Tup1 protein. *FEBS Lett.* **473**, 37-41

Grenert, J. P., Johnson, B. D., and Toft, D. O. (1999) The importance of ATP binding and hydrolysis by hsp90 in formation and function of protein heterocomplexes. *J. Biol. Chem.* **274**, 17525-33

Gross, M., and Hessefort, S. (1996) Purification and characterization of a 66-kDa protein from rabbit reticulocyte lysate which promotes the recycling of Hsp 70. *J. Biol. Chem.* **271**, 16833-16841

Hamilton, J. A., Steinrauf, L. K., Braden, B. C., Liepnieks, J., Benson, M. D., Holmgren, G., Sandgren, O., and Steen, L. (1993) The x-ray crystal structure refinements of normal human transthyretin and the amyloidogenic Val-30-->Met variant to 1.7-Å resolution. *J. Biol. Chem.* **268**, 2416-2424

Harrison, C. J., Hayer-Hartl, M., Diliberta, M., Hartl, F. U., and Kuriyan, J. (1997) Crystal structure of the nucleotide exchange factor GrpE bound to the ATPase domain of the molecular chaperone DnaK. *Science* **276**, 431-435

Hartl, F.U. (1996) Molecular chaperones in cellular protein folding. *Nature* **381**, 571-580

Hartl, F. U., and Hayer-Hartl, M. (2002) Molecular chaperones in the cytosol: from nascent chain to folded protein. *Science* **295**, 1852-1858

Heine, H., Delude, R. L., Monks, B. G., Espevik, T., and Golenbock, D. T. (1999) Bacterial lipopolysaccharide induces expression of the stress response genes hop and H411. *J. Biol. Chem.* **274**, 21049-21055

Hendrick, J. P., and Hart, F. U (1993) Molecular chaperone functions of heat-shock proteins. *Annu. Rev. Biochem.* **62**, 349-84

Hernandez, M. P., Sullivan, W. P., and Toft, D. O. (2002) The assembly and intermolecular properties of the hsp70-Hop-hsp90 molecular chaperone complex. *J. Biol. Chem.* **277**, 38294-38304

Hernandez Torres, J., Chatellard, P., and Stutz, E. (1995) Isolation and characterization of gmsti, a stress-inducible gene from soybean (*Glycine max*) coding for a protein belonging to the TPR (tetratricopeptide repeats) family. *Plant Mol. Biol.* **27**, 1221-1226

Heyrovska, N., Frydman, J., Hohfeld, J., and Hartl, F. U. (1998) Directionality of polypeptide transfer in the mitochondrial pathway of chaperone-mediated protein folding. *Biol. Chem.* **379**, 301-9

Hightower, L. E. (1980) Cultured animal cells exposed to amino acid analogues or puromycin rapidly synthesize several polypeptides. *J. Cell Physiol.* **102**, 407-427

Hirano, T., Kinishita, N., Morikawa, K., and Yanagida, M. (1990) Snap helix with knob and hole, essential repeats in *Schizosaccharomyces pombe* nuclear protein *nuc*2+. *Cell* **60**, 319-328

Hohfeld, J., and Hartl, F. U. (1994) Role of the chaperonin cofactor Hsp10 in protein folding and sorting in yeast mitochondria. *J. Cell Biol.* **126**, 305-315

Hohfeld, J., Minami, Y., and Hartl, F. U. (1995) Hip, a novel cochaperone involved in the eukaryotic Hsc70/Hsp40 reaction cycle. *Cell* **83**, 589-598

Honore, B., Leffers, H., Madsen, P., Rasmussen, H. H., Vandeckerckhove, J., and Celis, J. E. (1992) Molecular cloning and expression of a transformation –sensitive human protein containing TPR motif and sharing identity to the stress-inducible yeast protein STI1. *J. Biol. Chem.* **267**, 8485-8491

Irmer, H., and Hohfeld, J. (1997) Characterization of functional domains of the eukaryotic co-chaperone Hip. *J. Biol. Chem.* **272**, 2230-2235

Irniger, S., Piatti, S., Michaelis, C., and Nasmyth, K. (1995) Genes involved in sister chromatid separation are needed for B-type cylcin proteolysis in budding yeast. *Cell* **81**, 269-278

Jaenicke, R. (1998) Protein self-organization *in vitro* and *in vivo*: partitioning between physical biochemistry and cell biology. *Biol. Chem.* **379**, 237-243.

Jaenicke, R. (1991) Protein folding: local structures, domains, subunits, and assemblies. *Biochemistry* **30**, 3147-3161

Jindal, S. (1996) Heat shock proteins, applications in health and disease. *TIBTECH.* **14**, 17-21

Johnson, J. L., and Toft, D. O. (1994). A novel chaperone complex for steroid receptors involving heat shock proteins, immunophilins, and p23. *J. Biol. Chem.* **269**, 24989-24993.

Johnson, B. D., Schumacher, R. J., Ross, E. D., and Toft, D. O. (1998) Hop modulates Hsp70/90 interactions in protein folding. *J. Biol. Chem.* **273**, 3679-3686

Johnson, J. L., and Craig, E. A. (2000) A role for the Hsp40 Ydj1 in repression of basal steroid receptor activity in yeast. *Mol. Cell Biol.* **20**, 3027-36

Joshi, M., Dwyer, D. M., and Nakhasi, H. L. (1993) Cloning and characterization of differentially expressed genes from in vitro-grown 'amastigotes' of *Leishmania donovani*. *Mol. Biochem. Parasitol.* **58**, 345-354

Kanelakis, K. C., Morishima, Y., Dittmar, K. D., Galigniana, M. D., Takayama, S., Reed, J. C., and Pratt, W. B. (1999) Differential effects of the hsp70-binding protein

BAG-1 on glucocorticoid receptor folding by the hsp90-based chaperone machinery. *J. Biol. Chem.* **274**, 34134-40

Kaufmann, S. H. E. (1990) Heat shock proteins and the immune response. *Immunol. Today* **11**, 129-136

Kelly, J. W. (1996) Alternative conformations of amyloidogenic proteins govern their behaviour. *Curr. Opin. Struct. Biol.* **6**, 11-17.

Kelly, J. W. (1997) Amyloid fibril formation and protein misassembly: a structural quest for insights into amyloid and prion diseases. *Structure* **5**, 595-600.

Kimura, Y., Yahara, I., and Lindquist, S. (1995). Role of the protein chaperone YDJ1 in establishing Hsp90-mediated signal transduction pathways. *Science* **268**, 1362-1365.

Kimura, Y., Rutherford, S. L., Miyata, Y., Yahara, I., Freeman, B. C., Yue, L., Morimoto, R. I., and Lindquist, S. (1997) Cdc37 is a molecular chaperone with specific functions in signal transduction. *Genes Dev.* **11**, 1775-1785

Kluck, C. J., Patzelt, H., Genevaux, P., Brehmer, D., Rist, W., Mergener-Scheider, J., Bukau, B., and Mayer, M. P. (2002) Structure-function analysis of HscC, the *Escherichia coli* member of a novel subfamily of specialized Hsp70 chaperones. *J. Biol. Chem.* **277**, 41060-41069

Kordes, E., Savelyeva, L., Schwab, M., Rommelaere, J., Jauniaux, J. C., and Cziepluch, C. (1998) Isolation and characterization of human SGT and identification of homologues in *Saccharomyces cerevisiae* and *Caenorhabditis elegans Genomics* **52**, 90-94

Kraulis, P. J. (1991) MOLSCRIPT, a program to produce both detailed and schematic plots of protein structures. *J. App. Cryst.* **24**, 946-950

Kumar, A., Roach, C., Hirsh, I. S., Turley, S., deWalque, S., Michels, P. A. M., and Hol, W. G. J. (2001) An unexpected extended conformation for the third TPR motif of the peroxin PEX5 from *Trypanosoma brucei*. *J. Mol. Biol.* **307**, 271-282

Laemmli, U. K. (1970) Cleavage of structural proteins during the assembly of the head of bacteriophage T4. *Nature* **227**, 680-685

Lamb, J. R., Tugendreich, S., and Hieter, P. (1995) Tetratricopeptide repeat interactions, to TPR or not to TPR. *Trends Biochem. Sci.* **20**, 257-259

Langer, T., Lu, C., Echols, H., Flanagan, J., Hayer, M. K., and Hartl, F. U. (1992) Successive action of DnaK, DnaJ and GroEL along the pathway of chaperone-mediated protein folding. *Nature* **356**, 683-689

Lapouge, K., Smith, S. J. M., Walker, P. A., Gamblin, S. J., Smerdon, S. J., and Rittinger, K. (2000) Structure of the TPR domain of $p67^{phox}$ in complex with Rac.GTP. *Mol. Cell.* **6**, 899-907

Laskey, R. A., Honda, B. M., Mills, A. D., and Finch, J. T. (1978) Nucleosomes are assembled by an acidic protein, which binds histones and transfers them to DNA. *Nature* **275**, 416-420

Lassle, M., Blatch, G. L., Kunra, V., Takatori, T., and Zetter, B. R. (1997) Stress-inducible, murine protein mSTI1; Characterization of binding domains for heat shock proteins and *in vitro* phosphorylation by different kinases. *J. Biol. Chem.* **272**, 1876-1884

Laufen, T., Mayer, M. P., Beisel, C., Klostermeier, D., Mogk, A., Reinstein, J., and Bukau, B. (1999) Mechanism of regulation of Hsp70 chaperones by DnaJ cochaperones. *Biochemistry* **96**, 5452-5457

Liberek, K., Skowyra, D., Zylicz, M., Johnson, C., and Georgopoulos, C. (1991) The *Escherichia coli* DnaK chaperone, the 70-kDa heat shock protein eukaryotic equivalent, changes conformation upon ATP hydrolysis, thus triggering its dissociation from a bound target protein. *J. Biol. Chem.* **266**, 14491-14496

Lindenthal, C., and Klinkert, Mo-Q. (2002) Identification and biochemical characterisation of a protein phosphatase 5 homologue from *Plasmodium falciparum*. *Mol. Biochem. Parasitol.* **120**, 257-268

Liu, F., Wu, S., Hu, S., Hsiao, C., and Wang, C. (1999) Specific interaction of the 70-kDa heat shock cognate protein with tetratricopeptide repeats. *J. Biol. Chem.* **274**, 34425-34432

Longshaw, V. M., Dirr, H. W., Blatch, G. L., and Lassle, M. (2000) The *in vitro* phosphorylation of the co-chaperone mSTI1 by cell cycle kinases substantiates a predicted casein kinase II-p34cdc2-NLS (CcN) motif. *Biol. Chem.* **381**, 1133-1138

Lowry, D. H., Rosebrough, N. J., Fan, A. L., and Randall, R. J. (1951) Protein measurement with the Folin-phenol reagent. *J. Biol. Chem.* **193**, 265-275

Malek, S. N., Yang, C. H., Earnshaw, W. C., Kozak, C. A., and Desiderio, S. (1996) p150, a conserved nuclear phosphoprotein that contains multiple tetratricopeptide repeats and binds specifically to SH2 domains. *J. Biol. Chem.* **271**, 6952-6962

Maruya, M., Sameshima, M., Nemoto, T., and Yahara, I. (1999) Monomer arrangement in HSP90 dimer as determined by decoration with N and C-terminal region specific antibodies. *J. Mol. Biol.* **285**, 903-907

Mayer, M. P., Brehmer, D., Gassler, C. S., and Bukau, B. (2001) in *Advances in Protein Chemistry: Protein Folding in the cell* (Horwich, A. L., ed) Vol. **59**, pp. 1-44, Academic Press, San Diego

Mayr, C., Richter, K., Lilie, H., and Buchner, J. (2000) Cpr6 and Cpr7, two closely related Hsp90-associated immunophilins from *Saccharomyces cerevisiae*, differ in their functional properties. *J. Biol. Chem.* **275**, 34140-34146

Minton, A. P. (2000) Protein folding: Thickening the broth. *Curr. Biol.* **10**, R97-9

Minton, A. P. (2000) Implications of macromolecular crowding for protein assembly. *Curr. Opin. Struct. Biol.* **10**, 34-9.

Morimoto, R. I., Tissieres, A., and Georgopoulos, C. (1994) In, *The biology of heat shock proteins and molecular chaperones,* (Morimoto, R.I., Tissieres, A. and Georgopoulos, C., eds.) Cold Spring Harbor Laboratory, Cold Spring Harbor, NY., pp 1-30

Morishima, Y., Murphy, P. J., Li, D. P., Sanchez, E. R., and Pratt, W. B. (2000). Stepwise assembly of a glucocorticoid receptor hsp90 heterocomplex resolves two sequential ATP-dependent events involving first hsp70 and then hsp90 in opening of the steroid binding pocket. *J. Biol. Chem.* **275**, 18054-18060.

Morishima, Y., Kanelakis, K. C., Murphy, P. J. M., Shewach, D. S., and Pratt, W. B. (2001) Evidence for iterative ratcheting of receptor-bound hsp70 between its ATP and ADP conformations during assembly of glucocorticoid receptor.hsp90 heterocomplexes. *Biochemistry* **40**, 1109-1116

Moro, F., Okamoto, K., Donzeau, M., Neupert, W., and Brunner, M. (2002) Mitochodrial protein import: molecular basis of the ATP-dependent interaction of MtHsp70 with Tim44. *J. Biol. Chem.* **277**, 6874-6880

Murre, C., McCaw, P. S., Vaessin, H., Caudy, M., Jan, Y. N., Cabrera, C. V., Buskin, J. N., Hauschka, S. D., and Lassar, A. B. (1998) Interactions between heterologous helix-loop-helix proteins generate complexes that bind specifically to a common DNA sequence. *Cell* **58**, 537-544

Murphy, P. J., Kanelakis, K. C., Galigniana, M. D., Morishima, Y., and Pratt, W. B. (2001) Stoichiometry, abundance, and functional significance of the hsp90/hsp70-based multiprotein chaperone machinery in reticulocyte lysate. *J. Biol. Chem.* **276**, 30092-30098

Murthy, A. E., Bernards, A., Church, D., Wasmuth, J., and Gusella, J. F. (1996) Identification and characterization of two novel tetratricopeptide repeat-containing genes *DNA Cell Biol.* **15**, 727-735

Nakatsu, Y., Asahina, H., Citterio, E., Rademakers, S., Vermeulen, W., Kamiuchi, S., Yeo, J-P., Khaw, M-C., Saijo, M., Kodo, N., Matsuda, T., Hoeijmakers, J. H. J., and Tanaka, K. (2000) XAB2, a novel tetratricopeptide repeat protein involved in transcription-coupled DNA repair and transcription. *J. Biol. Chem.* **275**, 34931-34937

Nemoto, T., Nemoto-Ohara, Y., Takagi, T., and Yokoyama, K. (1995) Mechanism of dimer formation of the 90-kDa heat-shock protein. *Eur. J. Biochem.* **233**, 1-8

Nicolet, C. M., and Craig, E. A. (1989) Isolation and characterization of STI1, a stress-inducible gene from *Saccharomyces cerevisiae. Mol.Cell Biol.* **9**, 3638-3646

Odunuga, O. O., Hornby, J. A., Bies, C., Zimmermann, R., Pugh, D. J., and Blatch, G. L. (2003) Tetratricopeptide repeat motif-mediated Hsc70-mSTI1 interaction:

molecular characterization of the critical contacts for successful binding and specificity. *J. Biol. Chem.* **278**, 6896-6904

O'Farrell, P. H. (1975) High resolution two-dimensional electrophoresis of proteins. *J. Biol. Chem.* **250**, 4007-4021

Ordway, R. W., Pallanck, L., and Ganetzky, B. (1994) A TPR domain in the SNAP secretory proteins. *Trends Biochem. Sci.* **19**, 530-531

Owens-Grillo, J. K., Czar, M. J., Hutchison, K. A., Hoffman, K., Perdew, G. H., and Pratt, W. B. (1996) A model of protein targeting mediated by immunophilins and other proteins that bind to hsp90 via tetratricopeptide repeat domains. *J. Biol. Chem.* **271**, 13468-13475

Panaretou, B., Prodromou, C., Roe, S. M., O'Brien, R., Ladbury. J. E., Piper, P. W., and Pearl, L. H. (1998) ATP binding and hydrolysis are essential to the function of the Hsp90 molecular chaperone *in vivo*. *EMBO J.* **17**, 4829-4836

Parsell, D. A., and Lindquist, S. (1993) The function of heat-shock proteins in stress tolerance, degradation and reactivation of damaged proteins. *Annu. Rev. Genet.* **27**, 437-496

Pearl, L. H., and Prodromou, C. (2000). Structure and *in vivo* function of Hsp90. *Curr. Opin. Struct. Biol.* **10**, 46-51.

Picard, D., Khursheed, B., Garabedian, M. J., Fortin, M. G., Lindquist, S., and Yamamoto, K. R. (1990). Reduced levels of hsp90 compromise steroid receptor action *in vivo*. *Nature* **348**, 166-168.

Prapapanich, V., Chen, S., Nair, S. C., Rimerman, R. A., and Smith, D. F. (1996) Molecular cloning of human p48, a transient component of progesterone receptor complexes and an Hsp70-binding protein. *Mol. Endocrinol.* **10**, 420-31

Prapapanich, V., Chen, S., and Smith, D. F. (1998) Mutation of Hip's carboxy-terminal region inhibits a transitional stage of progesterone receptor assembly. *Mol. Cell Biol.* **18**, 944-52

Pratt, W. B. (1990). Interaction of hsp90 with steroid receptors: organizing some diverse observations and presenting the newest concepts. *Mol. Cell. Endocrinol.* **74**, C69-76.

Pratt, W. B. (1993). The role of heat shock proteins in regulating the function, folding, and trafficking of the glucocorticoid receptor. *J. Biol. Chem.* **268**, 21455-21458.

Pratt, W. B., and Toft, D. O. (1997). Steroid receptor interactions with heat shock protein and immunophilin chaperones. *Endocr. Rev.* **18**, 306-360.

Pratt, W. B. (1998) The hsp90-based chaperone system: involvement in signal transduction from a variety of hormone and growth factor receptors. *Proc. Soc. Exp. Biol. Med.* **217**, 420-34

Preker, P. J., and Keller, W. (1998) The HAT helix, a repetitive motif implicated in RNA processing. *Trends Biochem. Sci.* **23**, 15-16

Prodromou, C., Roe, S. M., O'Brien, R., Ladbury, J. E., Piper, P. W., and Pearl, L. H. (1997) Identification and structural characterization of the ATP/ADP-binding site in the Hsp90 molecular chaperone. *Cell* **90**, 65-75

Prodromou, C., Roe, S. M., Piper, P. W., and Pearl, L. H. (1997) A molecular clamp in the crystal structure of the N-terminal domain of the yeast Hsp90 chaperone. *Nat. Struct. Biol.* **4**, 477-482

Prodromou, C., Siligardi, G., O'Brien, R., Woolfson, D. N., Regan, L., Panaretou, B., Ladbury, J. E., Piper, P. W., and Pearl, L. H. (1999) Regulation of Hsp90 ATPase activity by tetratricopeptide repeat (TPR)-domain co-chaperones. *EMBO J.* **18**, 754-762

Prodromou, C., Panaretou, B., Chohan, S., Siligardi, G., O'Brien, R., Ladbury, J. E., Roe, S. M., Piper, P. W., and Pearl, L. H. (2000) The ATPase cycle of Hsp90 drives a molecular 'clamp' via transient dimerization of the N-terminal domains. *EMBO J.* **19**, 4383-92

Queitsch, C., Sangster, T. A., and Lindquist, S. (2002) Hsp90 as a capacitor of phenotypic variation. *Nature* **417**, 618-624

Ratajczak, T., and Carrello, A. (1996) Cyclophilin 40 (cyp-40), mapping of its hsp90 binding domain and evidence that FKBP52 competes with cyp-40 for hsp90 binding. *J. Biol. Chem.* **271**, 2961-2965

Richter, K., Reinstein, J., and Buchner, J. (2002) N- terminal residues regulate the catalytic efficiency of the Hsp90 ATPase cycle. *J. Biol. Chem.* **277**, 44905-44910

Ritossa, F. (1962) A new puffing pattern induced by temperature shock and DNP in Drosophila. *Experimentia* **18**, 571-573

Rudiger, S., Buchberger, A., and Bukau, B. (1997) Interaction of Hsp70 chaperones with substrates. *Nat. Struct. Biol.* **4**, 342-349

Russell, L. C., Whitt, S. R., Chen, M., and Chinkers, M. (1999) Identification of conserved residues required for the binding of a tetratricopeptide repeat domain to heat shock protein 90. *J. Biol. Chem.* **274**, 20060-20063

Rutherford, S. L., and Lindquist, S. (1998) Hsp90 as a capacitor for morphological evolution. *Nature* **396**, 336-342

Scanlan, M. J., Chen, Y. T., Williamson, B., Gure, A. O., Stockert, E., Gordan, J. D., Tureci, O., Sahin, U., Pfreundschuh, M., and Old, L. J. (1998) Characterization of human colon cancer antigens recognized by autologous antibodies *Int. J. Cancer* **76**, 652-658

Scheibel, T., Weikl, T., and Buchner, J. (1998) Two chaperone sites in Hsp90 differing in substrate specificity and ATP dependence. *Proc. Natl. Acad. Sci. USA,* **95**, 1495-1499

Scheibel, T., Siegmund, H. I., Jaenicke, R., Ganz, P., Lilie, H., and Buchner, J. (1999) The charged region of Hsp90 modulates the function of the N-terminal domain. *Proc. Natl. Acad. Sci. USA,* **96**, 1297-1302

Scheufler, C., Brinker, A., Bourenkov, G., Pegoraro, S., Moroder, L., Barfunlk, H., Hartl, F. U., and Moerefl, J. (2000) Structure of TPR domain-peptide complexes, critical elements in the assembly of the Hsp70-Hsp90 multichaperone machine. *Cell* **101**, 199-210

Schmid, F. X. (1993) Prolyl isomerase: enzymatic catalysis of slow protein-folding reactions. *Annu. Rev. Biophys. Biomol. Struct.* **22**, 123-142

Serpell, L. C., Sunde, M., Fraser, P. E., Luther, P. K., Morris, E. P., Sangren, O., Lundgren, E., and Blake, C. C. (1995) Examination of the structure of the transthyretin amyloid fibril by image reconstruction from electron micrographs. *J. Mol. Biol.* **254**, 113-118

Shaw, D. J. (ed.) (1995) Molecular Genetics of human inherited disease. J. Wiley & Sons.

Sikorski, R. S., Boguski, M. S., Goebl, M., and Hieter, P. (1990) A repeating amino acid motif in CDC23 defines a family of proteins and a new relationship among genes required for mitosis and RNA synthesis. *Cell* **60**, 307-317

Silverstein, A. M., Galigniana, M. D., Kanelakis, K. C., Radanyi, C., Renoir, J. M., and Pratt, W. B. (1999) Different regions of the immunophilin FKBP52 determine its association with the glucocorticoid receptor, hsp90, and cytoplasmic dynein.. *J. Biol. Chem.* **274**, 36980-36986

Small, I. D., and Peteers, N. (2000) The PPR motif – a TPR-related motif prevalent in plant organellar proteins. *Trends Biochem. Sci.* **25**, 46-47

Smith, D. F., Sullivan, W. P., Marion, T. N., Zaitsu, K., Madden, B., McCormick, D. J., and Toft, D. O. (1993) Identification of a 60-Kilodalton stress-related protein, p60, which interacts with hsp90 and hsp70. *Mol. Cell. Biol.* **13**, 869-876

Smith, D. F. (1998) Sequence motifs shared between chaperone components participating in the assembly of progesterone receptor complexes. *Biol. Chem.* **379**, 283-288

Smith, D. F., and Toft, D. O. (1993). Steroid receptors and their associated proteins. *Mol. Endocrinol.* **7**, 4-11.

Sriram, M., Osipiuk, J., Freeman, B. C., Morimoto, R. I., and Joachimiak, A. (1997) Human Hsp70 molecular chaperone binds two calcium ions within the ATPase domain. *Structure* **5**, 403-414

Stebbins, C. E., Russo, A. A., Schneider, C., Rosen, N., Hartl, F. U., and Pavletich, N. P. (1997) Crystal structure of an Hsp90-geldanamycin complex: targeting of a protein chaperone by an antitumor agent. *Cell* **89**, 239-50

Strickler, J. E., Berka, T. R., Gorniak, J., Fornwald, J., Keys, R., Rowland, J. J., Rosenberg, M., and Taylor, D. P. (1992) Two novel Streptomyces protein protease inhibitors. Purification, activity, cloning, and expression. *J. Biol. Chem.* **267**, 3236-3241

Suh, W. C., Lu, C. Z., and Gross, C. A. (1999) Structural features required for the interaction of the Hsp70 molecular chaperone DnaK with its cochaperone DnaJ. *J. Biol. Chem.* **274**, 30534-30539

Sullivan, W. P., Owen, B. A., and Toft, D. O (2002) The influence of ATP and p23 on the conformation of Hsp90. *J. Biol. Chem.* **277**, 45942-45948

Sunde, M. (1999) Amyloid formation and disease. In: Oxford Innovation Society Seminar, *Isis Innovation Newsletter*, edition **27**

Szabo, A., Korszum, R., Hartl, F. U., and Flanagan, J. (1996) A zinc finger-like domain of the molecular chaperone DnaJ is involved in binding to denatured protein substrates. *EMBO J.* **15**, 408-417

Takayama, S., Sato, T., Krajewski, S., Kochel, K., Irie, S., Millan, J. A., and Reed, J. C. (1995) Cloning and functional analysis of BAG-1: a novel Bcl-2-binding protein with anti-cell death activity. *Cell* **80**, 279-284

Terry, C. J., Damas, A. M., Oliveira, P., Saraiva, M. J., Alves, I. L., Costa, P. P., Matias, P. M., Sakaki, Y., and Blake, C. C. (1993) Structure of Met30 variant of transthyretin and its amyloidogenic implications. *EMBO J.* **12**, 735-741

Teter, S. A., Houry, W. A., Ang, D., Tradler, T., Rockabrand, D., Fischer, G., Blum, P., Georgopoulos, C., and Hartl, F. U. (1999) Polypeptide flux through bacterial Hsp70: DnaK cooperates with trigger factor in chaperoning nascent chains. *Cell* **97**, 755-65

Thomas, J. G., and Baneyx, F. (2000) ClpB and HtpG facilitate *de novo* protein folding in stressed *Escherichia coli* cells. *Mol. Microbiol.* **36**, 1360-1370

Thompson, J. D., Higgins, D. G., and Gibson, T. J. (1994) CLUSTAL W: improving the sensitivity of progressive multiple sequence alignment through sequence weighting, positions-specific gap penalties and weight matrix choice. *Nuc. Acid Res.* **22**, 4673-4680

Tzamarias, D., and Struhl, K. (1995) Distinct TPR motifs of Cyc8 are involved in recruiting the Cyc8-Tup1 corepressor complex to differentially regulated promoters. *Genes Dev.* **9**, 821-831

Thomas, P. J., Qu, B-H., and Pederson, P. L. (1995) Defective protein folding as a basis of human disease. *Trends Biochem, Sci.* **20**, 456-459

Uparanukraw, P., Toyoshima, T., Aikawa, M., and Kumar, N. (1993) Molecular cloning and localization of an abundant novel protein of *Plasmodium berghei*. *Mol. Biochem. Parasitol.* **59**, 223-234

van der Spuy, J., Kana, B. D., Dirr, H. W., and Blatch, G. L. (2000) Heat shock cognate protein 70 chaperone-binding site in the co-chaperone murine stress-inducible protein 1 maps to within three consecutive tetratricopeptide repeat motifs. *Biochem. J.* **345**, 1-7

van der Spuy, J., Cheetam, M. E., Dirr, H. W., and Blatch, G. L. (2001) The cochaperone murine stress-inducible protein 1: overexpression, purification, and characterization. *Protein Expr. Purif.* **21**, 462-469

Vector NTI Advance, the newest version of Vector NTI Suite 8 software packages developed by InforMax, Inc. Bethesda, Maryland.

Vriend, G. (1990) WHAT IF, A molecular modeling and drug design program. *J. Mol. Graph.* **8**, 52-56

Walsh, D. M., Klyubin, I., Fadeeva, J. V., Cullen, W. K., Anwyl, R., Wolfe, M. S., Rowan, M. J., and Selkoe, D. J. (2002) Naturally secreted oligomers of amyloid β protein potently inhibit hippocampal long-term potentiation *in vivo*. *Nature* **416**, 535-539

Ward, B. K., Allan, R. K., Mok, D., Temple, S.E., Taylor, P., Dornan, J., Mark, P. J., Shaw, D. J., Kumar, P., Walkinshaw, M. D., and Ratajczak, T. (2002) A structure-based mutational analysis of cyclophilin 40 identifies key residues in the core tetratricopeptide repeat domain that mediate binding to Hsp90. *J. Biol. Chem.* **277**, 40799-40809

Wang, H., and Stillman, D. J. (1993) Transcriptional repression in *Saccharomyces cerevisiae* by a SIN3LexA fusion protein. *Mol. Cell Biol.* **13**, 1805-1814

Wang, T. F., Chang, J., and Wang, C. (1993) Identification of the peptide-binding domain of Hsc70. *J. Biol. Chem.* **268**, 26049-26051

Waterston, R. (1998) Genome sequence of the nematode *C. elegans*: a platform for investigating biology. The *C. elegans* Sequencing Consortium. *Science* **282**, 2012-2018

Wetzel, R. (1996) For protein misassembly, it's the "I" decade. *Cell* **86**, 699-702

Whitesell, L., Mimnaugh. E. G., De Costa, B., Myers, C. E., and Neckers, L. M. (1994) Inhibition of heat shock protein HSP90-pp60$^{v\text{-}src}$ heteroprotein complex formation by benzoquinone ansamycins: Essential role for stress proteins in oncogenic transformation. *Proc. Natl. Acad. Sci.* **91**, 8324-8328

Wishart, D. S., Fortin, S., Woloschuk, D. R., Wong, W., Rosborough, T. A., van Domselaar, G., Schaeffer, J., and Szafron, D. (1997) A platform-independent graphical user interface for SEQSEE and XALIGN. *CABIOS.* **13**, 561-562

Wood, V., Gwilliam, R., Rajandream, M. A., *et al.*, (2002) The genome sequence of *Schizosaccharomyces pombe*. *Nature* **415**, 871-880

Yonehara, M., Minami, Y., Kawata, Y., Nagai, J., and Yahara, I. (1996) Heat-induced chaperone activity of HSP90. *J. Biol. Chem.* **271**, 2641-5

Young, J. C., Schneider, C., and Hartl, F. U. (1997) *In vitro* evidence that hsp90 contains two independent chaperone sites. *FEBS Lett.* **418**: 139-143

Young, J. C., Obermann, W. M., and Hartl, F. U. (1998) Specific binding of tetratricopeptide repeat proteins to the C-terminal 12-kDa domain of hsp90. *J. Biol. Chem.* **273**, 18007-10

Young, J. C., and Hartl, F. U. (2000) Polypeptide release by Hsp90 involves ATP hydrolysis and is enhanced by the co-chaperone p23. *EMBO J.* **19**, 5930-5940

Young, J. C., Moarefi, I., and Hartl, F. U. (2001) Hsp90: a specialized but essential protein-folding tool. *J. Cell Biol.* **154**, 267-273

Zanata, S. M., Lopes, M. H., Mercadante, A. F., Hajj, G. N. M., Chiarini, L. B., Nomizo, R., Freitas, A. R. O., Cabral, A. L. B., Lee, K. S., Juliano, M. A., de Oliveira, E., Jachieri, S. G., Burlingame, A., Huang, L., Linden, R., Brentani, R. R., and Martins, V. R. (2002) Stress-inducible protein 1 is a cell surface ligand for cellular prion that triggers neuroprotection. *EMBO J.* **21**, 3307-3316

Zhu, X., Zhao, X., Burkholder, W. F., Gragerov, A., Ogata, C. M., Gottesman, M. E., and Hendrickson, W. A. (1996) Structural analysis of substrate binding by the molecular chaperone DnaK. *Science* **272**, 1606-1614

Zimmermann, S. B., and Minton, A. P (1993) Macromolecular crowding: biochemical, biophysical, and physiological consequences. *Annu. Rev. Biophys. Biomol. Struct.* **22**, 27-65.

Zimmermann, S. B., and Trach, S. O (1991) Estimation of macromolecule concentrations and excluded volume effects for the cytoplasm of *Escherichia coli J. Mol. Biol.* **222**, 599-620

Zoghbi, H., and Botas, J. (2002) Mouse and fly models of neurodegeneration. *Trends Genet.* **18**, 463-471

Appendix A

General Experimental Procedures

A.1 Preparation of competent bacterial cells

Escherichia coli (*E. coli*)(XLI Blue) cells carefully picked from a fresh Luria Broth (LB) agar plate containing 100 μg/ml ampicillin, were grown overnight in LB broth containing 100 μg/ml ampicillin with shaking at 37^0C. The culture was diluted 1:200 into 50 ml LB broth containing 100 μg/ml ampicillin and grown with shaking at 37^0C to early log phase; about 3 hours (absorbance = 0.3 - 0.6). The cells were collected by centrifugation at 5,000 x g for 5 minutes at 4^0C. In all further steps, the cells were kept on ice. The cells were resuspended in 50 ml (1 x culture volume) of ice-cold 0.1 M $MgCl_2$ and left on ice for 2 minutes. The cells were pelleted as before and gently resuspended in 25 ml (1/2 x culture volume) of ice-cold 0.1 M $CaCl_2$ and allowed to stand on ice for 2-3 hours. Finally, the cells were collected as before, resuspended in 5 ml (1/10 x culture volume) of ice-cold 0.1 M $CaCl_2$ and immediately stored in 30 % glycerol (ratio 1:1) at -70^0C in suitable aliquots.

A.2 Transformation of competent bacterial cells

Transformation was done using *E. coli* (XLI Blue) bacterial cells. Competent bacterial cells were prepared as described in section A.1. Epicurean *E. coli* (XLI Blue) super-competent cells were purchased from Stratagene. Frozen competent or super-competent bacterial cells were thawed on ice and aliquoted into prechilled 1.5-ml Falcon tubes. To each 100 μl aliquot of competent cells (or 50 μl of super-competent cells) was added 2 μl of 1:10 dilution of β-mercaptoethanol, the mixture was swirled gently and incubated for 10 minutes with gentle swirling every two minutes. To each transformation reaction was added 100 ng of DNA (or 1 to 5 μl of whole plasmid amplification products) and the reaction mixture swirled gently. 0.1 ng of pUC18 was used as control plasmid to calculate competence and transformation efficiency. All tubes were allowed to stand on ice for 30 minutes. The cells were heat-shocked at 42^0C for 2 minutes (for competent cells) or 45 seconds (for super-competent cells).

The tubes were immediately transferred onto ice and allowed to stand for another 2 minutes (cold shock). Pre-warmed LB broth was then added to the 1 ml mark and the reaction incubated for 30 - 60 minutes at 37^0C to allow for the expression of the ampicillin resistance gene. Afterwards, the cells were collected by centrifugation at 12,000 x g for 1 minute in a microcentrifuge; 900 µl of the supernatant was carefully removed, and the cells resuspended in the remaining 100 µl. The transformed cells were then plated out onto LB-ampicillin agar plates and incubated at 37^0C for > 16 hours.

A.3 Calculation of Transformation Efficiency (TE)

N = number of colony forming units (cfu) per 100 µl of transformation reaction

10 x N cfu per 1000 µl (1 ml) of transformation reaction

10 x N cfu per 100 ng of DNA

10 x 10 x N per 1000 ng (1 µg) of DNA

With the super-competent cells, transformation with pUC18 control plasmid yielded >250 colonies giving a transformation efficiency $>10^8$ cfu/µg DNA.

A.4 Small-scale preparation of plasmid DNA

A.4.1 Conventional miniprepping by alkaline lysis

E. coli (XLI Blue) cells transformed with the plasmid of interest were carefully picked from a single colony on a fresh LB-ampicillin agar plate and grown overnight in 4 ml of LB-ampicillin broth at 37^0C with shaking. I ml of the overnight culture was put into a 1.5-ml Falcon tube and centrifuged at 12,000 x g for 1 minute in a microcentrifuge. The cell pellets were resuspended in 100 µl of solution I (Resuspension buffer: 50 mM glucose, 25 mM Tris-HCl, 10 mM EDTA, pH 8.0) and incubated at room temperature for 5 minutes. Into the mixture was added 200 µl of solution II (Lysis buffer: 0.2 M NaOH, 1 % SDS) and allowed to stand for 2 minutes on ice. 150 µl of solution III (Neutralisation buffer: 3 M potassium acetate, pH 5.0) was added and the mixture was further incubated on ice for 5 minutes. After incubation, the mixture was centrifuged for 10 minutes at 12,000 x g at room temperature. The supernatant was carefully collected into a new 1.5-ml tube and the DNA was precipitated by adding 1 volume of isopropanol, incubating at room temperature for 2 minutes and centrifuging at 12,000 x g for 20 minutes at 4^0C. The

pellet was washed by gentle inversion in 200 µl of room temperature 70 % ethanol and centrifuging as above for 1 minute. The DNA was allowed to dry slightly before resuspending in appropriate volume of Tris-EDTA (TE buffer; 10 mM Tris-HCl, 1 mM EDTA, pH 8.0). To further remove contaminating salts, after isopropanol precipitation, the DNA pellet was resuspended in 400 µl of TE buffer and one tenth volume of 3 M sodium acetate solution (pH 5.2) and precipitated with 2 volumes of ice-cold absolute ethanol at -20^{0}C for 30 minutes. The DNA precipitant was then collected by centrifugation at 12,000 x g for 20 minutes before washing with 70 % ethanol. The plasmid DNA was stored at -20^{0}C. Alternatively, extra-pure plasmid DNA was isolated using the High Pure Plasmid Isolation Kit for mini preparations (Roche Diagnostics, Hilden, Germany) or the QIAprep Spin Miniprep kit, (QIAGEN Hilden, Germany). Manufacturers protocols were followed.

A.5 Large-Scale preparation of plasmid DNA

Extra-pure plasmid DNA was isolated in large scale using the QIAGEN Plasmid Maxi Kit (QIAGEN, Hilden, Germany), according to manufacturer's protocols.

A.6 Determination of DNA purity and concentration

DNA absorbance spectrum was scanned between 220 and 300 nm and the purity calculated according to the formula:

$$\frac{\text{Absorbance at 260 nm}}{\text{Absorbance at 280 nm}}$$

A value ≥2 was taken as indication of 100 % DNA purity.

Plasmid DNA concentration was calculated as follows:

1.0 Absorbance unit of double stranded DNA at 260 nm = 50 µg/ml

Therefore DNA concentration (µg/ml) = Absorbance unit at 260 nm x 50 µg/ml x dilution factor

A.7 Restriction endonuclease digestion of double-stranded DNA

For each single and double digestion, the following protocol was used:

Reagents	Volume (µl)
Sterile de-ionised H_2O	16
10 x Restriction buffer	02
ds DNA (100 – 500 ng)	02

Adding 2 units of restriction endonuclease started the reaction. The mixture was incubated for at least 2 hours at the recommended temperature for the enzyme and the reaction stopped by the addition of 4 µl of 6 x DNA gel loading buffer (0.25 % bromophenol blue and 30 % glycerol). For double digestion, restriction endonuclease enzyme that required low ionic strength buffer or low temperature was first used to digest the DNA before adding high ionic strength buffer or incubating at higher temperature. For bulk digestion, 2 µg of DNA and 20 - 40 units of enzyme were used. Lambda DNA molecular weight marker was prepared by digesting Lambda DNA with *Pst* I as follows:

Reagents	Volume (µl)
Sterile de-ionised H_2O	160
10 x Restriction buffer	20
Lambda DNA (10 ug)	20

Adding 20 - 40 units of Pst I initiated reaction. The reaction was allowed to occur overnight to ensure that the DNA was properly cut, and stopped by adding 40 µl of 6 x DNA gel loading buffer. The digestion products were analysed on a 1 % agarose gel.

A.8 Agarose gel electrophoresis

For a 1 % gel, 1 g agarose was suspended in Tris-Borate-EDTA (TBE; 0.045 M Tris-base, 0.045 M Borate, 0.001 M EDTA, pH 8.3) buffer to a total volume of 100 ml. The agarose was melted in a microwave oven for 30 to 60 seconds and allowed to cool down to about 55^0C. 5 µl of 10 mg/ml ethidium bromide was added to give a final concentration of 0.5 µg/ml before the agarose was poured into the gel casting

platform. A comb was inserted at one end of the gel platform. After hardening, the comb was carefully removed to avoid tearing of the sample wells. The gel casting platform was lowered into an electrophoretic tank and TBE added to a depth of about 3 mm above the gel. All air bubbles trapped in the wells were carefully removed before loading the DNA samples with a pipetteman. The leads were set such that the DNA would move towards the anode. A voltage of 100 V was applied and the samples were allowed to run to 75 % of the length of the gel. The DNA was visualised and photographed by placing on an ultraviolet (UV) light source.

A.9 Oligonucleotide-directed mutagenesis

Oligonucleotide-directed mutagenesis was done by non-PCR based double-stranded whole plasmid linear amplification using complementary mutagenic oligonucleotide primers. The QuikChange site-directed mutagenesis kit (Stratagene, La Jolla, USA) was used. The following reagents were put into thin-walled 0.2-ml PCR tubes.

Control Reaction

Reagent	**Volume (µl)**
Sterile de-ionised H_2O	38.5
10 x Reaction buffer	5
dNTPs mix (10 mM each)	1
Primer #1 (100 ng/µl)	1.25
Primer #2 (100 ng/µl)	1.25
pWhiteScript plasmid DNA (5 ng/µl)	2
PfuTurbo DNA polymerase (2.5 U/µl)	1
Total volume	50

Test Reaction

Reagent	**Volume (µl)**
Sterile de-ionised H_2O	32
10 x Reaction buffer	5
dNTPs mix (10 mM each)	1
Forward primer (250 ng/µl)	5
Reverse primer (250 ng/µl)	5

Template DNA (100 ng/µl)	2
PfuTurbo DNA polymerase (2.5 U/µl)	1
Total volume	50

The reaction was not overlaid with mineral oil since the temperature cycler block was sealed. The reactions were cycled using the cycling parameters outlined in Table A.1 below.

Table A.1: Cycling parameters for the QuikChange site-directed mutagenesis protocol

Segment	No of Cycles	Temperature	Time
1	1	95^0C	30 seconds
2	18	95^0C	30 seconds
		52^0C	1 minute
		68^0C	2 minutes/kilobase of plasmid length
3	1	78^0C	1 minute/kilobase of plasmid length

After cycling, the reaction was removed and allowed to cool down to 4^0C. To digest the contaminating parental plasmid DNA, 1 µl of *Dpn* I (10 units) was added, after which the mixture was incubated at 37^0C for 1 to 2 hours. The final products were analysed on a 1 % agarose gel using 15 µl of mutagenesis products and 5 µl of 6 x DNA gel loading buffer.

A.10 Polymerase chain reaction (PCR)

Polymerase chain reaction was done using the Expand High Fidelity PCR System (Roche Diagnostics, Hilden, Germany). A 50-µl reaction volume was set up as shown in the protocol below.

Reagents	**Volume (µl)**
Master Mix 1	
Sterile de-ionised H_2O	21
dNTPs mix (10 mM each)	1
Forward primer (300 nM)	1
Reverse primer (300 nM)	1

Template DNA (500 ng)	1
Master Mix 2	
Sterile de-ionised H_2O	19
10 x Reaction buffer containing 15 mM $MgCl_2$	5
Expand High Fidelity Enzyme mix	1
Total volume	50

DNA amplification was done using the cycling parameters in Table A.2.

Table A.2: Cycling parameters for Polymerase Chain Reaction

Segment	No of Cycles	Temperature	Time
1	1	94^0C	2 minutes
2	25	94^0C	0.5 minute
		55^0C	1 minute
		72^0C	2 minutes/kilobase of plasmid length
		72^0C	10 minutes

The PCR products were analysed on a 1 % agarose gel using 5 µl of mutagenesis products and 1 µl of 6 x DNA gel loading buffer.

A.11 DNA ligation

Ligation reaction was set up as follows:

Reagents	**Volume (µl)**
Sterile de-ionised H_2O	X
10 x Ligase buffer	1
Vector DNA (100 ng/µl)	1
Insert DNA	X
T4 DNA Ligase (1 Weiss Unit/µl)	1
Total volume	10

The amount of insert used was calculated based on a molar ratio of 3:1 (insert : vector) using the formula below.

$$\frac{\text{ng of vector x kilobase size of insert}}{\text{kilobase size of vector}} \times \frac{3}{1}$$

The reaction was incubated either at room temperature for 3-5 hours or at 4^0C overnight. After ligation, 1 µl of the reaction mixture was used to transform *E. coli* (XL1 Blue) as described in section A.2.

A.12 Automated DNA sequencing

DNA sequencing was done using the ABI 3100 Genetic Analyser, which is based on capillary electrophoresis. Extra-pure DNA samples were obtained using the QIAprep Spin Miniprep kit. The DNA was resuspended in sterilised ultra-pure water to reduce salt contamination that might interfere with sequencing. Reactions for thermocycling were prepared by mixing 200 – 500 ng of double stranded plasmid DNA, 3.2 pmol primer and the volume made up to 12 µl with sterile de-ionised water. To the mixture was added 8 µl of BigDye V3.0 terminator Cycle Sequencing System (*PE* Biosystems, Foster City, U.S.A) before amplification was carried out using the parameters below.

1. Rapid thermal ramp to 96^0C
2. 96^0C for 10 seconds
3. Rapid thermal ramp to 50^0C
4. 50^0C for 5 seconds
5. Rapid thermal ramp to 60^0C
6. 60^0C for 4 minutes
7. Rapid thermal ramp to 4^0C and hold until ready to clean.

To clean up the DNA after cycling, DNA Clean and Concentrator-5 columns (Zymo Research, California, U.S.A) was used, following manufacturer's instructions. The samples were dried either in an incubator or in a vacuum drier before sequencing.

A.13 Determination of solubility of target recombinant protein(s)

Generally, before large-scale production of recombinant proteins, the solubilities of the proteins were determined in a small-scale culture. A 10 ml LB-ampicillin culture of freshly picked colony of *E. coli* XLI Blue cells carrying pGEX3X derived plasmid construct encoding the protein of interest was grown overnight at 37^0C with vigorous shaking. The culture was used to inoculate (1:10 dilution) a 50 ml fresh LB-ampicillin medium, and the culture was allowed to grow for 2 – 3 hours until the cells reached

the log phase (OD_{600} = 0.5 - 0.7). A 1 ml sample of the culture was aliquoted before inducing with isopropyl-1-thio-β-D-galactopyranoside (IPTG) and served as uninduced sample. The culture was grown for another 4 hours before a second 1 ml sample was taken which served as induced sample. Each 1 ml sample taken was centrifuged, and the cell pellets resuspended in 50 µl of phosphate-buffered saline (PBS; 137 mM NaCl; 2.7 mM KCl; 10 mM Na_2HPO_4; and 2 mM KH_2PO_4; pH 7.4) and 50 µl of SDS-PAGE sample buffer (100 mM Tris, pH 6.8; 5 % β-mercaptoethanol; 4 % SDS; 0.2 % Bromophenol blue; and 20 % glycerol). The remaining cells were harvested by centrifugation at 5000 x g for 5 minutes and resuspended in 5 ml ice-cold PBS. The cells were lysed by sonication using 3 x 30 seconds bursts with 30 seconds pause at 200-300 W, on ice. The lysate was centrifuged at 12,000 x g for 20 - 30 minutes at 4^0C. The supernatant was carefully decanted and served as crude extract A containing the soluble proteins. The pellets were resuspended in 5 ml PBS and regarded as crude extract B containing the insoluble proteins and cell debris. To 50 µl each of crude extracts A and B was added 50 µl of SDS sample buffer. All the samples were heated at 95^0C for 3 - 5 minutes before resolving on SDS-PAGE gel.

A.14 Large-scale heterologous production and purification of recombinant GST fusion mSTI1 proteins

A 200 ml LB-ampicillin culture of freshly picked colony of *E. coli* XLI Blue cells carrying pGEX3X derived plasmid constructs was grown overnight at 37^0C with vigorous shaking. The culture was used to inoculate (1:10 dilution) a 1 L fresh LB-ampicillin medium, and the culture was allowed to grow for 2 – 3 hours until the cells reached the log phase (OD_{600} = 0.5 - 0.7). Over-production of recombinant GST fusion proteins was induced for 5 - 6 hours at 37^0C with 1 mM IPTG. The cells were harvested 5000 x g for 5 minutes and lysed by mild sonication in one-hundredth-culture volume of ice-cold PBS containing phenylmethylsulphonyl fluoride (PMSF; 1 mM final concentration). The sonicate was incubated, with gentle agitation, for 30 - 60 minutes at room temperature after the addition of Triton X-100 to 1 % final concentration. The extracts were clarified by centrifugation at 12,000 x g for 20 - 30 minutes at 4^0C.

The overexpressed GST-mSTI1 proteins were purified using S-hexyl glutathione agarose affinity chromatography. Aliquots of clarified extracts were added to 50 % (w/v) slurry of glutathione agarose beads (2 ml bed volume per 100 ml of extract) previously equilibrated with PBS. Binding was allowed to occur for 1 h at 4^0C with gentle rocking. Afterwards, the beads were washed extensively with ice-cold PBS by centrifugation at 500 x g for 5 minutes at 4^0C. To the sedimented matrix was added glutathione elution buffer (10 mM reduced glutathione in 50 mM Tris-HCl, pH 8.0; 50 µl per 100 µl glutathione agarose used). The matrix was resuspended gently in the elution buffer and incubated for 10 minutes at room temperature to elute the bound proteins. Eluted proteins were resolved by electrophoresis on a 12 % sodium dodecyl sulphate (SDS) polyacrylamide gel.

A.15 Large-scale heterologous production and purification of recombinant $(His)_6$-tagged mSTI1 proteins

Heterologous production of $(His)_6$-tagged mSTI1 proteins in exponentially growing *E. coli* cells was induced by 1 mM IPTG. The *E. coli* cells were treated and lysed as described in section A.14 above. The clarified lysate was loaded onto a nickel-chelating sepharose resin column. Washing of the column was done using a buffer containing 50 mM Na_2HPO_4, pH 7.5, 20 mM imidazole, and 1 mM PMSF. The protein was eluted with a linear gradient of 20 - 300 mM imidazole. The imidazole ligand was removed from the protein by gel filtration in a Sephadex G-25 column. Buffer exchange was achieved by loading the purified protein onto a hydroxyapatite column previously equilibrated with 20 mM K_2HPO_4, pH 7.5 and eluting with a linear gradient of 20 - 300 mM K_2HPO_4. The homogeneity of the protein was assessed by SDS-PAGE and SEC-HPLC using a LKB model 2150.

A.16 Culture and lysis of NIH3T3 mouse fibroblast cells

NIH3T3 mouse fibroblast cells (Highveld Biological, Lyndhurst, South Africa) were cultured in complete DMEM (Dulbecco's modified Eagle's medium supplemented with 10 % foetal calf serum and 1 % penicillin (100 U/ml)/streptomycin (100 µg/ml) solution), at 37^0C and 5 % CO_2 in humidified incubator until they reached 80 - 100 % confluency. The cells were harvested by trypsinization followed by three washes with room temperature PBS. The harvested cells were resuspended in appropriate volume

of lysis buffer (50 mM Tris-HCl; 150 mM NaCl; 0.02 % sodium azide; 100 μg/ml PMSF; 1 μg/ml Aprotinin; and 1 % Triton X-100) and incubated at 4^0C for 10 minutes to allow lysis to occur. The lysate was centrifuged at 12,000 x g for 30 minutes at 4^0C, and the supernatant used immediately.

A.17 Transfection of NIH3T3 mouse fibroblast cells

Prior to transfection, exponentially growing NIH3T3 mouse fibroblasts were harvested by trypsinization and re-plated in 60-mm tissue culture dishes in complete DMEM. The cultures were incubated for 24 hours to a confluency of 40 – 60 %, at 37^0C and 5 % CO_2 in a humidified incubator. The medium was changed 1 hour before transfection. Calcium phosphate-mediated transfection of the cells was done using the CellPhect Transfection kit (Amersham Biosciences, Buckinghamshire, England). Approximately 3 μg of DNA was dissolved in 120 μl of sterile de-ionised water before mixing with 120 μl of Buffer A. The mixture was vortexed briefly and incubated for 10 minutes at room temperature. To the mixture was added 240 μl of Buffer B, followed by vortexing for several seconds and incubation for 15 at room temperature, to allow precipitates to form. The calcium phosphate-DNA precipitate was added to the cell culture and mixed properly with the medium. Incubation was continued for another 12 hours to allow the cell to take up the precipitate. The cells were washed twice with ordinary DMEM to remove any remaining precipitate after which 1.5 ml of 15 % (v/v) glycerol in 1 x HEPES-buffered saline (140 mM NaCl; 1.5 mM $Na_2HPO_4{\cdot}2H_20$; and 50 mM HEPES) was added and followed by another incubation for 3 minutes at room temperature. The cells were rinsed with ordinary DMEM; 3 ml of complete DMEM was added and incubation was continued for 48 - 72 hours before harvesting.

A.18 Glutathione affinity pull down assays

In separate 1 ml reactions, GST-mSTI1 fusion proteins were added to 100 μl of 50 % slurry of glutathione agarose beads to a final concentration of 0.3 μM. Binding was allowed to occur for 1 h at 4^0C after which unbound fusion protein was removed by washing three times in ice-cold PBS. Hsc70 binding assays were conducted by incubating the coupled agarose beads with 250 μg of crude extracts of NIH3T3 mouse fibroblast cells (see section A.16) and making up to 1 ml with ice-cold PBS. In Hsp90

binding assays, purified rat or chicken Hsp90 (kind gifts from Dr Csaba Soti and Dr David Smith respectively) rather than extract proteins was added to a final concentration of 0.025 μM. After incubation for 2 hours at 4^0C, the beads were collected and washed extensively in ice-cold PBS to remove non-specifically bound extract proteins. The bound proteins were solubilised in 50 μl of SDS sample buffer and 30 μl was analysed on a 0.1 % SDS- 12 % PAGE (see section A.19). After transferring onto nitrocellulose membrane (see section A.20), co-precipitation of Hsc70 or Hsp90 with the GST-mSTI1 fusion proteins was revealed by immunodetection and chemiluminescent autoradiography (see section A.21) using the mouse monoclonal primary antibodies H5147 and H9010 specific for Hsc70 and Hsp90, respectively.

A.19 Sodium dodecyl sulphate polyacrylamide gel electrophoresis (SDS-PAGE)

Proteins were resolved on a 0.1 % SDS- 10 or 12 % PAGE gel in a discontinuous buffer, according to Laemmli (1970) using a Bio-Rad Mini-Protean 3 electrophoresis system (Bio-Rad Laboratories, Hercules, U.S.A). The resolving and stacking gels were prepared as shown in Table A.3. The gels were allowed to stand for about 30 minutes for polymerisation to occur after which they were clamped in a frame and transferred into a buffer tank. Previously, protein samples were mixed with 2 x SDS-PAGE sample buffer in 1:1 ratio and boiled for 3 - 5 minutes at 95^0C. 25 μl of the denatured protein samples were carefully loaded into the wells. The Bio-Rad premixed wide-range protein molecular weight marker was loaded as standards. Electrophoresis was carried out in 1 x Tris-glycine electrophoresis buffer (25 mM Tris, pH 8.3; 250 mM glycine; and 0.1 % (w/v) SDS) at 150 volts for 1 hour. The resolved proteins were visualized by staining the gel with Coomassie Brilliant Blue solution (0.25 % Coomassie Brilliant Blue (R250); 50 % methanol; 7.5 % acetic acid) for 2 - 3 hours, and destaining in a solution containing 20 % methanol and 7.5 % acetic acid.

Table A.3: Solutions for preparing stacking and resolving gels for Tris-glycine SDS-PAGE

Reagents (ml)	5 % Stacking gel	10 % Resolving gel	12 % Resolving gel
Distilled H_2O	4.1	5.9	4.9
30 % Acrylamide mix	1.0	5.0	6.0
1.5 M Tris (pH 8.8)	-	3.8	3.8
1.0 M Tris (pH 6.8)	0.75	-	-
10 % SDS	0.06	0.15	0.15
10 % Ammonium persulphate	0.06	0.15	0.15
TEMED	0.006	0.006	0.006
Total volume	6 ml	15 ml	15 ml

A.20 Western blotting analysis of proteins

Western transfer of proteins was done using the Bio-Rad Mini Trans-Blot Cell (Bio-Rad Laboratories, Hercules, U.S.A). After electrophoresis, the SDS-PAGE gel was removed from the glass plates and the stacker was cut off. The gel, together with 2 pieces of 3 mm Whatman filter papers, 2 Scotchbrite fibre pads and nitrocellulose paper (Hybond-C extra, ECL; Amersham, Buckinghamshire, England) were pre-equilibrated in the transfer buffer (25 mM Tris; 192 mM glycine; and 20 % methanol) for 30 minutes. The gel was aligned on the filter paper placed on a Scotchbrite pad, and air bubbles were expelled. Next, the nitrocellulose was carefully aligned on the gel, followed by the other filter paper. The other Scotchbrite pad was laid on the filter paper to complete the sandwich. The sandwich was inserted into clamps with the nitrocellulose facing the clear panel (anode) and the gel facing the black panel (cathode). Transfer was allowed to occur for 1 hour at 100 volts while using a magnetic stirrer to stir the buffer continuously. Cooling was achieved by inserting a heat trap into the buffer. To visualise the proteins, the membrane was stained with Ponceau S stain (0.5 % Ponceau S; and 1 % glacial acetic acid) for 3 - 5 minutes, and destained by washing with distilled water.

A.21 Chemiluminescence-based immunodetection of proteins

The BM chemiluminescence Western blotting kit (mouse/rabbit) from Roche Diagnostics Hilden, Germany, was used to detect proteins with peroxidase (POD)-labelled secondary antibodies and the chemiluminescent substrate luminol on Western blots. Ponceau S-stained nitrocellulose membrane was washed with distilled water followed by ample washes in Tris-buffered saline (TBS) (50 mM Tris, pH 7.4; and 150 mM NaCl). The membrane was blocked with blocking solution (5 % non-fat milk in TBS) either for 1 hour with shaking or overnight with no shaking at 4^0C. Blocking was followed by incubation of membrane for 1 hour, in the primary antibody appropriately diluted in blocking solution. Next, the membrane was washed twice in TBS-Tween (TBST; 0.1 % Tween 20 in TBS) for 10 minutes each, and twice in blocking solution for 10 minutes each. The membrane was then incubated in secondary antibody (anti-mouse IgG-POD/anti-rabbit IgG-POD) diluted 1:6000 in blocking solution, for 30 - 60 minutes with rocking. Washing was done four times in large volumes of TBST 15 minutes each before chemiluminescent detection.

A.22 Spectroscopic measurements

Fluorescence emission spectra and other fluorescence measurements were made at 25^0C in 20 mM sodium phosphate, 1 mM EDTA, pH 7.5. The intrinsic fluorescence of the lone tryptophan (excitation at 295 nm) in mSTI1 was measured for 2 μM protein between 300 and 400 nm in a Perkin-Elmer fluorescence spectrophotometer (27). Circular dichroism measurements were made using 8 μM of each protein sample in a Jasco J-710 spetropolarimeter. Ellipticity values were collected (average of 10 runs) in both the near-UV (350-250 nm) and far-UV (250-200 nm) regions.

A.23 Binding studies using the Biacore Surface Plasmon Resonance Spectroscopy-based real time analysis

Biomolecular interactions in real time were monitored using the Biacore X apparatus machine (Biacore, Uppsala, Sweden). All experiments were performed at 25^0C in buffer A (PBS containing 0.005 % P20 surfactant (Biacore, Uppsala, Sweden). Monoclonal goat anti-GST antibody was covalently attached to carboxy-methlylated dextran on a research grade sensor chip CM5 via amine coupling according to manufacturer's protocol (Biacore, Uppsala, Sweden). As a reference, GST was bound

to the immobilised antibody on the chip by diluting 0.2 mg/ml recombinant GST, (Biacore, Uppsala, Sweden) in buffer A, and loading 5 - 10 µl of the solution into the first flow-cell at a flow-rate of 5 µl/min, to give approximately 700 response units (RU). GST-mSTI1 fusion protein was immobilised on the chip in the second flow-cell to give approximately the same number of response units as the recombinant GST. The chip was equilibrated with buffer A before injecting solutions containing increasing concentrations of purified Hsc70 or Hsp90 (analyte) over the bound proteins at a flow-rate of 10 µl/min. For competition experiments, a mixture of full-length Hsc70 and Hsp90 (8 µM and 5 µM respectively) was pre-incubated at 25^0C before passing it over the immobilised mSTI1 proteins. Washing of chip was programmed to occur two minutes after injection of analyte. Anti-GST sensor chip was regenerated by injecting 10 µl of Biacore regeneration buffer (10 mM glycine, pH 2.2) into both flow-cells at a flow-rate of 5 µl/min and washing with buffer A. Background binding to GST was subtracted from each signal to account for non-specific binding to GST. Data were analysed using the BIA evaluation software version 2.2.4 (Biacore, Uppsala, Sweden).

A.24 Dialysis of purified proteins

Purified proteins were dialysed to exchange the Tris-HCl buffer used to prepare glutathione elution buffer with PBS, before using them for SPR studies. Dialysis membrane was equilibrated two times in 10 ml of solution containing 5 mM EDTA and 0.1 M $NaHCO_3$ to inhibit protease activities. The equilibrated membranes were then washed two times in 10 ml each of ultra-pure water. After washing, 500 µl of purified protein was introduced into the membranes, and the membrane was clipped at both ends. The protein was thereafter dialysed against 500 ml of ice-cold PBS for two hours at 4^0C with gentle agitation. The PBS buffer was changed and the dialysis continued for another 3 hours. After dialysis, the protein mixture was centrifuged at 14,000 x g for 10 minutes to remove any precipitate.

Appendix B

Vector Plasmid Maps

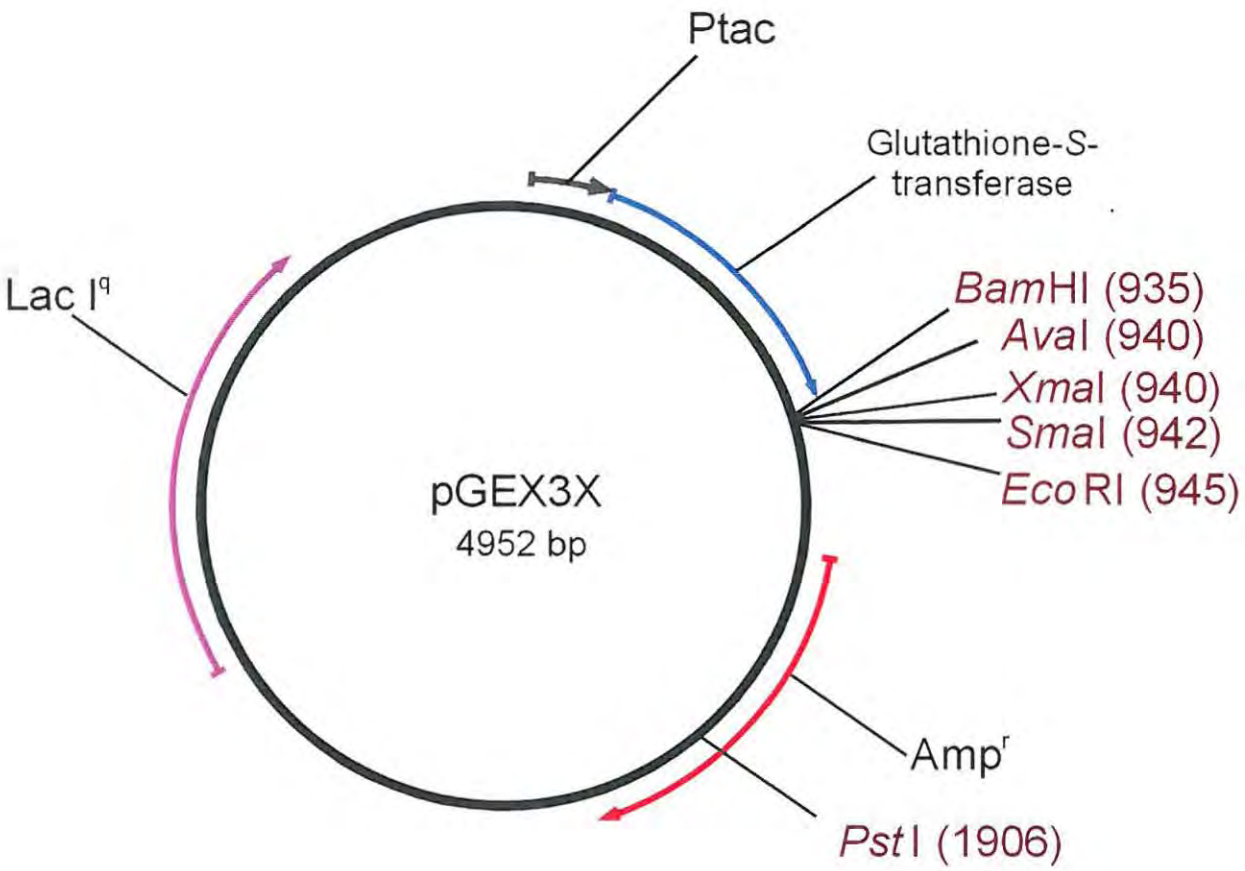

Figure B.1: Map of pGEX3X expression plasmid vector
The figure was drawn using Vector NTI Advance computer software.

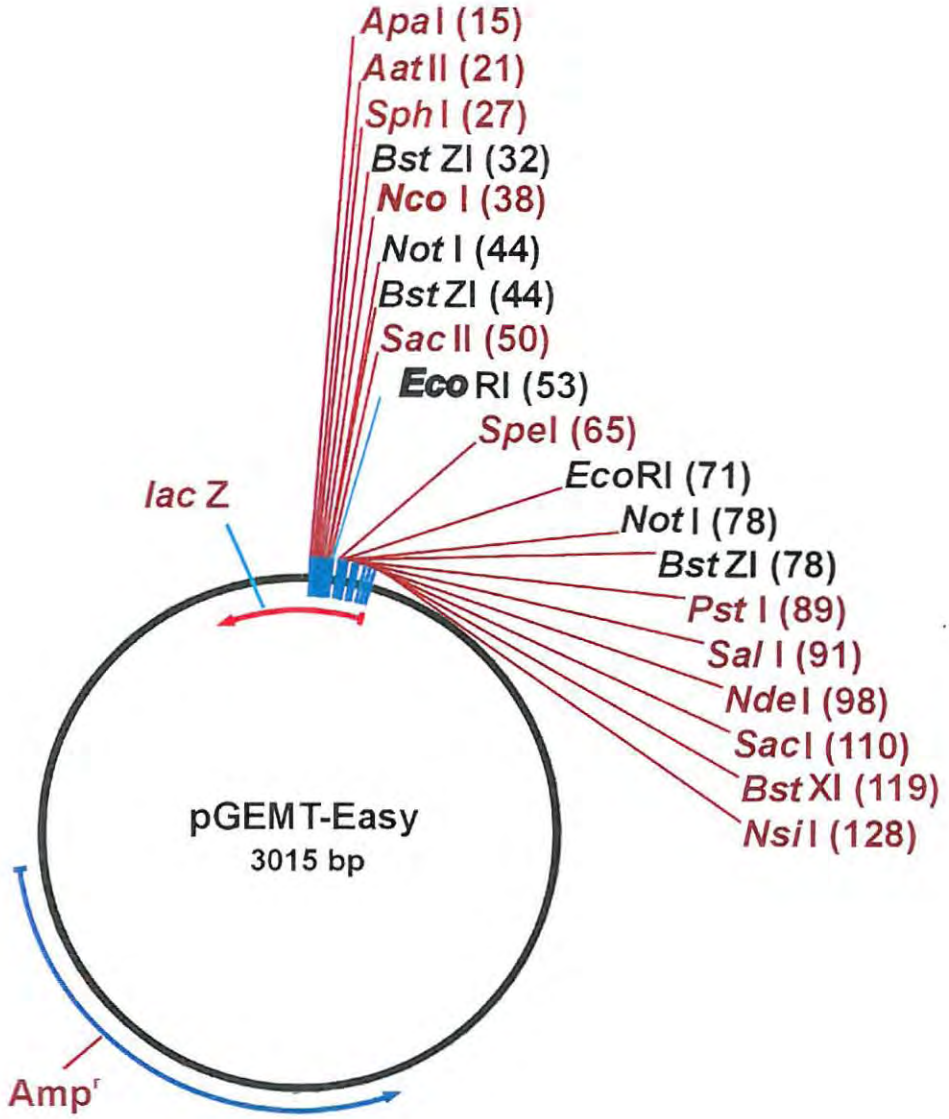

Figure B.2: Map of pGEMT-Easy cloning plasmid vector
The figure was drawn using Vector NTI Advance computer software.

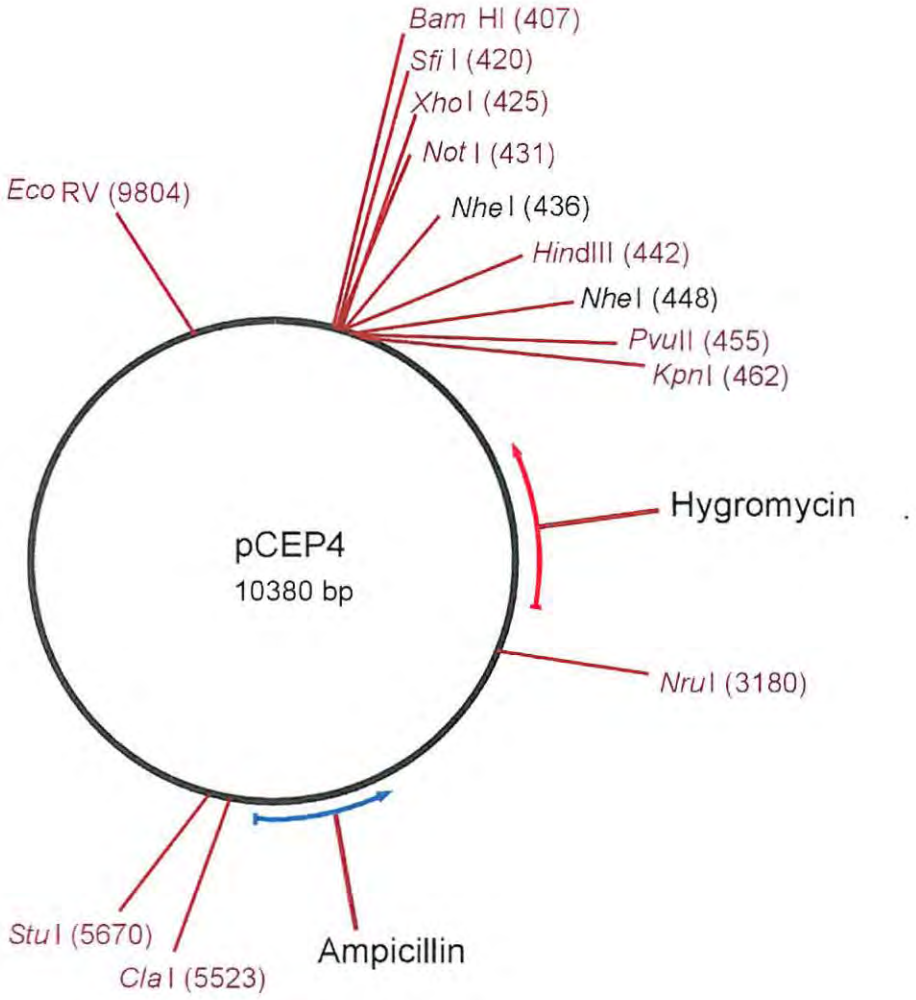

Figure B.3: Map of pCEP4 mammalian expression plasmid vector
The figure was drawn using Vector NTI Advance computer software.

Appendix C

Sequences of the Stress-inducible protein 1 homologues

>gi|5803181|ref|NP_006810.1| stress-induced-phosphoprotein 1 (Hsp70/Hsp90-organizing protein); transformation-sensitive, similar to *Saccharomyces cerevisiae* STI1 [*Homo sapiens*] Honore *et al.*, 1992

MEQVNELKEKGNKALSVGNIDDALQCYSEAIKLDPHNHVLYSNRSAAYAKKGDYQKAYEDGCKTVDLKPD
WGKGYSRKAAALEFLNRFEEAKRTYEEGLKHEANNPQLKEGLQNMEARLAERKFMNPFNMPNLYQKLESD
PRTRTLLSDPTYRELIEQLRNKPSDLGTKLQDPRIMTTLSVLLGVDLGSMDEEEEIATPPPPPPPKKETK
PEPMEEDLPENKKQALKEKELGNDAYKKKDFDTALKHYDKAKELDPTNMTYITNQAAVYFEKGDYNKCRE
LCEKAIEVGRENREDYRQIAKAYARIGNSYFKEEKYKDAIHFYNKSLAEHRTPDVLKKCQQAEKILKEQE
RLAYINPDLALEEKNKGNECFQKGDYPQAMKHYTEAIKRNPKDAKLYSNRAACYTKLLEFQLALKDCEEC
IQLEPTFIKGYTRKAAALEAMKDYTKAMDVYQKALDLDSSCKEAADGYQRCMMAQYNRHDSPEDVKRRAM
ADPEVQQIMSDPAMRLILEQMQKDPQALSEHLKNPVIAQKIQKLMDVGLIAIR

>gi|6324601|ref|NP_014670.1| Heat shock protein also induced by canavanine and entry into stationary phase; Sti1p [*Saccharomyces cerevisiae*] Goffeau *et al.*, 1996

MSLTADEYKQQGNAAFTAKDYDKAIELFTKAIEVSETPNHVLYSNRSACYTSLKKFSDALNDANECVKIN
PSWSKGYNRLGAAHLGLGDLDEAESNYKKALELDASNKAAKEGLDQVHRTQQARQAQPDLGLTQLFADPN
LIENLKKNPKTSEMMKDPQLVAKLIGYKQNPQAIGQDLFTDPRLMTIMATLMGVDLNMDDINQSNSMPKE
PETSKSTEQKKDAEPQSDSTTSKENSSKAPQKEESKESEPMEVDEDDSKIEADKEKAEGNKFYKARQFDE
AIEHYNKAWELHKDITYLNNRAAAEYEKGEYETAISTLNDAVEQGREMRADYKVISKSFARIGNAYHKLG
DLKKTIEYYQKSLTEHRTADILTKLRNAEKELKKAEAEAYVNPEKAEEARLEGKEYFTKSDWPNAVKAYT
EMIKRAPEDARGYSNRAAALAKLMSFPEAIADCNKAIEKDPNFVRAYIRKATAQIAVKEYASALETLDAA
RTKDAEVNNGSSAREIDQLYYKASQQRFQPGTSNETPEETYQRAMKDPEVAAIMQDPVMQSILQQAQQNP
AALQEHMKNPEVFKKIQTLIAAGIIRTGR

>gi|23491036|gb|EAA22670.1| stress-induced protein sti1-like protein [*Plasmodium yoelii yoelii*] Carlton *et al.*, 2002

MINKEEAQRLKELGNKCFQEGKFEDSVKYFSDAIKNDPSDHVLYSNLSGAYSSLGRFYEALESANKCINI
KNDWPKGYIRKACAEHGLRQLDNSEKTYLEGLKLDPNNKSLKDGLEKVRKDKEMENMEYINHINNIINND
AKLKSYKEENSNYPIELLNTIKAINANPMNIRFILSSCNPKISEGVEKFFGIKFNDEASYEAERERQRKK
EEEEKKEKERKMKEEEKKKNRTPEEILGEEHKLKGNDFYKQKKFEEALKEYDEAIKVNPNDIMYYYNKAA
VYLEMKSYEKCIETCIYAIENRYNFKAEFSQVAKVYNRLAIGYINIKNYDKAIEAYRKSLVEDNNRATRN
ALKELERKKEKEEREAYIDPVKAEEHKNKGNEFFKNNDFPNAKKEYDEAIRRNPNDAKLYSNRAAALTKL
IEYPSALEDVMKAIELDPKFVKAYSRKGNLHFFMKDYYKAIQAYNKGLELDPNNKECIEGYQRCVYKIDE
MSKSEKVDEEQIKKSMADPEIQQIISDPQFQIILQKINENPNSISEYIKDPKIFNGLQKLIAAGILTVR

>gi|548993|sp|P28591] Protease inhibitor precursor (SLPI) (Trypsin inhibitor STI1) (SILA-3) (*Streptomyces coelicolor*) Strickler *et al.*, 1992

MRNTARWAATLGLTATAVCGPLAGASLASPATAPASLYAPSALVLTVGHGESAATAAPLRAVTLTCAPTA
SGTHPAAAAACAELRAAHGDPSALAAEDSVMCTREYAPVVVTVDGVWQGRRLSYERTFANECVKNAGSAS
VFTF

>gi|22788769|ref|NP_690481.1| stress-induced protein STI1 [*Heliothis zea virus* 1] Cheng *et al.*, 2002

MASSASSHMSFNIIEYGTPQIKMDLPRLKNPRTSAENPYGTEPHKPFFDYQELMARKVAEVGVDTDVELA
DTDNTDIERQRNRAKRASLESDSDADSDYSGIKVDGEQLLRKAAKCVTEHNRKRGILDATDSESEAKRRR
QVDDEMENFKFLNEHVFNKLDNITKKAQAESSQEEPSVPVRRSRPQTPHHKRKPKVQSRRDDSQDASDED
DECNNRELSRNSFNRSVNSGRGSGGKGSRASEANSRSSSRVSSRASSRANSRSSSRASSRGGNRSDDEAE
EEDDEVNNEGNGENANTEVNANESNVDGSNVDGSNVNDVDYESNTIVENVGVEGDFNKENLAPSGKESNI
ETVALGSAKSNIDVYNFDEDDNASVKSGTSASQSRKSKTKSTIAVGKNLDDRLKSLQLNLELTDANKGNS
TKGGSLLNANGSAKNSVKNGSAKGGSVKGGSVNSKVNNSNSKSASKSKANNSSSEKTIKPKVAKPTPTPV
PTKTLASNSQSNNQTSNNQTSSQSNNQNSQSSQSNESTSNDSSSNNSSSNSQSTVVNVNAQSNDNTQSNN

NTQSNVQSNVQVNDQIDTQANDQINTQSNTQSNTQPNTQSSTAPTKRPTLINHANTKVSDRMHELKLKMN
PPRRTDEATILAIERAALTCKQCNKTYKTARNLSKHTCKPKKSAAPKRGKKRTSSESSACSEPENKSEAP
EKKRKLPSTPLGVPVPLTSNSADKQALYDEFKVVEPGFKHMHKLNAIDTHKHPIELHETYACKVSELAYA
QYHNETNCTAAEFKRETANVRQSLSKQIASIQNQLKDKSMDKELSGKLKLRIKFLRAYKQMKLAEYSYTC
PKLKMFSKKMERIFTGNRVDSKGSLPNKITNADVQNAISSIGKMQVDDGDLTCIARSLENYITLITLSVL
ATMVNKRSCRVTRANIASVLALQYAMNHDKESYPMPEHGTIKTPSDGKLNVIICRNVLDLNNITSVDQVM
DVLMDEFNGELKNLWVKFLFYFKPSSDYFKVIKEFYIKYIMASYMALCKMEEKRASGKPSNFRQCMAIVI
NNCTWFPFKDYANHTDVNLDRQADDLFEQCDVKRSTSSAGTKRKANRATKEVPSKRQRCDSSDNESVASR
SPSPVKSAPVQSSLANKAMANKVMASAPMASTPLANKPTTPAVTKPKRDDMIEGGYFPMSRVVKIRRLEQ
RRMEANAANRGNLNSNTNSNLNSNPNSNSNPTPTNNTDSNTNSAKSTNNTDTTNNTTNNTNPTNNANSTN
TTNPTNNNSSNPSNSAPKKRTSNGSRKSSASSKIDPSRIKSRELIENDDFSSDEN

>gi|22655105|gb|AAM98143.1| stress-induced protein sti1-like protein [*Arabidopsis thaliana*] Tripp *et al.*, 2002 Direct submission

MAEEAKSKGNAAFSSGDYATAITHFTEAINLSPTNHILYSNRSASYASLHRYEEALSDAKKTIELKPDWS
KGYSRLGAAFIGLSKFDEAVDSYKKGLEIDPSNEMLKSGLADASRSRVSSKSNPFVDAFQGKEMWEKLTA
DPGTRVYLEQDDFVKTMKEIQRNPNNLNLYMKDKRVMKALGVLLNVKFGGSSGEDTEMKEADERKEPEPE
MEPMELTEEERQKKERKEKALKEKGEGNVAYKKKDFGRAVEHYTKAMELDDEDISYLTNRAAVYLEMGKY
EECIEDCDKAVERGRELRSDFKMIARALTRKGSALVKMARCSKDFEPAIETFQKALTEHRNPDTLKKLND
AEKVKKELEQQEYFDPTIAEEERKKGNGFFKEQKYPEAVKHYSEAIKRNPNDVRAYSNRAACYTKLGALP
EGLKDAEKCIELDPSFTKGYSRKGAIQFFMKEYDKAMETYQEGLKHDPKNQEFLDGVRRCVEQINKASRG
DLTPEELKERQAKAMQDPEVQNILSDPVMRQVKAVASIVF

>gi|20095129|gb|AAM07995.1| TraN [*Providencia rettgeri*] Boltner *et al.*, 2002

MKPTLFTRVLAGILSITMACLPLHGVAADVQRQSGLSGQQEGKQLLQNWTMPALNGNTLSVPNGSGNESI
NLQELFPGMDQGSLDVLTGVYGSDASMNQLGTQRQESMASENGATGEAFRSLQQIKDRSRPDMVNDPLWA
LTDAVQTDPNLLTQSFPGCESQGEGSPNYQQCDRLNTAVNSCTITHDYTAGIIEHVSGPMNLRSCGEGCL
EVWIGRIGDNYWSGRCKVFEQAITLKVVNPDAITSAVLEYAKWDDYMQVWLGDQKVWSGPNNNFPPETAG
RCELSTSWERNPNTDLTAKLKAVEPGLEVPVKIRVSVTGSGEGYARIKVRFDPTKVVMNDSWSPQSCIEQ
AADIPAKFSDYSIQCTDQPSSTNGCTVVNGVSVCESYFVPSPVAGISPLCRRVQVSVDDESYKGIENEAC
QVLEANPSCGFMSSECAETNDKGECIRFTDTYDCGLQTSDPKCVVSNLMPSSFEACEPTHTITPFTETKY
VPDYQVCEKISTLTQCQLERRVSAETHQQSWSIELGCFSSETLSFVPQHSSTMQTGNATLRVFDNQNTEI
KITESPSKANGWKTTLSLTGNKETVTETKPSIKYPEMTCPKGTLVGSLCKVVNGSIISWHEPQEVTRSKC
ESGWNKVDFDTCSREVQKCLAPAKLSASLAFSGKYLEQDVVHQSSDPGIDQCLMQTDQFTAVQWQCLDTG
TKRIDGLTVGSGELANLGSLYPAVVSSPAHLTSRGSSDGLGLSCWRARATYNASTAHPEFNMGSSDSWVD
ASGNTQTIVNNGQNTTTNMCAELEQNPACQYVRTECTEGGAGHEGFCYIQSLVYDCGQSVEVQNARMETQ
YNCEGPVRCMGTDCLEPESIKQANFAEAAAMLNAAQFMTNDMSCTGADGQDNVECTVFKGNAGQCKKAVG
GIVDCCEKPSGVSLSDYITMIVAVNKLDTAVMAMNPSSAIYGSWNTLREPITSTWSAVKEPFVSAWDSLM
GAGPSTAAGAGAEQAATGFMQVLTNKTAEWVGTTFGSGAQSALFSNVGGAVGADGVVSGGNFALGGAAGA
VLSTVMTAYMIYSVTMILIQLIWKCEQSEFEMNAKRVLKSCHYVGSYCKSKFLGACVEKRQSYCCFTSPL
SRIIQEQVRPQLGLGWGSAKSPNCEGLTASQLNQVDWSQVNLDEWIGILSITGNLPEVPSLDLERLTGSG
STLNVDGNRQSAADRAIERLNGMDAQKLRQEATEEISGNN

>gi|15234549|ref|NP_192977.1| stress-induced protein sti1 -like protein; protein id: At4g12400.1 [*Arabidopsis thaliana*] Town *et al.*, 2002 Direct submission

MAEEAKSKGNAAFSSGDYATAITHFTEAINLSPTNHILYSNRSASYASLHRYEEALSDAKKTIELKPDWS
KGYSRLGAAFIGLSKFDEAVDSYKKGLEIDPSNEMLKSGLADASRSRVSSKSNPFVDAFQGKEMWEKLTA
DPGTRVYLEQDDFVKTMKEIQRNPNNLNLYMKDKRVMKALGVLLNVKFGGSSGEDTEMKEADERKEPEPE
MEPMELTEEERQKKERKEKALKEKGEGNVAYKKKDFGRAVEHYTKAMELDDEDISYLTNRAAVYLEMGKY
EECIEDCDKAVERGRELRSDFKMIARALTRKGSALVKMARCSKDFEPAIETFQKALTEHRNPDTLKKLND
AEKVKKELEQQEYFDPTIAEEEREKGNGFFKEQKYPEAVKHYSEAIKRNPNDVRAYSNRAACYTKLGALP
EGLKDAEKCIELDPSFTKGYSRKGAIQFFMKEYDKAMETYQEGLKHDPKNQEFLDGVRRCVEQINKASRG
DLTPEELKERQAKAMQDPEVQNILSDPVMRQVLVDFQENPKAAQEHMKNPMVMNKIQKLVSAGIVQVR

>gi|18595340|ref|XP_093065.1| similar to Stress-induced-phosphoprotein 1 (STI1) (Hsp70/Hsp90-organizing protein) (Transformation-sensitive protein IEF SSP 3521) [*Homo sapiens*] NCBI Annotation Project 2002, Direct submission

MTYITNQAAVYFEKGDYNKCWELCEKSIEVGRENREDYLQIAKVCARIGNSYFKEEKYKDAIHFYNKSLA
EHRTPDVLKKCQQAEKILKEQERLAYINPDLALEEKNKGNECFQKGDYPHAMKHYTEAIKRNPKDAKLYS
NRAACYTKLLDSSWHSRTVKNGYTRKAVALEAMKDYTKVMDVYRKALDPDSSCKEAADGYQRCMMAQYNR
HHSPEDVKRRAMADPEVQQIMSDIAMHLILEQMQKDPPGTQRTLKESCNRKEDPEADGCGSDCNSTMTCP
SPLPFALMRKEERGPRQAARSGRESRGREGLTSLYLYPSRLENVASLQMLETLFSVFRNATAAPFSTIPI
SLGFSDPLELVPGAQGLLSVPCYGSYSIIEITIKELLAVCESSQERLRILYTKIFDVPEKMPKNATYRRP
IFDDFRVAK

>gi|21779939|gb|AAM77586.1|AF506290_1 stress-induced phosphoprotein STI1; XSTI1 [*Xenopus laevis*] Goto *et al.*, 2002 Direct submission

MEAANALKEKGNKALSAGNLDEAVKCYTEAIKLDPKNHVLYSNRSAAYAKKKEFTKALEDGSKTVELKAD
WGKGYSRKAAALEFLNRFEEAKKTYEEGLRHEPTNAQLKEGLQNMEARLAEKKFMNPFNSPNLFQKLESD
PRTRALLSDPSYKELIEQLRNKPSDLGTKLQDPRVMTTLSVLLGVELGNVDEEEEDTPSPAPSQPKKETK
PEPMEEDLPENKKRAQKEKELGNEAYKKKDFETALKHYGQARELDPANMTYITNQAAVYFEMGDYSKCRE
LCEKAIEVGRENREDYRLIAKAYARIGNSYFKEEKNKEAIQFFNKSLAEHRTPEVLKKCQQAEKILKEQE
RVAYINPDLALEAKNKGNESFQKGDYPQAMKHYSEAIKRNPNDAKLYSNRAACYTKLLEFLLAVKDCEEC
IRLEPSFIKGYTRKAAALEAMKDFTKAMDAYQKAMELDSTSKEATDGYQRCMMSQYNRNDNPEDVKRRAM
ADPEVQQIMSDPAMRLILEQMQKDPQALSDHLKNPVIAQKIQKLMDVGLIAIR

>gi|12643907|sp|Q9USI5|Heat shock protein sti1 homolog (*Schizosaccharomyces pombe*) Wood *et al.*, 2002

MAEELKAKGNAAFSKKDYKTAIDYFTQAIGLDERNHILYSNRSACYASEKDYADALKDATKCTELKPDWA
KGWSRKGAALHGLGDLDAARSAYEEGLKHDANNAQLLNGLKSVEAAQTQAASGAGGFNPFAKLGSQLSDP
KFMEKLASNPETASLLADSAFMAKLQKIQQNPGSIMAELNDPRMMKVIGMLMGIDINMNAGEGAAEEQEK
KEEFAPSSSTPSADSAKPETTNPPPQPQASEPMEEDKTAEELEEAATKEALKKKADQEKQIGNENYKKRN
FPVAIEQYKKAWDTYKDITYLNNLAAAYFEADQLDDCIKTCEDAIEQGRELRADFKLIAKALGRLGTTYQ
KRGDLVKAIDYYQRSLTEHRTPDILSRLKDAEKSKELQDREAYIDPDKAEESRVKGNELFKSGDFANAIK
EYTEMTKRAPSDPRGFGNRAAAYLKVMAPAECIRDCNKAIELDPNFAKAYVRKAQALFMLKDYNKCIDAC
NEASEVDRREPNTGKNLREIESQLSKCMSAMASQRQNETEEETMARIQKDPEVLGILQDPAMQAILGQAR
ENPAALMEHMKNPTVKSKIEKLIASGVIRLG

>gi|15967134|gb|AAA91253.2| Hypothetical protein ZK328.7 [*Caenorhabditis elegans*] Waterston, 1998

MDSESDDNPNDPEDRKKWGHKDVEHWRAVSNVHYYAREGYFGTAILVCDGRLATIKDPALAILKGVCLTL
LGKIPDAIRHLETFVTDNDVALGALHALKWAHASAFNPDNKSIVEIETEISTRARNEKTPYTSYATASEV
LYFAGEYQKSKQMLDIARKRATEKHAKHYCLLGWIELALGKKQKSTQELFEKAGGQEYPDGNIGRCKILE
GHHSAPEMKVAANELAISTIHFLPGHIEKAKASIMMKDWRGVMDCIMNADQPEGSNPYIEVLRTVHGICY
AGEVSMLKRTLQLLLKSLDENEATNHVLYARITKLLVSISGRDEKILRHARDFLTRALKISRKPDYVALS
MRIAFGLGGAKEVSTLSQELVALDCEDSYAVLSSVVSMLMISRVSDARAQFDILPSAHPKLLESPLYYLI
ASVLAKQSKDKSFENFRQHIENLVEMLRNQLQSFPFGLDYLSLFSSDLLYSAVEQCFDFYPLVPIKAPDD
CMKLTAKTLQMIYDVAPGLAHCTLQLARNSYLCSNTNAAEKWIEKVLDKDDSLADAHILRAELILDRGGK
ITDADDALVTGLNFNFKLRETSLYHLIKSKTFKKRNENDEAIKTLKMALQIPRKEPSKNLFQPKESADTH
KISVQLELIDTLQHMKRIQEAETTMTDALAEWAGQPEQDQLVIAQAQLYLTKGHVERALGILKKIQPGQS
NFHLSRIKMAEIYLEEKKDKRMFAACYRELLKVEATPGSYSLLGDAFMKVQEPEDAINFYEQALKMQSKD
VQLAEKIGEAYVMAHLYSKAVNFYESSMNIYKDKNMRLKLANLLLKLRNFEKCEKVLRAPFERDPEPVGT
ETIQTYIQFLLLLAECHEMMDNVPEAMNDFEKAKSLHSRIQDKTLTAALKKEGARICNLQAELLYRRREF
SQAVDICKQALAYHETDLKANLLLSKIFKEENKWTLVLQPCQTVIQVDPHNDEANSILADFYYIRSEAAH
ASTSYTTLLNTNPQHWHALSRVVELFCRNGEQNAAEKHLDRAKEVNPRCVTESGYNVCRGRFEWYTGDQN
EALRYYSRTKDSAAGWREKALYYMIDICLNPDNEIIIDENSVENPETTKIIYLVSELWKKLVNSKNLPNI
TSIYSENFQSTDRFLLAQNFIRMHTTDKSAIQAALDEFNRMAFNADRSQVTNVGAVFGVARGHVLLKQVQ
KAKTVLKMVNGRVWNFDDSDYLEKCWLMLADIYINQNKNDQAVTFLDLVFKYNCNCLKAFELYGYMREKE
QKYVEAYKMYEKAFMATKERNPGFGYKLAFTYLKAKRLFACIETCQKVLDLNPQYPKIKKEIMDKAKALI
RT

>gi|465507|sp|P33313|Cyclophilin seven suppressor 1 (STI1 stress-inducible protein homolog) (*Saccharomyces cerevisiae*) Baur *et al.*, 1993

MSSVNANGGYTKPQKYVPGPGDPELPPQLSEFKDKTSDEILKEMNRMPFFMTKLDETDGAGGENVELEAL
KALAYEGEPHEIAENFKKQGNELYKAKRFKDARELYSKGLAVECEDKSINESLYANRAACELELKNYRRC
IEDCSKALTINPKNVKCYYRTSKAFFQLNKLEEAKSAATFANQRIDPENKSILNMLSVIDRKEQELKAKE
EKQQREAQERENKKIMLESAMTLRNITNIKTHSPVELLNEGKIRLEDPMDFESQLIYPALIMYPTQDEFD
FVGEVSELTTVQELVDLVLEGPQERFKKEGKENFTPKKVLVFMETKAGGLIKAGKKLTFHDILKKESPDV
PLFDNALKIYIVPKVESEGWISKWDKQKALERRSV

>gi|14389431|ref|NP_058017.1| stress-induced phosphoprotein 1; IEF SSP 3521; Hsp70/Hsp90 organizing protein; stress-inducible protein [*Mus musculus*] Blatch *et al.*, 1997

MEQVNELKEKGNKALSAGNIDDALQCYSEAIKLDPQNHVLYSNRSAAYAKKGDYQKAYEDGCKTVDLKPD
WGKGYSRKAAALEFLNRFEEAKRTYEEGLKHEANNLQLKEGLQNMEARLAERKFMNPFNLPNLYQKLEND
PRTRSLLSDPTYRELIEQLQNKPSDLGTKLQDPRVMTTLSVLLGVDLGSMDEEEEAATPPPPPPPKKEPK
PEPMEEDLPENKKQALKEKELGNDAYKKKDFDKALKHYDRAKELDPTNMTYITNQAAVHFEKGDYNKCRE
LCEKAIEVGRENREDYRQIAKAYARIGNSYFKEEKYKDAIHFYNKSLAEHRTPDVLKKCQQAEKILKEQE
RLAYINPDLALEEKNKGNECFQKGDYPQAMKHYTEAIKRNPRDAKLYSNRAACYTKLLEFQLALKDCEEC
IQLEPTFIKGYTRKAAALEAMKDYTKAMDVYQKALDLDSSCKEAADGYQRCMMAQYNRHDSPEDVKRRAM
ADPEVQQIMSDPAMRLILEQMQKDPQALSEHLKNPVIAQKIQKLMDVGLIAIR

>gi|17473522|gb|AAL38384.1| At1g12270/F5O11_1 [*Arabidopsis thaliana*] Cheuk *et al.*, 2001, Direct submission

MAEEAKAKGNAAFSSGDFTTAINHFTEAIALAPTNHVLFSNRSAAHASLHQYAEALSDAKETIKLKPYWP
KGYSRLGAAHLGLNQFELAVTAYKKGLDVDPTNEALKSGLADAEASVARSRAAPNPFGDAFQGPEMWTKL
TSDPSTRGFLQQPDFVNMMQEIQKNPSSLNLYLKDQRVMQSLGVLLNVKFRPPPPQGDEAEVPESDMGQS
SSNEPEVEKKREPEPEPEPEVTEEKEKKERKEKAKKEKELGNAAYKKKDFETAIQHYSTAIEIDDEDISY
LTNRAAVYLEMGKYNECIEDCNKAVERGRELRSDYKMVARALTRKGTALTKMAKCSKDYEPAIEAFQKAL
TEHRNPDTLKRLNDAERAKKEWEQKQYFDPKLGDEEREKGNDFFKEQKYPEAIKHYTEAIKRNPNDHKAY
SNRAASYTKLGAMPEGLKDAEKCIELDPTFSKGYSRKAAVQFFLKEYDNAMETYQAGLEHDPSNQELLDG
VKRCVQQINKANRGDLTPEELKERQAKGMQDPEIQNILTDPVMRQVLSDLQENPSAAQKHMQNPMVMNKI
QKLISAGIVQMK

>gi|2129844|pir||S56658 stress-induced protein sti1 - soybean [*Glycine max*] Hernandez *et al.*, 1995

MAEEAKAKGNAAFSAGDFAAAVRHLSDAIALSPSNHVLYSNRSAATLPPELRGGPSRRQKTVDLKPDWPK
AYSRLGAAHLGLRRHRDASPPTKPASNSNPDNAALKSGLADAQAAASRPPPTSPFATAFSGPDMWARSPP
TPPHVQPPGPRVRQDHAGHPEGPQQVQPAFEYQRVMHAIGVLLNVKIQTPNHDENDHDADDDVSEDEVVS
QPEPEHEPEAAVEVAEEEEEEEKETRDRKGQAQKEKEAGNAAYKKKDFETAIGHYSKALELDDEDISYLT
NRAAVYLEMGKFEDCIKDCEKAVERGKELRSDYKMIARALTRKGTALAKMAKCSKDFEPAIEIFQKALTE
NRNPDTLKKLNEAEKAKKELEQQEYFDPKLADEAREKGNELFKQQKYPEATKHYTEAIKRNPKDAKAYSN
RAACYTKLGAMPEGLKDAEKCIELDPTFSKGYTRKGAVQFSMKEYDKALETYREGLKHDPNNQELLDGIR
RCVEQINKASRGDFTPEELKERQAKAMQDPEIQSILQDPVMTQVLTDFQENPRAAEEHVKNPMVMNKTQN
VTVPGCQMR

>gi|83553|pir||A32567 stress-induced protein STI1 - yeast (*Saccharomyces cerevisiae*) Nicolet and Craig, 1989

MSLTADEYKQQGNAAFTAKDYDKAIELFTKAIEVSETPNHVLYSNRSACYTSLKKFSDALNDANECVKIN
PSWSKGYNRLGAAHLGLGDLDEAESNYKKALELDASNKAAKEGLDQVHRTQQARQAQPDLGLTQLFADPN
LIENLKKNPKTSEMMKDPQLVAKLIGYKQNPQAIGQDLFTDPRLMTIMATLMGVDLNMDDINQSNSMPKE
PETSKSTEQKKDAEPQSDSTTSKENSSKAPQKEESKESEPMEVDEDDSKIEADKEKAEGNKFYKARQFDE
AIEHYNKAWELHKDITYLNNRAAAEYEKGEYETAISTLNDAVEQGREMRADYKVISKSFARIGNAYHKLG
DLKKTIEYYQKSLTEHRTADILTKLRNAEKELKKAEAEAYVNPEKAEEARLEGKEYFTKSDWPNAVKAYT
EMIKRAPEDARGYSNRAAALAKLMSFPEAIADCNKAIEKDPNFVRAYIRKATAQIAVKEYASALETLDAA
RTKDAEVNNGSSAREIDQLYYKASQQRFQPGTSNETPEETYQRAMKDPEVAAIMQDPVMQSILQQAQQNP
AALQEHMKNPEVFKKIQTLIAAGIIRTGR

>gi|478009|pir||C48583 stress-inducible protein STI1 homolog - *Leishmania donovani* Joshi *et al.*, 1993

MESMGKYDEAQKAFQKALQLSPGNEEVMDKLHTVNTKVRERNEKTKSQQCKTPEEAKQLGNSFFKDGKYD
QAAEFYTRAIELQTEPVKEKAVYYTNRAACHQQTHMYSLMVDDCNAAIEIDPANVKAYLRRGIAYEGMEK
WKLALEDYTKAQSISPGVAGASQGILRCQRVLRN

>gi|1708299|sp|Q08168| 58 KD PHOSPHOPROTEIN (HEAT SHOCK-RELATED PROTEIN) *Plasmodium berghei* Uparanukraw *et al*, 1993

MDIEKIEDLKKFVASCEENPSILLKPELSFFKDFIESFGGKIKKDKMGYEKMKSEDSTEEKSDEEEEDEE
EEEEEEEDDDPEKLELIKEEAVECPPLAPIIEGELSEEQIEEICKLKEEAVDLVENKKYEEALEKYNKII
SFGNPSAMIYTKRASILLNLKRPKACIRDCTEALNLNVDSANAYKIRAKAYRYLGKWEFAHADMEQGQKI
DYDENLWDMQKLIQEKYKKIYEKRRYKINKEEEKQRLKREKELKKKLAAKKKAEKMYKENNKRENYDSDS
SDSSYSEPDFSGDFPGGMPGGMPGMPGGMGGMGGMPGMPGGFPGMPGGMPGGMPGGMGGMPGMPGGMPGG
MGGMPGMPGGMPDLNSPEMKELFNNPQFFQMMQNMMSNPDLINKYASDPKYKNIFENLKNSDLGGMMGEK
PKP

>gi|2745838|gb|AAB94760.1| Hsp70/Hsp90 organizing protein; hop [*Cricetulus griseus*] Heine *et al.*, 1999

MEQVNELKEKGNKALSAGNIDDALQCYSEAIKLDPQNHVLYSNRSAAYAKKGDYQKAYEDGCKTVDLKPD
WGKGYSRKAAALEFLNRFEEAKRTYEEGLKHEANNLQLKEGLQNMEARLAERKFMNPFNLPNLYQKLEND
PRTRTLLSDPTYRELIEQLRNKPSDLGTKIQDPRIMTTLSVLLGVDLGSMDEEEEAATPPPPPPSKKEAK
PEPMEEDLPENKKQALKEKEMGNEAYKKKDFDMALKHYDRAKELDPTNMTYITNQAAVHFEKGDYNKCRE
LCEKAIEVGRENREDYRQIAKAYARIGNSYFKEERYKDAIHFYNKSLAEHRTPDVLKKCQQAEKILKEQE
RLAYINPDLALEEKNKGNECFQKGDYPQAMKHYTEAIKRNPKDAKLYSNRAACYTKLLEFQLALKDCEEC
IQLEPTFIKGYTRKAAALEAMKDYTKAMDVYQKALELDSSCKEAADGYQRCMMAQYNRHDSPEDVKRRAM
ADPEVQQIMSDPAMRLILEQMQKDPQALSEHLKNPVIAQKIQKLMDVGLIAIR

>gi|4038461|gb|AAC97378.1| TcSTI1 [*Trypanosoma cruzi*] Minning et al., 1998 Direct submission

MDATELKNRGNQEFSSGRYKEAAEFFSQAINLDPSNHVLYSNRSACHAALHQYPNALQDAEKCVSIKPDW
VKGYVRKGAALHGLRRYETAAAYNKGLSLDPSSAACTEGIAAVEKDKVASRMQNPFANVFGPDAIGKIQA
HPKLSLFLLQPDYVRMIDEVMKDPSSVQKYLKDQRFMATFMVLSGLELPEDEDEEEEKVRRQQQKQKEKE
MKEEQEKKKAAATELSPEAKEALRKKEEGNALYKQRKFDEALQKYQEALSKDSTNTVYLLNITAVIFEKG
EYAACVEKCEEALEHGRENRCDYTVLAKLMTREALCLQRLKRFDEAIALFKKALVEHRNPDTLAKLTACE
KEKEKFEIEAYLDPEIALQKKEEGNTFFKSDKFPEAVEAYTEAIKRNPDEHTTYSNRAAAYLKLGAYSQA
LADAEKCISLKPEFVKAHARRGHAFFWTKQYNKALQAYDEGLKHDKENAECKEGRMRTLMKIQEWLLATL
PTEMKWQNAPWQIQRLLLSCRTAICSWYWVRCSGTPHASKNTCGIRRLPQRSTPLFLLESFALESKREAK
QAMIR

>gi|2511703|emb|CAA75351.1| p60 protein [*Rattus norvegicus*] Hohfeld, 1997

MEQVNELKEKGNKALSAGNIDDALQCYSEAIKLDPQNHVLYSNRSAAYAKKGDYQKAYEDGCKTVDLKPD
WGKGYSRKAAALEFLNRFEEAKRTYEEGLKHEANNLQLKEGLQNMEARLAERKFMNPFNLPNLYQKLEND
PRTRTLLSDPTYRELIEQLQNKPSDLGTKLQDPRVMTTLSVLLGVDLGSMDEEEEAATPPPPPPKKEAK
PEPMEEDLPENKKQALKEKELGNDAYKKKDFDKALKHYDKAKELDPTNMTYITNQAAVHFEKGDYNKCRE
LCEKAIEVGRENREDYRQIAKAYARIGNSYFKEERYKDAIHFYNKSLAEHRTPDVLKKCQQAEKILKEQE
RLAYINPDLALEEKNKGNECFQKGDYPQAMKHYTEAIKRNPRDAKLYSNRAACYTKLLEFQLALKDCEEC
IQLEPTFIKGYTRKAAALEAMKDYTKAMDVYQKALDLDSSCKEAADGYQRCMMAQYNRHDSPEDVKRRAM
ADPEVQQIMSDPAMRLILEQMQKDPQALSEHLKNPVIAQKIQKLMDVGLIAIR

>gi|1890281|gb|AAB49720.1| transformation-sensitive protein homolog [*Acanthamoeba castellanii*] Xu and Zot, 1997 Direct submission

MADIALEEKNKGNAAMSAGDFKAAVEHYTNAIQHDPQNHVLYSNRSAAYASLKDYDQALADGEKTVELKP
DWSKGYSRKGAALCYLGRYADAKAAYAAGLEVEPTNEQLKQALQEAEEQEQASGGGPDIGNVFGQMLQGD
IWTKLRQSDLTRAYLDDPAFVSLLSRLQKNPNELPMYIQSDPRIANVFAVILGISQKPPGAETQEPAQQP
KKEEPKKEEKPKAEEKPKEPEPELPTEKKQALEEKELGNQAYKKKDFDTAIVHYKKAFELDPDNMTYLTN
LAAVYMEQKNYEECVNTCTEAIEVGRRVFADYKLISRAFHRKGNAYMKMEKYAEAIDSYNRALTEHRNPD
SLNALRKAEQLKKESEEKNYVNPEISQQEKEKGNDCFRNAQYPDAIKHYTEAIRRNPTDHVLYSNRAACY
MKLGRVPMAVKDCDKAIELSPTFVKAYTRKGHCQFFMKQYHKCLETYEQGLKVEPNNEELNEGLRRTMEA
INKRQEGSSKAEDKEAMAAAASDPEIQKILGDPMMKKVLSELGTNPAAVQSYMKDPVIMNNIQKLIAAGI
IKVK

Appendix D

Table D.1: Sequence Statistics for Murine stress-inducible protein 1 (mSTI1)

Molecular Weight (Daltons)	62584.24
Number of Amino Acids	543
Mean Amino Acid Weight (Daltons)	115.3
Average Hydrophobicity	-9.5
Ratio of Hydrophilicity to Hydrophobicity	1.97
Percentage of Hydrophilic Amino Acids	58.2
Percentage of Hydrophobic Amino Acids	41.8
Ratio of %Hydrophilic to %Hydrophobic	1.39
Number of Basic Amino Acids	90
Number of Acidic Amino Acids	93
Estimated pI for Protein	7.00
Total Linear Charge Density	0.34
Polar Area of Extended Chain (Angs^2)	39595.4
Non-Polar Area of Extended Chain (Angs^2)	59484.5
Total Area of Extended Chain (Angs^2)	99079.9
Polar ASA of Folded Protein (Angs^2)	8477.2
Non-Polar ASA of Folded Protein (Angs^2)	11276.2
ASA of Folded Protein (Angs^2)	19753.4
Ratio of Folded to Extended Area	0.21
Buried Polar Area of Folded Protein (Angs^2)	25422.5
Buried Non-Polar Area of FP (Angs^2)	44307.8
Buried Charge Area of FP (Angs^2)	2905.4
Total Buried Surface (Angs^2)	72635.7
Number of Buried Amino Acids	233
Packing Volume (est) (Angs^3)	76123.0
Packing Volume (act) (Angs^3)	73324.1
Interior Volume of Protein (Angs^3)	28214.2
Exterior Volume of Protein (Angs^3)	45109.9
Partial Specific volume (ml/g)	0.720
Fisher Volume Ratio (act)	1.6
Fisher Volume Ratio (idealized)	0.5
Protein Solubility	2.7
Est. Radius of Folded Protein (Angs)	31.6
RMS End-to-End Dist. of Ext. Chain (Angs)	244.4
Radius of Gyration of Ext. Chain (Angs)	99.8
Solv. Free Energy of Folding (kcal/mol)	-521.5

Appendix E

Table E.1: Oligonucleotide Primers

Name of Oligo	Oligo sequence	Tm ^{0}C
K8A(FWD)	5'GTGAATGAGCTAGCGGAGAAGGGC	63.4
K8A(REV)	5'GCCCTTCTCCGCTAGCTCATTCAC	63.4
pGEX3X2000N12AF	5'GCTAAAGGAGAAGGGCGCCAAGGCCCTGAGTGC	73.2
pGEX3X2000N12AR	5'GCACTCAGGGCCTTGGCGCCCTTCTCCTTTAGC	73.2
pGEXKN812FWD	5'GAATGAGCTAGCGGAGAAGGGCGCCAAGGCCCTGAG	74.4
pGEXKN812REV	5'CTCAGGGCCTTGGCGCCCTTCTCCGCTAGCTCATTC	74.4
pGEXN43AFWD	5'GTGCTCTACAGCGCTCGCTCTGCAG	66.8
pGEXN43AREV	5'CTGCAGAGCGAGCGCTGTAGAGCAC	66.8
pGEX301AF	5'GCAGATCGCCGCCGCTTATGCCCG	69.9
pGEX301AR	5'CGGGCATAAGCGGCGGCGATCTGC	69.9
PGEXL15YFWD	5'GAAGGGCAATAAAGCCTATAGTGCTGGGAAC	64.3
PGEXL15YREV	5'GTTCCCAGCACTATAGGCTTTATTGCCCTTC	64.3
PGEXA49FK50EF	5'CAATCGCTCTGCGGCCTACTTCGAGAAAGGAGAC	69.1
PGEXA49FK50ER	5'GTCTCCTTTCTCGAAGTAGGCCGCAGAGCGATTG	69.1
Y/Lfwd	5'GGAAATGATGCCCTTAAGAAGAAAG	55.9
Y/Lrev	5'CTTTCTTCTTAAGGGCATCATTTCC	55.9
FE/AKfwd	5'GCTGTGCATGCTAAGAAGGGCGAC	64.0
FE/AKrev	5'GTCGCCCTTCTTAGCATGCACAGC	64.0
pCEP4-2000F	5'GGTACCAGAATGGGACATCATCATCATCATCATGGAA TGGAGCAGGTGAATGAG	71.7
pCEP4-2000R	5'CTCGAGTTATCATTATCACCGAATTGCGATGAG	62.3
pCEP4-1400F	5'GGTACCAGAATGGGACATCATCATCATCATCATGAAC CCAAGCCAGAACCAATG	72.1
pCEP4-700R	5'CTCGAGTTATCAGATCTTCTTCCATTGG	58.6
EBVrev	5'GTGGTTTGTCCAAACTCATC	52.7
PCEPfwd	5'AGCAGAGCTCGTTTAGTGAACCG	60.6
PGEXK8EFWD	5'GGTGAATGAGCTCGAGGAGAAGGGC	64.5
PGEXK8EREV	5'GCCCTTCTCCTCGAGCTCATTCACC	64.5
PGEXN12EFWD	5'GGAGAAGGGCGAGAAAGCCCTGAGTG	66.3
PGEXN12EREV	5'CACTCAGGGCTTTCTCGCCCTTCTCC	66.3
pGEXK73AFWD	5'CTGACTGGGGCGCCGGTTATTCAAG	65.3
pGEXK73AREV	5'CTTGAATAACCGGCGCCCCAGTCAG	65.3
pGEXR77AFWD	5'GGTTATTCAGCAAAAGCGGCCGCCCTTG	67.9
pGEXR77AREV	5'CAAGGGCGGCCGCTTTTGCTGAATAACC	67.9
pGEX229AF	5'CACTGAAAGAGGCGGAGCTCGGAAATGATGC	67.7
pGEX229AR	5'GCATCATTTCCGAGCTCCGCCTCTTTCAGTG	67.7
pGEX233AF	5'GAGAAGGAGCTCGGAGCAGATGCCTACAAG	66.7
pGEX233AR	5'CTTGTAGGCATCTGCTCCGAGCTCCTTCTC	66.7
pGEXKNAF	5'CACTGAAAGAGGCGGAGCTCGGAGCTGATGCCTAC	71.6
pGEXKNAR	5'GTAGGCATCAGCTCCGAGCTCCGCCTCTTTCAGTG	71.6